

M.T.HESIS

25

AN EXPERIMENTAL AND THEORETICAL INVESTIGATION
OF THE THERMOSYPHON SOLAR WATER HEATER

Handwritten notes:
1985
11/10/85

A MASTER'S THESIS

in

Mechanical Engineering

Middle East Technical University

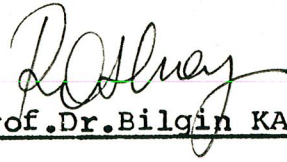
044114

By


İlyas ERDOĞAN

October 1985


Approval of the Graduate School of Natural and Applied Sciences.


for Prof. Dr. Bilgin KAFTANOĞLU
Director

I certify that this thesis satisfies all the requirements as a thesis for the degree of Master of Science in Mechanical Engineering Department.



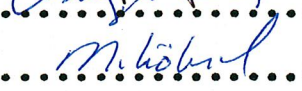



Prof. Dr. Alp ESİN
Chairman of the Department

We certify that we have read this thesis and that in our opinion it is fully adequate, in scope and quality, as a thesis for the degree of Master of Science in Mechanical Engineering Department.


Assoc. Prof. Dr. Mazhar ÜNSAL
Supervisor

Examining Committee in Charge:

Prof. Dr. ALP ESİN
Assoc. Prof. Dr. MAZHAR ÜNSAL
Assoc. Prof. Dr. ÖMER T. GÖKSEL
Assoc. Prof. Dr. MUHAMMED KÖKSAL
Assoc. Prof. Dr. MUSTAFA MERDAN


.....

.....

.....

.....

.....

ABSTRACT

AN EXPERIMENTAL AND THEORETICAL INVESTIGATION
OF THE THERMOSYPHON SOLAR WATER HEATER

ERDOĞAN, İlyas

M.S. in Mechanical Engineering

Supervisor : Assoc.Prof.Dr. Mazhar ÜNSAL

October 1985, 116 Pages

This study is an experimental and theoretical investigation of the most common type of thermosyphonic solar water heating system being used in Turkey. This system consists of two solar collectors and a jacketed hot water storage tank. Experiments are performed on a standard type solar thermosyphon water heating system manufactured by ÇİLTUĞ A.Ş. Temperatures and system heat input rates are measured in the experimental part of the study. The thermosyphoning fluid mass flow rate, the collector inlet to exit temperature difference, and the jacketed hot water storage tank overall heat transfer coefficient were estimated from an analysis of the experimental measurements. An analysis is developed for the computation of the thermosyphonic system mass flow rate, collector inlet to exit temperature difference, and

the system head loss in the theoretical part of this study. The results from the theoretical analysis are used to develop an interactive computer program in the Applesoft Basic Language using the Apple IIe microcomputer. This computer program is used to investigate the effects of system geometric parameters on the system performance and results are presented in graphical form. The experimental results and theoretical predictions are discussed with comparison.

Key Words : Solar energy, Thermosyphon system,
Jacketed hot water storage tank.

ÖZET

TERMOSİFON GÜNEŞ ENERJİLİ SU ISITMA SİSTEMİNİN DENEYSEL VE TEORİK OLARAK İNCELENMESİ

ERDOĞAN, İlyas

Yüksek Lisans Tezi, Makina Mühendisliği Bölümü

Tez Yöneticisi : Doç.Dr. Mazhar ÜNSAL

Ekim 1985, 116 Sayfa

Bu çalışma Türkiye'de en yaygın tip güneşli su ısıtma sistemi olan iki güneş toplayıcısı ve bir gömlekli sıcak su deposundan oluşan güneş enerjili termosifon su ısıtma sistemi üzerinde yapılmış olan teorik ve deneysel çalışmaları içermektedir. Deneysel çalışmalar ÇİLTUĞ A.Ş. tarafından üretilen standart tipteki termosifon, güneşli su ısıtma sistemi üzerinde yapılmıştır. Deneysel çalışmada sistem üzerinde sıcaklık ve ısıtma şiddeti ölçümleri yapılmıştır. Yapılan ölçümlerin analizi sonucunda sistemdeki termosifon su debisi, toplayıcı giriş-çıkış su sıcaklık farkı ve gömlekli eşanjör toplam ısı aktarım katsayısı saptanmıştır. Teorik çalışmada ise sistemdeki su akışının laminar olduğu varsayılarak termosifon sistem su debisinin, Güneş toplayıcıları su giriş-çıkış sıcaklık farkının ve sistemdeki basınç kaybının hesaplanmasını sağlayan bir analiz geliştirilmiştir.

Teorik analiz sonuçlarından yararlanılarak Apple IIe mikrobilgisayarında Applesoft Basic dilinde etkileşimli bir bilgisayar programı hazırlanmıştır. Bilgisayar programı kullanılarak sistem geometrik parametrelerinin sistem performansı üzerindeki etkileri hesaplanmış ve grafikler halinde gösterilmiştir. Teorik bulgular ile deneysel sonuçlar arasındaki uyum tartışılmıştır.

Anahtar Kelimeler : Güneş enerjisi, Termosifon sistemi,
Gömlekli sıcak su deposu.

ACKNOWLEDGEMENTS

I would like to express my gratitude to Assoc.Prof. Dr. Mazhar ÜNSAL for his inspiring and illuminating supervision and continual encouragement throught the progress of this thesis.

I am grateful to Prof.Dr. Alp ESİN, Assoc.Prof. Dr. Süleyman SARITAŞ and Asst.Prof.Dr. Sedat BAYSEÇ for their contributions in the experimental measurements.

I am grateful to Mr. İbrahim TUĞSUZ, chairman of the ÇILTUĞ A.Ş. for his kind encouragement, helps and supply of the equipments for this study.

I also thank my small brother, Salih ERDOĞAN for his typing, Mrs.Semiha KONU for technical drawings and Mrs. Emel BAHÇECİ for the photographes of the experimental set up.

TABLE OF CONTENTS

	Page
ABSTRACT	iii
ÖZET	v
ACKNOWLEDGEMENT	vii
LIST OF TABLES	xi
LIST OF FIGURES	xii
LIST OF SYMBOLS	xv
1. INTRODUCTION	1
2. LITERATURE SURVEY	9
3. EXPERIMENTAL STUDY	17
3.0. Introduction	17
3.1. Description of the Experimental Set-Up	17
3.2. Experimental Measurements	24
3.2.1. Calibration of the Temperature	
Recording System	26
3.2.2. Description of the Temperature	
Recording System	29
3.2.3. Measurement of Heat Input Rate	
to the Collector	30
3.2.4. Determination of Thermosyphonic	
Mass Flow Rate	31
3.2.5. Determination of the Overall Heat	
Transfer Coefficient, Number of	
Transfer Units and Effectiveness	
of the Storage Tank-Heat Exchanger.	31

	Page
4. THEORETICAL ANALYSIS	34
4.1. Analysis of the Thermosyphonic Cycle by the Application of the Mechanical Energy Equation	37
4.2. Mass Flow Rate and Head Loss Relationship for Laminar Flow Inside Pipes	40
4.3. Theoretical Estimation of Unequal Flow Rates in Different Collector Risers	43
4.4. The System Characteristic for the Thermosyphonic Loop and the Prediction of the Thermosyphonic Mass Flow Rate for Laminar Flow	51
5. RESULTS AND DISCUSSION	54
5.1. Evaluation of Results	54
5.2. Discussion of the Effects of System Parameters on System Performance	57
6. CONCLUSION	85
7. RECOMMENDATIONS FOR FURTHER STUDY	87
REFERENCES	89
APPENDICES	92
Appendix-1 A Triac Triggering Circuit	92
Appendix-2 Estimation of the Overall Heat Loss Coefficients	93
Appendix-3 Flowchart, Computer Program and Computer Outputs for Experimental Data Evaluation	97

Appendix-4 Expressions for Mass Flow Rate
Estimation of the Collector
Risers 106

Appendix-5 Flowchart, Computer Program and
Computer Outputs (Only Sample)
for Theoretical Results
Evaluation 110

LIST OF TABLES

Table	Page
1. Technical Data for the Collectors Unit.....	23
2. Technical Data for the Hot Water Heat Storage Tank-Heat Exchanger Unit.....	24
3. The estimated Reynolds Number in the Connecting Pipe and in the 8th Riser.....	63
4. Comparison of the Experimental Effectiveness Value of the Storage Tank-Heat Exchanger with the Theoretical Effectiveness Value for a Counter Flow Heat Exchanger.....	79
5. Percent Reduction in Double Loop Thermosyphon System Efficiency Because of the Storage Tank-Heat Exchanger Unit.....	83

LIST OF FIGURES

Figure	Page
1.1. Schematic Diagram of a Solar Aided Single Loop Forced Circulation System	3
1.2. Schematic Diagram of a Single Loop Natural Circulation System	3
1.3. Schematic Diagram of a "Once-Through" System with Temperature Controlled Valve	5
1.4. Schematic Diagram of a Self-Adjusting "Once-Through" System	5
3.1. Schematic of the Experimental Set-Up	18
3.2. Side View from the Experimental Set-Up	20
3.3. Front View from the Experimental Set-Up	21
3.4. Hot Water Heat Storage Tank-Heat Exchanger ...	25
3.5. Calibration of Thermometer	27
3.6. Calibration of Temperature Recorder Channel No.1	28
3.7. Calibration of Temperature Recorder Channel No.2	28
3.8. Calibration of Temperature Recorder Channel No.3	28
3.9. Calibration of Temperature Recorder Channel No.4	28
4.1. Schematic Diagram of a Double Loop Thermosyphon System	35

	Page
4.2. Double Loop Thermosyphon Solar Water Heating System	39
4.3. Schematic of Flow Net-Work in Collector Risers	45
4.4. Flow Through Riser No.1	46
4.5. Flow Through Loop No.1	47
5.1. The Effect of Dh on the Total Thermosyphonic Mass Flow Rate	58
5.2. The Effect of Dh on the Collector Exit-Inlet Temperature Difference	59
5.3. The Effect of Dh on the Total Thermosyphonic Head	60
5.4. Theoretical Mass Flow Rate Relationships for the Solar Collector Manufactured by ÇILTUĞ A.Ş.	62
5.5. The Effect of Dr on the Total Thermosyphonic Mass Flow Rate	64
5.6. The Effect of Dr on the Collector Exit-Inlet Temperature Difference	65
5.7. The Effect of Dr on the Total Thermosyphonic Head	66
5.8. The Effect of Dp on the Total Thermosyphonic Mass Flow Rate	68
5.9. The Effect of Dp on the Collector Exit-Inlet Temperature Difference	69
5.10. The Effect of Dp on the Total Thermosyphonic Head	70

	Page
5.11. The Effect of L_p on the Total	
Thermosyphonic Mass Flow Rate	72
5.12. The Effect of L_p on the Collector	
Exit-Inlet Temperature Difference	73
5.13. The Effect of L_p on the Total	
Thermosyphonic Head	74
5.14. The Effect of L_v on the Total	
Thermosyphonic Mass Flow Rate	76
5.15. The Effect of L_v on the Collector	
Exit-Inlet Temperature Difference	77
5.16. The Effect of L_v on the Total	
Thermosyphonic Head	78
5.17. Experimental U-Value Versus Heat	
Input Rate to the Collectors	81
5.18. Experimental U-Value Versus Tank	
Inlet-Exit Temperature Difference	82

LIST OF SYMBOLS

Q_c	Heat input rate to the collector, (W)
I_{rms}	Current, (Ampere)
V_{rms}	Voltage, (Volts)
m	Thermosyphonic total mass flow rate, (Kg/s)
c_p	Water constant pressure specific heat, (J /kg- $^{\circ}$ C)
T_1	Collectors water inlet temperature, ($^{\circ}$ C)
T_2	Collectors water exit temperature, ($^{\circ}$ C)
T_o	Average water temperature of the collectors, ($^{\circ}$ C)
T_{h_1}, T_{hi}	Tank hot side water inlet temperature, ($^{\circ}$ C)
T_{h_2}, T_{he}	Tank hot side water exit temperature, ($^{\circ}$ C)
T_{c_2}, T_{ce}	Tank cold side water exit temperature, ($^{\circ}$ C)
T_{c_1}, T_{ci}	Tank cold side water inlet temperature, ($^{\circ}$ C)
ΔT_m	Log-mean temperature difference of the tank, ($^{\circ}$ C)
U	Overall heat transfer coefficient of the tank, (W/m ² - $^{\circ}$ C)
Q_{ut}	Useful heat input rate to the storage tank, (W)
A_j	Heat transfer surface area of the tank, (m ²)
NTU	Number of transfer unit of the tank
ϵ	Effectiveness of the tank
C_h	Hot side capacity rate, (W/ $^{\circ}$ C)
C_c	Cold side capacity rate, (W/ $^{\circ}$ C)
m_t	Cold side (tank) mass flow rate, (Kg/s)
C_{min}	Minimum capacity rate, (W/ $^{\circ}$ C)
C_{max}	Maximum capacity rate, (W/ $^{\circ}$ C)
γ	Defined parameter

C	Capacity rate ratio
h_f	Lost head, (m)
p	Static pressure, (N/ m ²)
V	Average velocity of water, (m/s)
g_c	Constant, (1.0 kg-m/N-s ²)
g	Gravitational acceleration, (9.81 m/s ²)
z	Gravity direction, (+)
h_L	Total thermosyphonic head loss, (m)
C_o	Defined parameter, (N/m ² -°C)
C_l	Defined parameter, (m/ °C)
β	Volume coefficient expansion of water, (1/°C)
f	Moody friction factor
Re	Reynolds number, $Re = V D/\nu$
μ	Dynamic viscosity, (N-s/m ²)
ν	Kinematic viscosity, (m ² /s)
L	Length of the pipe, (m)
D	Diameter of the pipe, (m)
K_r	Resistance coefficient
α	L/D equivalent of flow fittings
K	Defined parameter, (1/m ³)
H	Defined parameter, (Kg/m ³ -s)
a	Distance between risers, (m)
b	Riser length, (m)
D_h	Header inside diameter, (m)
D_p	Connecting pipe inside diameter, (m)
D_r	Riser inside diameter, (m)
$m_{1,8}$	Mass flow rate through one collector, (Kg/s)
m_1	Mass flow rate through riser no.1, (Kg/s)

h_{L8}	Lost head in collector; the collector characteristic, (m)
C_2	Defined parameter, ($m\text{-s}^2/kg^2$)
C_3	Defined parameter, ($m\text{-s}/kg$)
Q_{uc}	Useful heat input rate to the collectors, (W)
C_4	Defined parameter; $C_4 = C_3/C_2$, (Kg/s)
C_5	Defined parameter; $C_5 = -C_1 Q_{uc} / (c_p c_2)$, (Kg^3/s^3)
L_p	Total length of the connecting pipes, (m)
L_v	Total vertical length of the connecting pipes, (m)
$T_2 - T_1$	Collector exit-inlet temperature difference, ($^{\circ}C$)
F_R	Collector heat removal factor
$k_{ins.}$	Insulation thermal conductivity, ($W/m^2\text{-}^{\circ}C$)
$t_{ins.}$	Insulation thickness, (m)
A_c	Collector area, (m^2)
r_i	Jacket outside radius, (m)
r_o	Outside insulation radius over the jacket, (m)
A_s	Jacket outside surface area, (m^2)
A_p	Tank circumferential insulated surface area, (m^2)
A_f	Convex end surface area of the tank, (m^2)
ϵ	Emissivity of the painted tank surface
σ	Stefan-Boltzmann constant, ($5.669 \times 10^{-8} W/m^2 \text{ } ^{\circ}K^4$)
F'_R	Modified collector-heat removal factor
$(mc_p)_c$	Collector side capacity rate, ($W/^{\circ}C$)
$(mc_p)_{min}$	Minimum capacity rate, ($W/^{\circ}C$)
he	Heat exchanger (storage tank)
F'_R / F_R	A ratio representing the decrease in system efficiency
Q	Heat input rate to the collectors, (kW)

CHAPTER 1

INTRODUCTION

The subject of this study is an experimental and theoretical investigation of the thermosyphonic solar water heater. The scope of the present investigation consists of the measurement and prediction of the thermosyphonic mass flow rate and the heat transfer characteristics of a double loop heat storage tank-heat exchanger system typical to most thermosyphon solar water heating systems in Turkey.

In our days the unit price of energy is steadily increasing at a rate which is greater than the inflation rates. As a result, the cost of energy for domestic hot water heating in residential buildings is also increasing as more conventional heating systems are installed in residential buildings. For this reason investigations into the technical and economic feasibility aspects of solar hot water heating systems have gained importance during the last decade all over the world. In parallel to this trend solar energy utilization in domestic hot water heating applications is progressively increasing in our country.

At the present time the production and installation of solar heating systems for domestic hot water heating is

the most common application of solar energy utilization in our country. There are now many industrial firms manufacturing solar collectors and hot water heat storage tanks in Turkey.

An investigation into the types of solar hot water heating systems presently used shows that these systems may be classified into three categories as follows :

- 1 - Forced circulation systems
- 2 - Thermosyphon (i.e., natural circulation) systems
- 3 - Once-through systems

A schematic of a forced circulation system is depicted in Figure 1.1. The flow in this solar hot water heating systems is maintained by a water pump. The hot water storage tanks in these systems are generally located in the boiler room. The systems in this category usually have a large number of solar collectors. These systems are used in applications where a large amount of hot water supply is required. Hotel, hospital and army soldier residence hall solar hot water heating systems are examples.

The second category as shown in Figure 1.2 is the most commonly used system in residential applications. These systems operate in the thermosyphonic mode. The hot water storage tank is located above the solar collectors. The system does not have a water pump. The circulation through the collectors takes place as a result of the thermostatic head induced by the temperature differences in the circulation loop. The systems of this category may be further classified according to the type of the storage

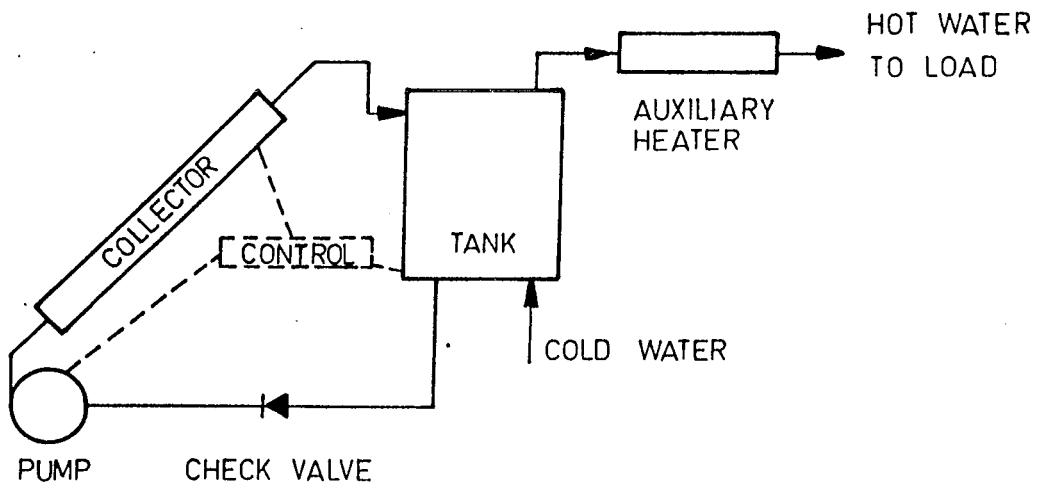


Fig.1.1 Schematic Diagram of a Solar Aided Single Loop Forced Circulation System

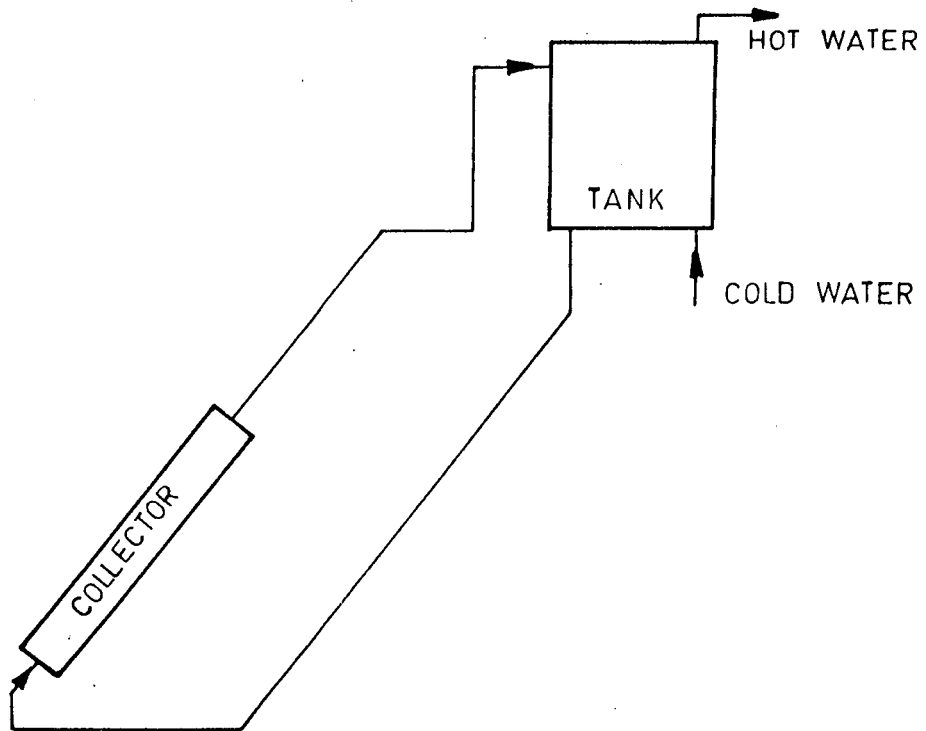


Fig.1.2 Schematic Diagram of a Single Loop Natural Circulation System

tank used as follows :

- 1 - Systems with a jacketed hot water storage tank
- 2 - Systems utilizing hot water storage tank with internal heat exchanger
- 3 - Systems without a heat exchanger (i.e., single loop systems).

In systems without a heat exchanger ; the domestic supply hot water itself circulates thru the collectors. This type of system is generally seen on the southern Mediterranean coast where temperatures below freezing are rarely observed throughout the winter months. In regions of strong winter conditions, systems of the first two categories are preferred. In practical applications an anti-freeze water solution is used for the thermosyphoning fluid in the solar collectors. This avoids danger of freeze damage to the collectors and piping. Systems in this category are the most commonly used systems in our country. Systems of the first two categories are called double loop solar hot water heating systems.

Once-through systems as shown schematically in Figures 1.3 and 1.4 have been proposed for use in China in place of thermosyphon systems due to some shortcomings of the natural circulation system as mentioned in (12). In a Once-through system the storage tank can be placed below the collector ; therefore the load on the roof of the building will be cut down significantly. These systems also have the advantages of no mixing of hot and cold water, no

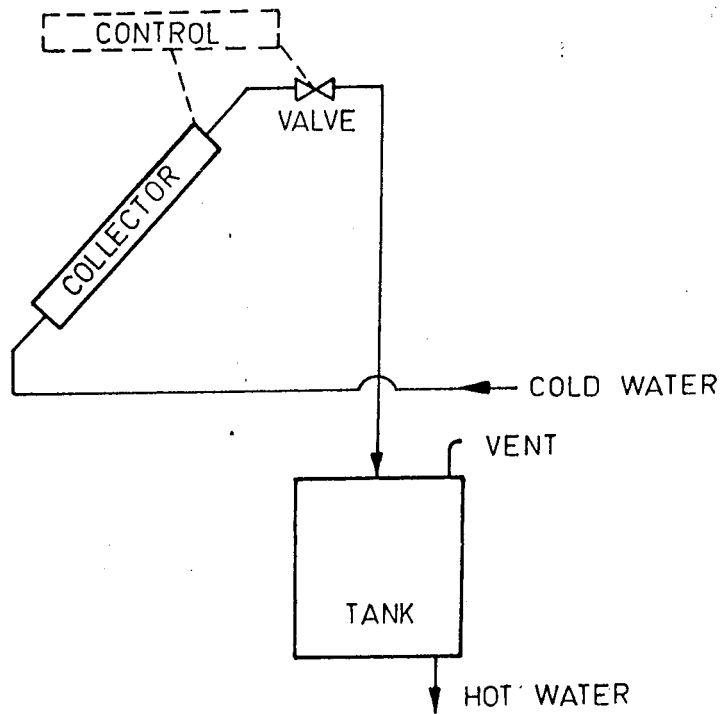


Fig.1.3 Schematic Diagram of a "Once-Through" System with Temperature Controlled Valve

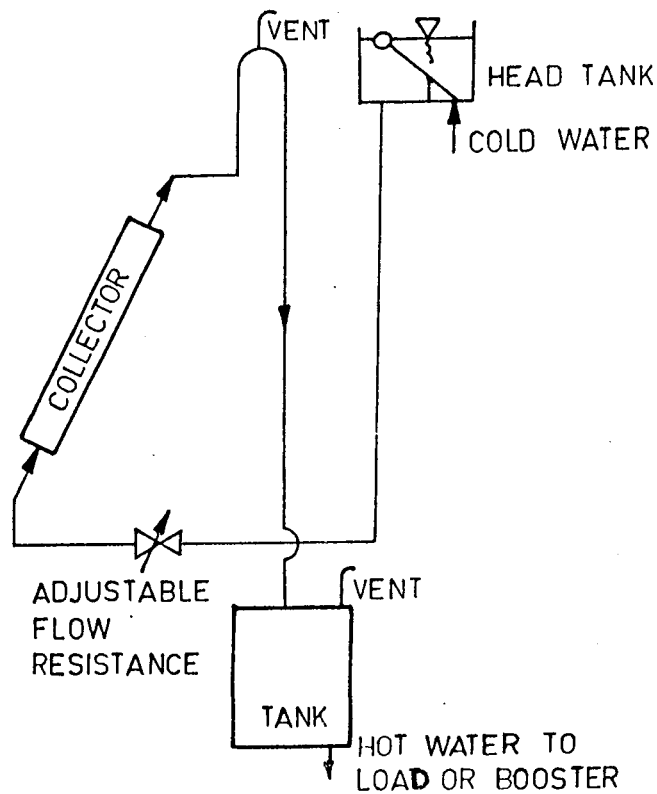


Fig.1.4 Schematic Diagram of a Self-Adjusting "Once-Through" System

reverse flow and capacity to provide hot water earlier in the day. According to Reference (12), the Once-through system performs worse in the morning but better in the afternoon as compared to the natural circulation systems. Under the same solar insolation conditions ; the difference of daily collector efficiency between these two systems has been noted to be negligible in (12).

The experimental and theoretical study in the present work utilizes the most commonly used double loop solar hot water heating system used in Turkey. This system is one consisting of two flat plate solar collectors and a jacketed hot water storage tank. The experiments are performed on a double loop hot water solar heating system which is manufactured and installed by " ÇİLTUĞ A.Ş " company located in Gaziantep. Double loop solar collector systems by other manufacturers in our country are of similar construction to that manufactured by " ÇİLTUĞ A.Ş. " and therefore results of the present study will be valid and are expected to apply to most of the existing thermosyphonic solar water heating systems in our country.

Design of the thermosyphonic loop and the establishment of an adequate thermosyphonic mass flow rate is critical in thermosyphonic solar water heating systems since malfunctioning in the circulation system can effect the system thermal efficiency drastically. The thermal and hydraulic characteristics of solar thermosyphon heating systems have been the subject of various theoretical and experimental investigations in the past. These previous

studies have been performed under solar heating of the collectors and consequently at unsteady state conditions. Additionally previous investigations have not accounted for the unequal flow rates in different collector risers. Information regarding the heat exchanger thermal characteristics of the double loop hot water storage tank is not available in the literature. The present analytical and experimental study is therefore aimed to investigate,

- 1- System performance under steady state conditions
- 2- The flow characteristics of the thermosyphon system taking into account the unequal flow rates in different collector risers
- 3- The thermal characteristics of the double loop jacketed hot water storage tank.

Firstly, experimental set up consisting of two solar water collectors connected in parallel to a jacketed hot water heat storage tank was fabricated at the ÇİLTUĞ A.Ş. workshop. Measurements were performed to evaluate the system performance experimentally. The mass flow rate within the system, the collector inlet-outlet temperature difference, the number of transfer units, NTU, the effectiveness, ϵ , and the overall heat transfer coefficient, U , of the jacketed hot water storage tank are determined experimentally.

A theoretical model was developed for the prediction of the thermosyphonic mass flow rate taking into account the unequal flow rates in different collector risers. The experimental results are compared with the predictions from the developed analytical model.

Chapter 2 includes review of the past literature on the subject. Chapter 3 includes description of the experimental set up, calibration of measuring instruments and experimental procedures. Chapter 4 includes the theoretical study for thermosyphonic mass flow rate estimation. Chapter 5 includes results and discussion. Conclusion is presented in Chapter 6. Recommendations for further study is given in Chapter 7.

CHAPTER 2

LITERATURE SURVEY

Thermosyphon solar water heaters have been in use since the beginning of the 20th century. Therefore single loop and double loop solar water heaters with natural circulation have been the subject of a large number of theoretical and experimental investigations during the last decades.

Close (1) developed a method for estimating the performance of solar water heaters with collector fluid circulating through a storage tank under the action of the thermosyphonic head. He studied a system with an unjacketed hot water storage tank. His analysis considers the case where heating is by solar energy and under unsteady conditions. Ideal conditions of no draw-off during the day and clear sunshine are assumed in his analysis. A single loop thermosyphoning solar heating system was tested experimentally and the results were compared with those estimated from his theoretical analysis. His results indicated that temperature increases across the collector of approximately 10°C are representative of well designed thermosyphon systems without serious flow restrictions.

Zvirin, Shitzer and Grossman (2) developed a theoretical method of solving the differential energy

equation and momentum equation to obtain the steady state temperature distributions and the flow rate for the thermosyphonic single loop solar water heater system consisting of a flat plate collector, a storage tank without jacket and connecting pipes. Their theoretical model was used to investigate the validity of the commonly used assumption of linear temperature distribution in the collector and the hot water storage tank. They did not consider the effect of unequal flow rates in different collector risers on system flow rate prediction.

Shitzer, Kalmanoviz, Zvirin and Grossman (3) tested a typical Israeli water heating system in thermosyphonic flow consisting of two flat plate collectors, a storage tank without jacket and connecting pipes. They measured the water temperature distributions along the collector tubes, the underside collector plate temperature profiles along the collector between adjacent tubes, and water flow rates in the system with a minimal amount of interference to the fluid flow by means of a specially designed flow meter. They also tested the validity of their analytical model (2) developed for the estimation of the water flow rate. They have performed their experiments under zero load conditions without any water consumption from the hot water heat storage tank throughout the day. Their measured results show that water flow rate in the system follows the pattern of daily solar insolation variation as expected. They found experimentally that the flow rate in their system increases during the morning hours, reaches a maximum of

about $950 \text{ cm}^3/\text{min}$. and then starts to decline in the afternoon hours. From their measurements it was estimated that the flow in the collectors are laminar throughout the day. In the connecting pipes the flow was also laminar for most of the day and transitional only around noon time.

Gupta and Garg (4) developed a computer model for predicting the thermal performance of domestic single loop thermosyphon solar water heaters. In their study the basic model previously presented by Close (1) was modified to take into account the system thermal capacity and the solar collector efficiency. Their analytical investigation included the effect of two different circulation pipe diameters, four different heights between the collector top and the tank bottom and three different ratios of tank dimensions (height / diameter-ratio) for a fixed tank volume. They also performed experiments on an experimental set up as described in their paper and compared the predicted results from their computer model with the experimental measurements. Their computer model and experimental investigation have been performed under no draw-off of hot water during the day, and under steady state conditions. In their study it was shown that inlet and outlet water temperatures of the collectors increase at nearly equal rates during the heat input period to the collectors.

Huang (5) developed a similarity theory for single loop solar water heating systems with natural circulation. In his model he divides the thermosyphonic solar system into

three components ; absorber plate, storage tank and connecting pipes. He developed two energy equations for the absorber plate and the storage tank together with a momentum equation for the entire flow system. These governing equations were then normalized resulting in ten dimensionless groups characterizing the performance of the thermosyphon collector system. Their similarity analysis yielded the important parameters for collector performance evaluation for collectors of arbitrary size. Thus he was able to present important design rules by means of the dimensionless parameters. His study indicates that the resistance to flow is the most important factor which should be carefully considered in the design of thermosyphonic solar collector systems. According to his results, low flow resistance would largely favor the collector performance by increasing the mean daily efficiency. Low flow resistance also allows for smaller solar collector-storage tank spacing and hence reduces structural cost. By studying the timewise variation of the temperature distribution in the tank, he also noted that flow mixing will occur near the top of the hot water storage tank. This reduces the system performance when the flow rate is low.

Ong (6) studied the performance of a single loop thermosyphonic solar water heating system theoretically by means of finite-difference formulation and also presented a solution procedure. The developed mathematical model follows closely the analyses of Close (1) and, Gupta and

Garg (4) . In accordance with Close (1) and, Gupta and Garg (4) he assumed that the mean temperatures of the absorber unit, the storage tank, the connecting piping as well as the mean temperature of the water contained inside the system are all equal. The difference between his model and those in references (1) and (4) lie mainly in the solution procedure and in the formulation for the collector plate efficiency factor. He also has performed experiments on the single loop thermosyphonic solar water heater consisting of a flat plate collector connected to a storage tank. Experimental mass flow rates were measured at half hour intervals while the temperature distribution of the system was monitored continuously. Some defects of his theory were noted which resulted from inaccurate assumptions for the mean temperatures of the various components of the system. These defects were noted to be significant only during the early and late periods of the day. Throughout the main insolation period, satisfactory qualitative and quantitative agreement was obtained between experimental and theoretical results.

Ong (7) developed an improved theoretical model to predict the thermal performance of a single loop natural recirculation solar water heating system. The model considers the entire system to be broken up into a finite number of sections and each individual section is assigned a temperature representing the mean temperature of that section. Finite-difference equations were written by applying an energy balance over each section. Solution of the finite difference equations

were presented yielding the temperatures for each section. The mass flow rate was evaluated from the temperature distribution of the whole system. He also performed experimental measurements on a single loop thermosyphonic solar water heater consisting of a flat plate collector connected to a storage tank. The experimental results presented showed that the mean collector plate temperature, the average water temperature in the storage tank and the mean water temperature in the collector tubes are not equal. Furthermore the tank temperature distribution was non linear. These results are contrary to the previous theoretical assumptions consisting of the equality in the mean temperatures within the system and the assumption of linear temperature distribution within the hot water storage tank.

Mertol, Place, Webster and Grief (8) developed an analytical detailed loop model (DLM) analysis to analyze the performance of the double loop solar thermosyphon water heaters. Their model was used to study the effect of the double loop shell and tube type heat exchanger characteristics, different heat transfer fluids, system flow resistances, tank thermal stratification and tank to collector elevation difference on system performance. Their results indicate that acceptable system performance can be attained in double-loop systems in comparison to thermosyphon systems without a heat exchanger.

De Winter (9) derived an expression which accounts for reduction in system efficiency resulting from the use

of a shell and tube heat exchanger in a double loop solar water heating system. Addition of antifreeze fluid to collector side fluid is usually practiced in double loop systems to prevent freezing within the collector loop and to avoid corrosion of metal parts. The presence of the heat exchanger forces the collector to operate at a higher temperature with a corresponding decrease in system thermal efficiency.

Orlando, Goldstein and Magnoli (10) designed and built a double loop thermosyphon solar water heater and measured its performance under different operating conditions. In their study heat exchanger design was found to be critical to the technical and economic performance of the thermosyphon solar water heater. The influence of the double loop heat exchanger was analysed in terms of the coefficient of performance, COP defined as the ratio of the useful solar energy from a double loop thermosyphon solar collector system to the useful solar energy from an identical size single loop thermosyphon solar collector system. They found that the COP is smaller for higher hot water temperatures. They found better double loop thermosyphon system efficiencies for larger ratios of heat exchanger surface to collector surface area.

Dutre, Cypers, Berghmans and Debosscher (11) developed a dynamic model describing the behaviour of a thermosyphon loop consisting of a number of solar collectors and a water tank placed above the collectors. Their study presents a mathematical model to simulate the time dependent behaviour

of double loop thermosyphon systems taking into account the temperature dependence of the fluid thermophysical properties and the time dependent meteorological data. The system considered in their study consists of a small array of collectors connected in parallel to a hot water tank with an internal heat exchanger. In their model the thermosyphon loop is segmented and the transient mass conservation, momentum and energy equations are written for each segment. The solutions of their equations are obtained numerically. They also tested a double loop thermosyphon system described in their paper which was physically compatible with their theoretical model. The mean storage tank temperature, inlet and exit temperatures of the heat exchanger, the ambient temperature and incident solar radiation on the collectors were measured experimentally. They showed that their model predicts well the dynamic behaviour of double loop system theoretically. The fast fluctuations of the solar radiation insolation resulted in rapid changes of the heat exchanger inlet and exit temperatures which were observed both theoretically and experimentally.

CHAPTER 3

EXPERIMENTAL STUDY

3.0 INTRODUCTION

The purpose of the experimental study is to measure the thermosyphonic mass flow rate in a double loop thermosyphonic solar water heating system and to determine the U-value of the jacketed hot water storage tank at steady state conditions. The experiments are carried out on a set up consisting of two flat plate solar collectors and a jacketed hot water storage tank. The solar collectors were electrically heated in order to obtain controlled steady-state conditions.

3.1 DESCRIPTION OF THE EXPERIMENTAL SET UP

The experiments are performed on the double-loop solar hot water heating system manufactured by ÇİLTUĞ A.Ş. The system consists of two 1.8 sq. m flat plate solar collectors, a jacketed hot water heat storage tank and the connecting pipes. A schematic diagram of the test set up is shown in Figure 3.1. The photographs of the test set up installation are shown in Figures 3.2 and 3.3 respectively.

The collectors are connected parallel and are made of two 1" pipe size headers and eight risers of 1/2" pipe size.

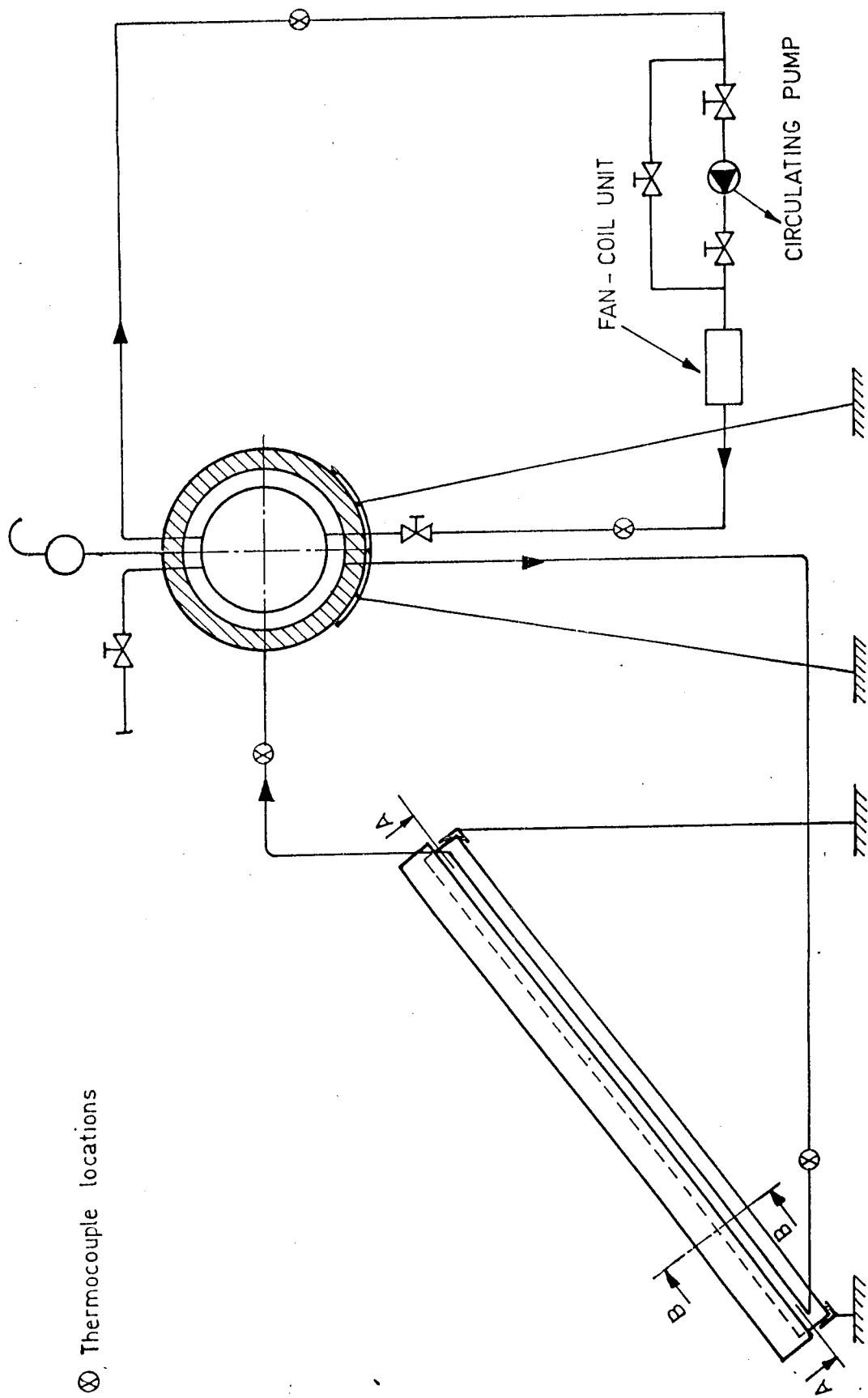


Fig.3.1 Schematic of the Experimental Set-Up

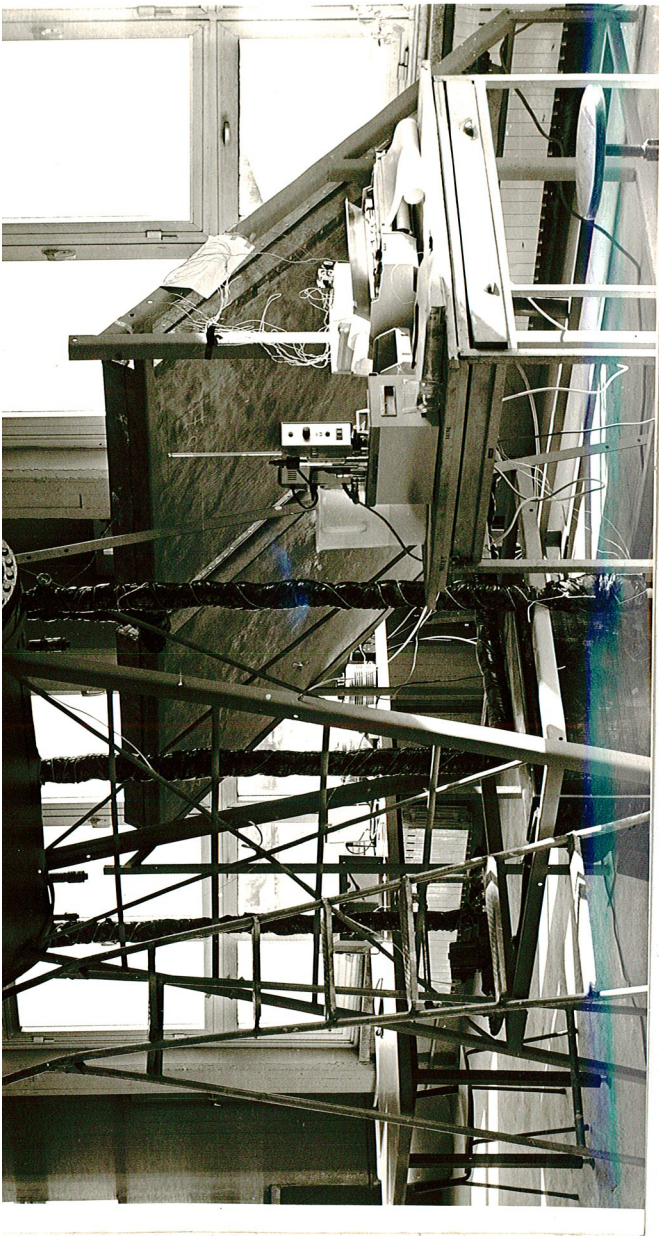


Fig. 3.2 Side View from the Experimental Set-Up

All measuring devices were calibrated and tested separately before the beginning of the experiment. All thermocouple junctions were calibrated with reference to a calibrated precision thermometer.

The heat to the collectors was supplied by means of an electrical resistance circuit mounted on the inner side of the insulated covers of the collectors. The set up consisted of the following units,

1 - Heat Supply Unit : A servo-motor controlled voltage regulator was used to provide a constant voltage source of 220 Volts to the system. An attempt was made to control the heat input by a triac triggering circuit described in Appendix 1. But it was not possible to supply a steady controlled power to the heating resistances by this circuit because of the unsteady and unpredictable behaviour of this triac circuit. This circuit was then replaced by two variacs controlling the voltages on the resistances on the two solar collectors. The electrical heating resistance wires were installed inside the collector cover in an arrangement to supply equal heat input to each of the risers of the collector.

2 - The Solar Collectors Unit : The solar collectors of identical construction were used. The collectors were covered by thermally insulated covers. The technical details of the collectors are given in Table 1.

Table 1. Technical Data for the Collectors Unit

<u>COMPONENT</u>	<u>DESCRIPTION</u>
COLLECTORS	
- Water flow pipes(risers)	- 8 parallel 16 mm I.D.(1/2") commercial steel pipe: 1821 mm long
- Supply and drain headers	- 27.2 mm I.D.(1") commercial steel pipe: 1075 mm long
- Insulation	- 50 mm glass wool
- Fins on risers (Collector plate)	- 1000 x 1800 x 1 mm galvanized steel plate
- Casing	- 0.5 mm thick galvanized sheet steel plate
COLLECTOR COVER	
- Heat supply	- By electrical heating resistance wires, 20 Ohm electrical resistance
- Insulation	- 50 mm glass wool
- Casing	- 0.5 mm thick galvanized sheet steel plate
CONNECTING PIPES	- 21.6 mm I.D.(3/4") commercial steel pipe insulated by 30 mm thick glass wool

3 - Hot Water Heat Storage Tank-Heat Exchanger Unit:

This is a standard double walled hot water tank with a removable flat circular cover on one end. The tank was insulated by 60 mm thick glass wool and enclosed by a 0.5 mm thick galvanized sheet steel casing. The unit has 200 liters water storage capacity. A technical drawing of the tank is

shown in Figure 3.4. The description of this unit is given in Table 2.

Table 2. Technical Data for the Hot Water Heat Storage Tank-Heat Exchanger Unit

COMPONENT	DESCRIPTION
HOT WATER TANK	<ul style="list-style-type: none"> - Cylindrical pressure tank with convex ends - Outside dimensions: 400 X 1715 mm - Material: 4 mm thick steel - Corrosion protection : Inside surface is painted
JACKET	<ul style="list-style-type: none"> - Fluid volume: 41 liters - Heat transfer area: 1.45 m²

- 4 - Heat Rejecting Unit: This unit mainly consists of
- Water circulating pump, Capacity: 2.4 m WG, 2m³/h
 - Heat rejecting fan-coil, Capacity: 13000 K cal/h.

3.2 EXPERIMENTAL MEASUREMENTS

The valve at the storage tank cold water inlet side was used to regulate the mass flow rate through the heat rejecting fan-coil unit to obtain steady state conditions. It was observed in the experiments that low mass flow rates are necessary to obtain steady conditions in the storage tank. High mass flow rates through the storage tank resulted in water surges and unstable operating conditions inside the storage tank eliminating the possibility of reaching true steady state hydraulic and thermal conditions in the system. All measurements were obtained at steady-state conditions.

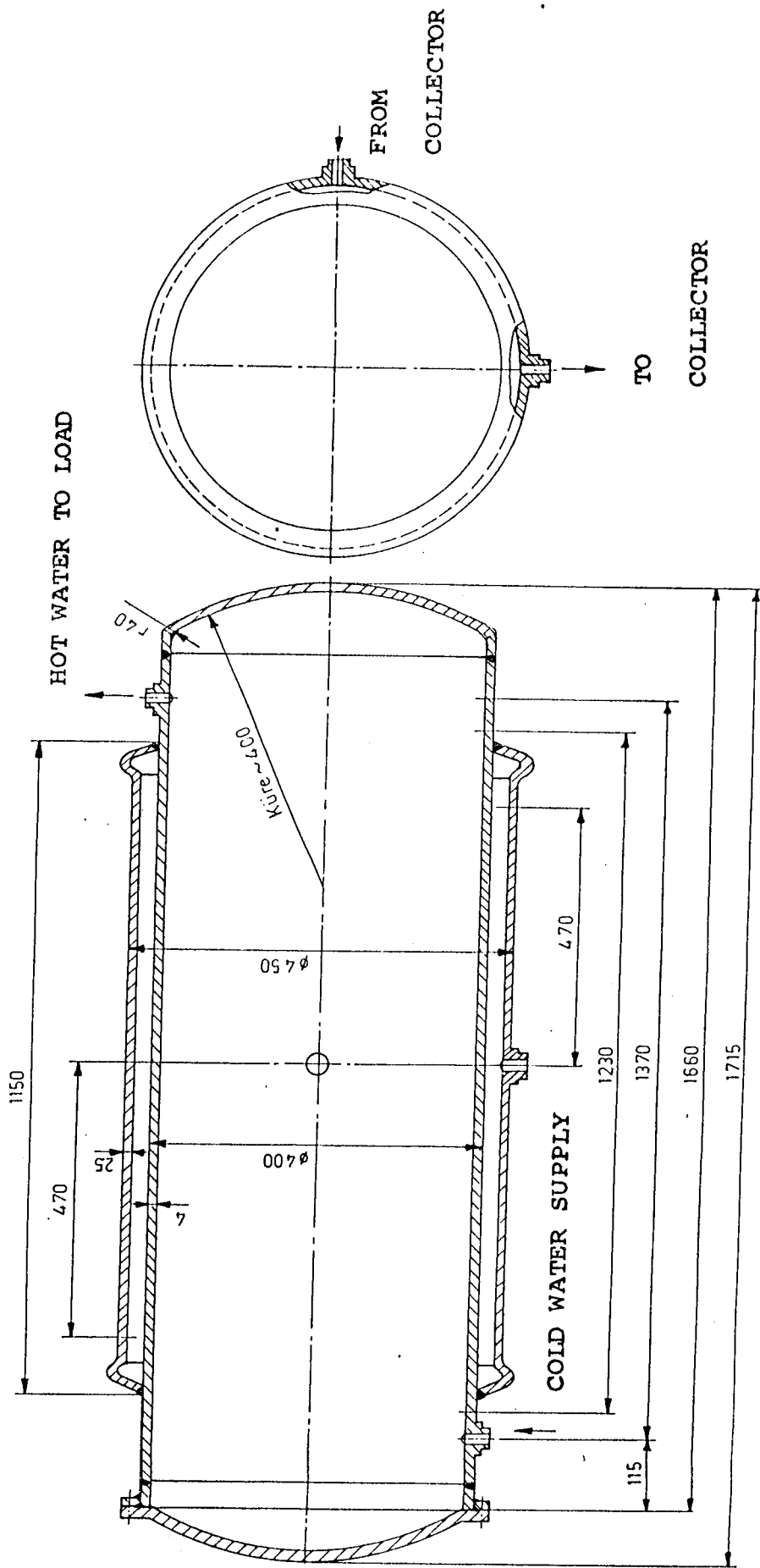


Fig.3.4 Hot Water Heat Storage Tank-Heat Exchanger

3.2.1 Calibration of the Temperature Recording System

A thermometer was calibrated which was then used to calibrate the channels of the temperature recorder.

1 - Calibration of the Thermometer: The thermometer was immersed into a mixture of crushed ice and water bath. After sufficient time the temperature of the bath was read as 0°C on the thermometer. The same thermometer was immersed in boiling water, after sufficient time the temperature reading was noted to reach steady-state and the boiling point of water was read as 98.2°C . The atmospheric pressure was measured by a mercury barometer as 685 mm Hg. This pressure reading was used to find the boiling temperature of water as 96.8°C from the saturated steam tables. The thermometer reading of 98.2°C was then taken as 96.8°C and a proportional correction was applied when calibrating the recorder channels with this thermometer. The calibration curve is shown in Figure 3.5.

2 - Calibration of the Recorder Channels: Each channel of the temperature recorder was calibrated for the $0 - 50^{\circ}\text{C}$ temperature range by using a constant temperature bath, the calibration thermometer and the 0°C reference point (crushed ice-water mixture). The calibration curves of the channels are shown in Figure 3.6, 3.7, 3.8, and 3.9. Following calibration, all thermocouple junctions were tested separately at the ice point (0°C) by using the ice bath and at 50°C temperature by using the calibration thermometer and a constant temperature bath. It was noted that all junctions gave 0°C

measurement at the ice point. The measurement at 50°C from the thermocouples showed a maximum deviation of $\pm 0.2^\circ\text{C}$.

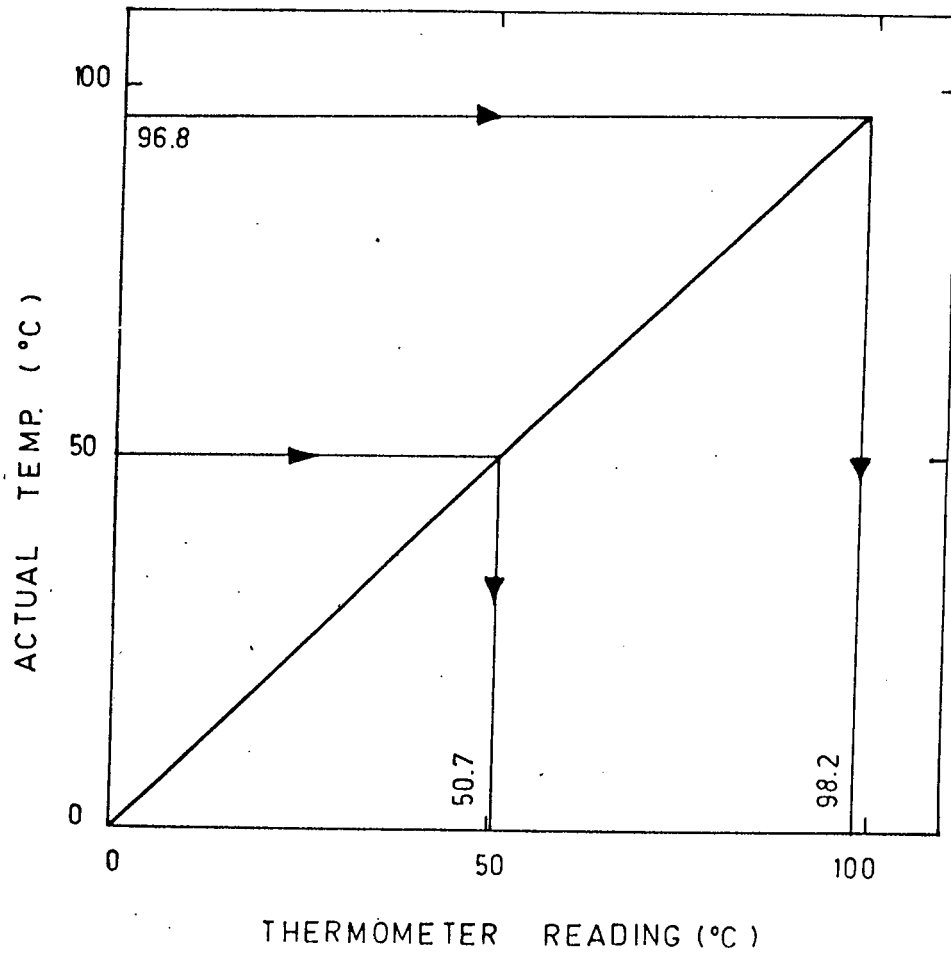
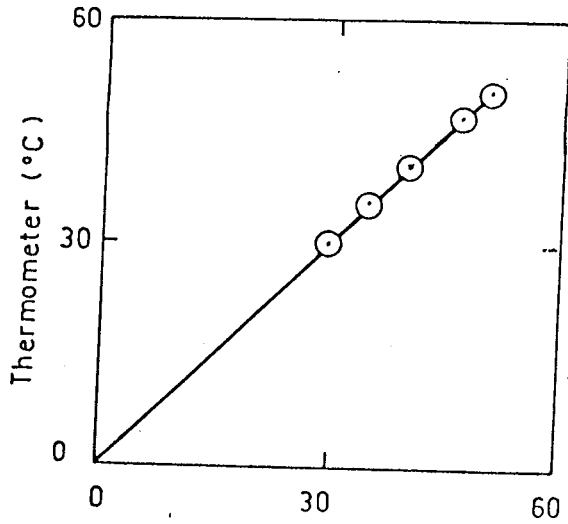
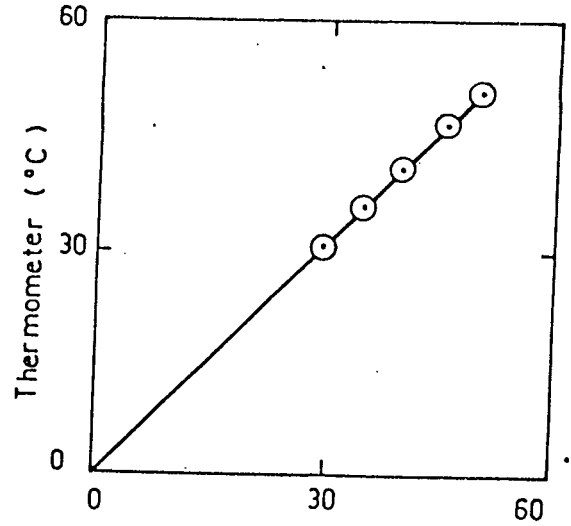


Fig.3.5 Calibration of Thermometer



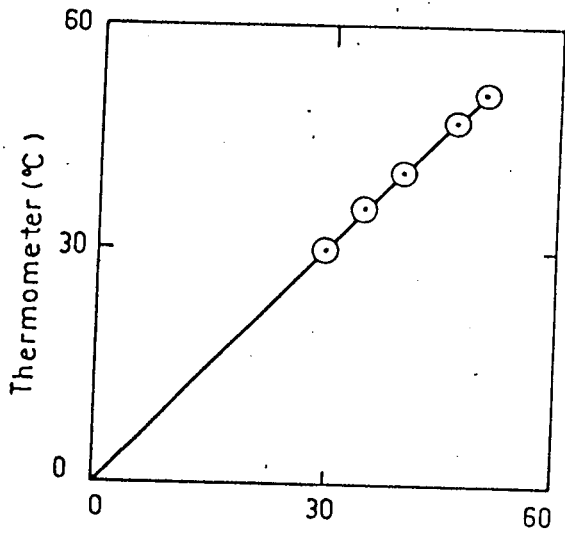
Channel no:1,(°C)

Fig.3.6 Calibration of Channel no.1



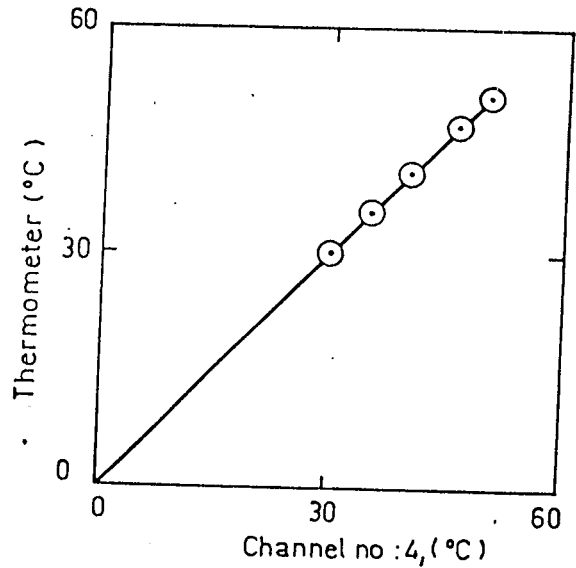
Channel no:2,(°C)

Fig.3.7 Calibration of Channel no.2



Channel no:3,(°C)

Fig.3.8 Calibration of Channel no.3



Channel no:4,(°C)

Fig.3.9 Calibration of Channel no.4

3.2.2 Description of the Temperature Recording System

The temperature recording system consists of a temperature recorder with four channels and an insulated thermos bottle filled with a mixture of crushed ice and water. The water-ice mixture is used for the reference junction corresponding to 0 celcius degrees. Copper-Constantan thermocouples of 0.3 mm diameter were used in the experimental measurements. The thermocouple junctions were all properly insulated against electrical contact with the metal parts of the experimental set up.

Four thermocouple measuring junctions were located at the collector inlet, the collector exit, the storage tank inlet and the storage exit. Eight additional thermocouple measuring junctions were placed at the top of the risers of one of the collectors (right collector). The following temperature measurements were made after the system has reached a steady state operating condition,

1 - Storage tank inlet temperature by channel no:1 of the temperature recorder

2 - Storage tank inlet to exit temperature difference by channel no:2 of the temperature recorder

3 - Collector inlet to exit temperature difference by channel no:3 of the recorder

4 - The temperature difference between the top side of each riser and the storage tank inlet by channel no:4 of the temperature recorder. The temperature difference between

the collector inlet and the storage tank inlet was also recorded by channel no:4 of the temperature recorder. A 16 contact switch was used for this purpose. These measurements were done only on one of the collectors.

5 - The inside air temperature was measured by the calibration thermometer.

The measurements were repeated 6 times at different heat input rates to the collectors. Before each measurement, the calibrations of the recorder channels were controlled.

3.2.3 Measurement of Heat Input Rate to the Collector

The heat input to the collectors were supplied by two parallel connected electrical heating resistances. Two variacs were used to regulate voltage on the electrical heating resistances. The heat input rate to the collector was determined by recording the current through the resistances and voltage across the resistances. Two ampermeters were used to measure the rms values of the current. The rms voltage across the resistances were measured by a Fluke brand digital multimeter. The rms voltage across the resistances and the rms value of the current flowing through the resistance wires were recorded for each experiment.

The heat input rate to the collector was calculated for each set of measurements made at steady state conditions from the following formula,

$$Q_C = I_{rms} \cdot V_{rms} \quad (3.1)$$

3.2.4 Determination of Thermosyphonic Mass Flow Rate

The experimental thermosyphonic mass flow rate through collectors was determined from the following formula,

$$m = Q_{uc} / c_p(T_2 - T_1) \quad (3.2)$$

where,

$T_2 - T_1$ is the temperature difference between the inlet and exit of the collector.

The fluid constant pressure specific heat, c_p , was evaluated at the average of the inlet and exit water temperatures of the collector.

3.2.5 Determination of the Overall Heat Transfer Coefficient, Number of Transfer Units and Effectiveness of the Storage Tank-Heat Exchanger

The theoretical expressions for a double pipe counter flow heat exchanger were used when estimating the heat exchanger characteristics for the jacketed hot water storage tank. The log-mean temperature difference analysis and effectiveness-NTU analysis for a counter flow heat exchanger are available in text books on heat transfer and the formulas presented below are taken from Reference (14).

1 - Experimental Evaluation of the Overall Heat Transfer Coefficient:

The following formulas were used to determine the overall heat transfer coefficient, U , of the jacketed hot water storage tank.

$$\Delta T_m = \frac{(T_{h_2} - T_{c_2}) - (T_{h_1} - T_{c_1})}{\ln \left(\frac{T_{h_2} - T_{c_2}}{T_{h_1} - T_{c_1}} \right)} \quad (3.3)$$

$$U = \frac{Q_{ut}}{A_j \cdot \Delta T_m} \quad (3.4)$$

2 - Experimental Estimation of the NTU and Effectiveness:

The following formulas were used to determine the number of transfer units, NTU, and the effectiveness of the jacketed hot water storage tank, ϵ :

$$C_h = m \cdot c_p \quad (3.6)$$

$$C_c = m_t \cdot c_p \quad (3.7)$$

If $C_h \leq C_c$; $C_{min} = C_h$ and $C_{max} = C_c$. For this case :

$$\epsilon = \frac{T_{hi} - T_{he}}{T_{hi} - T_{ci}} \quad (3.8)$$

If $C_c \leq C_h$; $C_{\min} = C_c$ and $C_{\max} = C_h$. For this case :

$$\epsilon = \frac{T_{ce} - T_{ci}}{T_{hi} - T_{ci}} \quad (3.9)$$

$$C = \frac{C_{\min}}{C_{\max}} \quad (3.10)$$

$$NTU = \frac{U \cdot A_j}{C_{\min}} \quad (3.11)$$

CHAPTER 4

THEORETICAL ANALYSIS

The aim of the present theoretical study is to develop a mathematical model to predict the thermosyphonic mass flow rate, the temperature difference between the inlet and exit of the collector panel and the total thermosyphonic head loss of the double loop thermosyphon solar water heating system as a function of the thermosyphonic solar heating system parameters.

The system under study is shown schematically in Figure 4.1. It consists of two flat plate solar collectors, a jacketed hot water heat storage tank and the connecting pipes. The mechanical energy equation is applied to the closed thermosyphonic loop to relate head loss to the thermosyphonic thermostatic head. Physical properties of the circulating fluid such as mass density, kinematic viscosity are evaluated at the average operating temperature of the system and heat losses from the hot and cold sides of the insulated connecting pipes are neglected.

The head losses through pipes and fittings are estimated by the Darcy-Weisbach head loss equation. The system mass flow rate is obtained from the solution of an equation obtained by balancing the system total head loss to the thermostatic head of the thermosyphonic cycle.

Results of the theoretical analyses are applied to the particular thermosyphonic solar water heating system studied experimentally and can also be applied to other thermosyphonic double loop solar water heating systems.

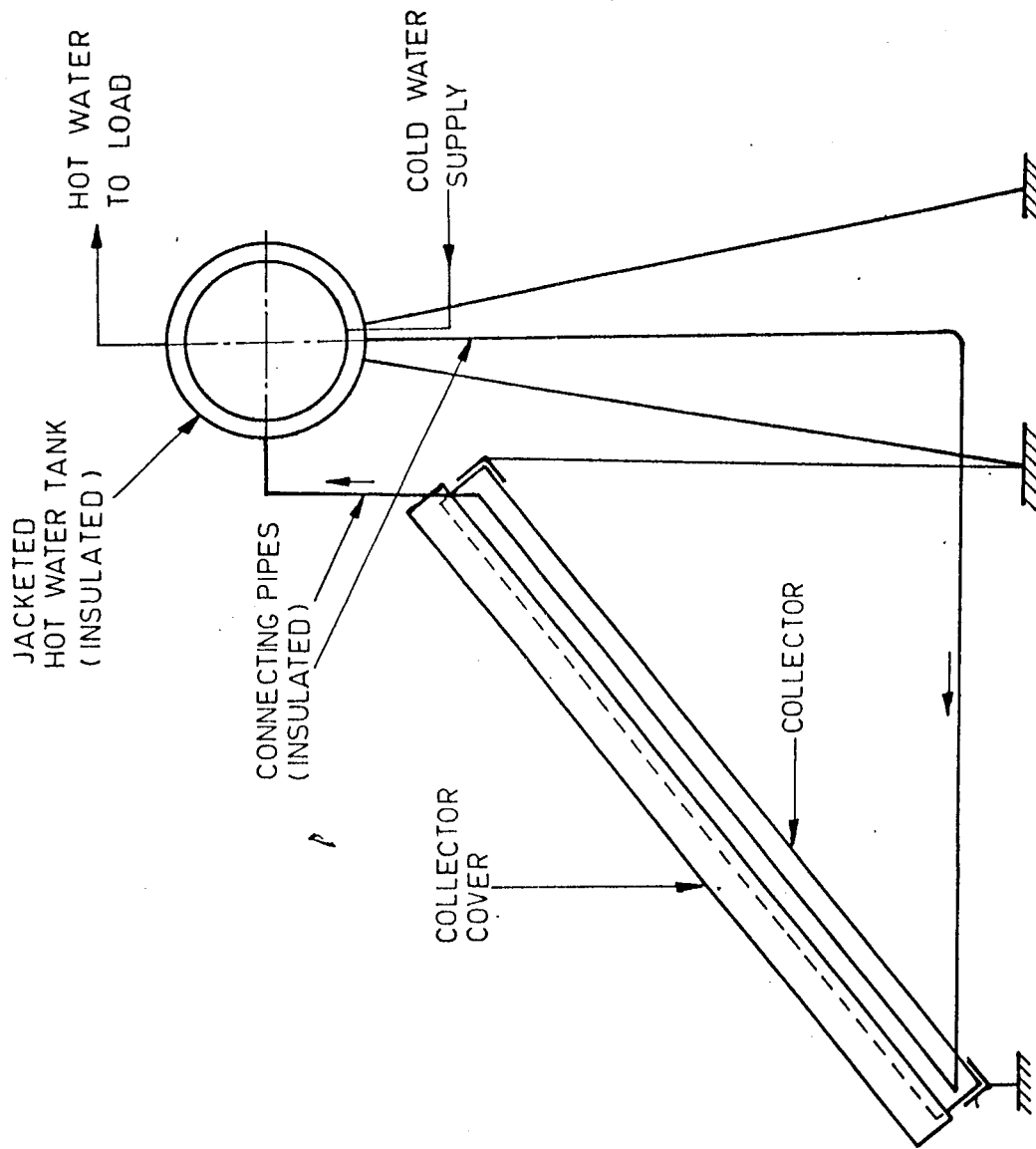


Fig.4.1 Schematic Diagram of a Double Loop Thermosyphon System

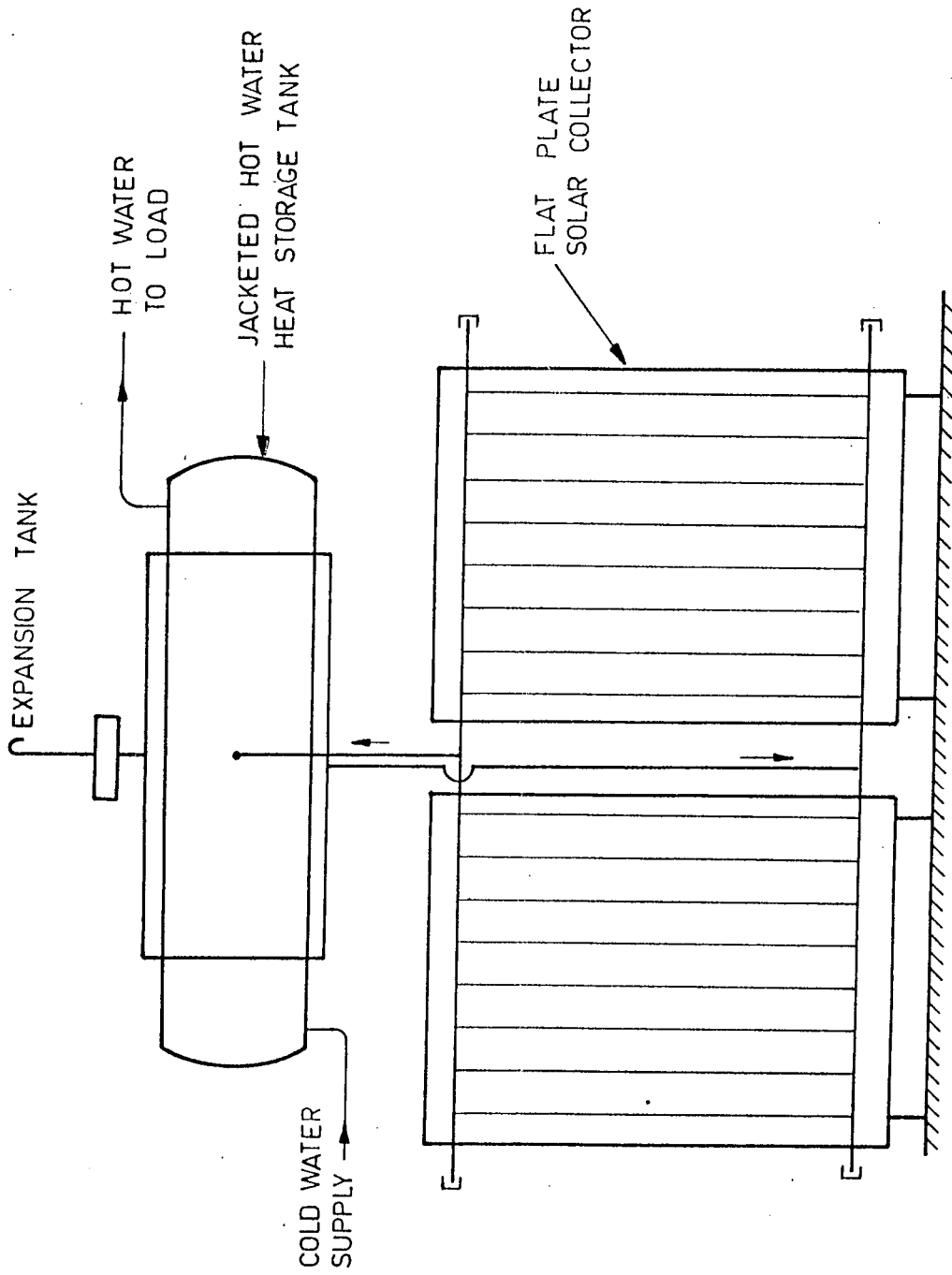


Fig.4.1 (Continued), Front View

4.1 ANALYSIS OF THE THERMOSYPHONIC CYCLE BY THE APPLICATION OF THE MECHANICAL ENERGY EQUATION

The mechanical energy equation (Bernoulli equation) is used to predict the flow in the thermosyphonic cycle. Application of mechanical energy equation to an infinitesimal section of the loop of length dz yields :

$$dh_f = dP + \frac{\rho v dv}{g_c} + \frac{\rho g dz}{g_c} \quad (4.1)$$

Here, dh_f is the head loss in the pipe section of length dz . The mass flow rates and velocities in the thermosyphon loop are small and velocity pressure is neglected. Integration of equation (4.1) over a closed loop of the thermosyphonic cycle yields the following expression :

$$h_f = \oint \rho g dz \quad (4.2)$$

The variation of density with temperature is written as :

$$\rho - \rho_0 = \rho_0 \beta (T_0 - T) \quad (4.3)$$

Substitution of equation (4.3) into equation (4.2) yields :

$$h_f = \rho_0 g \oint (1 - \beta (T - T_0)) dz \quad (4.4)$$

Here ρ_0 is reference density corresponding to the mean temperature of the thermosyphonic cycle. Equation (4.4) is

integrated by taking the temperature to be constant on the hot and cold sides of the loop and assuming a linear temperature variation inside the solar collector and the jacketed hot water storage tank. Integration of equation (4.4) in the gravity direction over a closed cycle of the system schematically shown in Figure 4.2 by taking the gravity direction as positive yields :

$$\begin{aligned}
 h_f = & \rho_0 g (1 - \beta (T_1 - T_0)) L_1 \sin \theta_1 + \\
 & \rho_0 g (1 - \beta (T_1 - T_0)) L_2 \sin \theta_2 + \\
 & \rho_0 g (1 - \beta ((T_1 + T_2) / 2 - T_0)) L_3 \sin \theta_3 + \\
 & \rho_0 g (1 - \beta (T_2 - T_0)) L_4 \sin \theta_4 + \\
 & \rho_0 g (1 - \beta (T_2 - T_0)) L_5 \sin \theta_5 + \\
 & \rho_0 g (1 - \beta ((T_1 + T_2) / 2 - T_0)) L_6 \sin \theta_6 \quad (4.5)
 \end{aligned}$$

where,

$$\begin{aligned}
 \theta_1 = 90^\circ, \theta_2 = 180^\circ, \theta_3 = -37.1^\circ \\
 \theta_4 = -90^\circ, \theta_5 = 0^\circ, \theta_6 = 90^\circ
 \end{aligned}$$

Taking $T_0 = (T_1 + T_2) / 2$, equation (4.5) reduces to the following form :

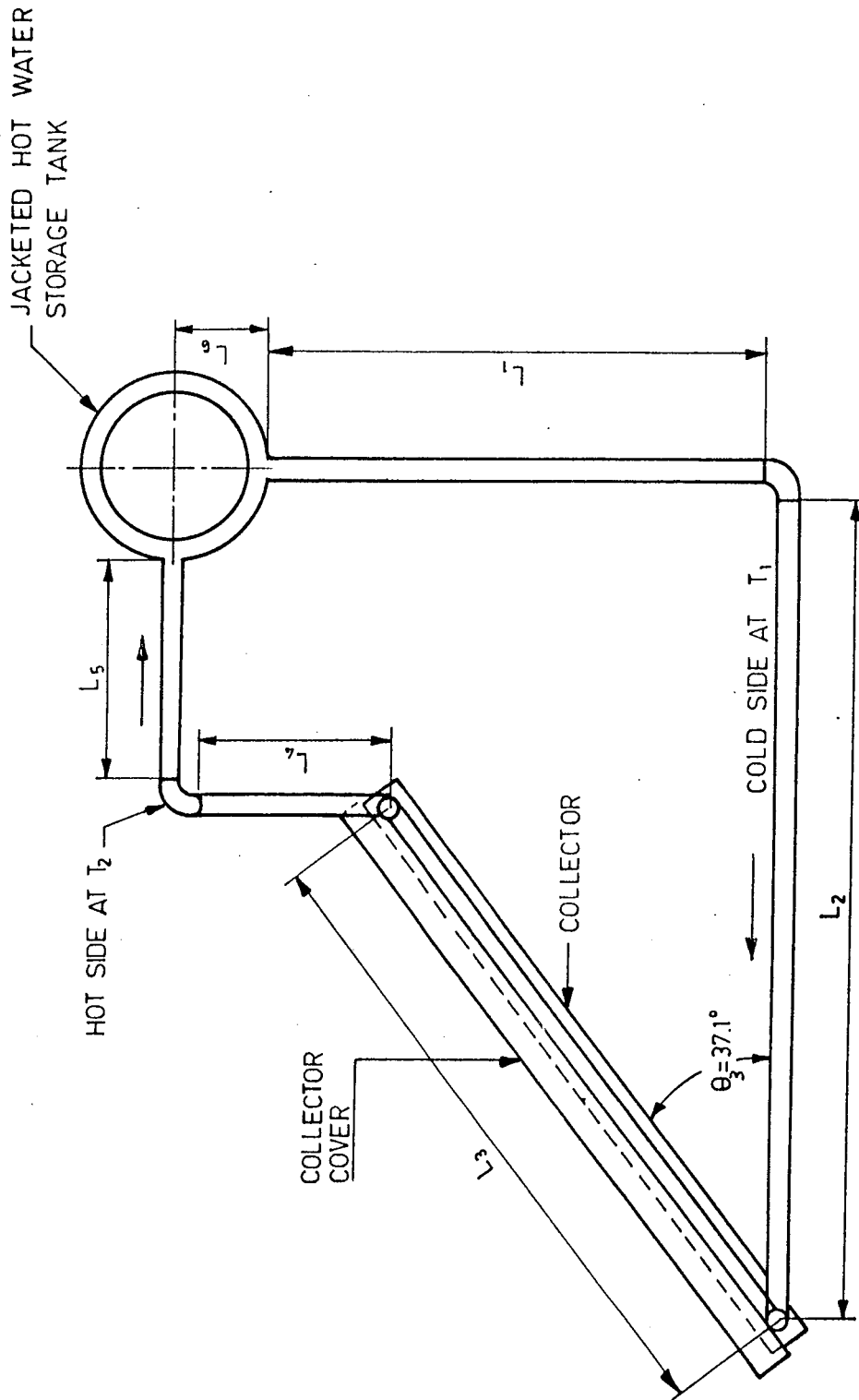


Fig.4.2 Double Loop Thermosyphon Solar Water Heating System

$$h_f = \rho_o g ((L_1 - L_3 \sin \theta_3 - L_4 + L_6) + (1/2) \beta (T_2 - T_1)(L_1 + L_4)) \quad (4.6)$$

Noting that $L_1 - L_3 \sin \theta_3 - L_4 + L_6 = 0$, equation (4.6) simplifies into,

$$h_f = (1/2) \rho_o g \beta (L_1 + L_4)(T_2 - T_1) \quad (4.7)$$

Letting $C_o = (1/2) \rho_o g \beta (L_1 + L_4)$, and $C_1 = C_o / (\rho_o g)$, the following final expression is obtained,

$$h_L = C_1(T_2 - T_1) \quad (4.8)$$

4.2 MASS FLOW RATE AND HEAD LOSS RELATIONSHIP FOR LAMINAR FLOW INSIDE PIPES

For incompressible flow in pipes the head loss is expressed by,

$$h_L = f(L / D) \cdot (V^2 / 2g) \quad (4.9)$$

The unit for head loss, h_L , is meters-height of the fluid flowing inside the pipe. The friction factor is a function of the Reynolds number and the relative roughness e / D of the pipe in the transition regime. It is a function of only the Reynolds number in the laminar flow regime.

The friction factor is a function of only relative roughness in the complete turbulence (fully rough flow) regime.

The flow inside the pipe in the closed loop thermosyphon cycle shown schematically in Figure 4.2 is assumed to be steady and laminar. In laminar tube flow the friction factor is given by,

$$f = 64 / Re \quad (4.10)$$

Reynolds number may be written in terms of mass flow rate as follows,

$$Re = 4 m / (\pi \mu D) \quad (4.11)$$

Substitution of equation (4.11) into equation (4.10) yields,

$$f = 64 \pi \mu D / (4 m) \quad (4.12)$$

The average fluid velocity may be written in terms of mass flow rate as follows,

$$V = 4 m / (\pi \rho D^2) \quad (4.13)$$

Substitution of equation (4.12) and equation (4.13) into equation (4.9) gives,

$$h_L = 128 \sqrt{L} m / (\pi \rho g D^4) \quad (4.14)$$

Pipe fittings losses are accounted for by us of a resistance coefficient, K_r , as follows,

$$h_L = K_r V^2 / (2g) \quad (4.15)$$

Comparing equation (4.15) with equation (4.9) it is seen that,

$$K_r = f (L / D) \quad (4.16)$$

L is considered as the equivalent length of straight pipe that will cause the same pressure drop as a flow fitting. The values of ($\alpha = L / D$) are given for different flow fittings in reference (20) as follows,

1 - For standard Tees

- | | |
|-------------------------------------|-----------------|
| i. Separation - thru flow | $\alpha_1 = 20$ |
| ii. Separation - branch flow | $\alpha_2 = 60$ |
| iii. Union - thru flow, branch flow | $\alpha_3 = 40$ |

2 - For standard 90° Elbows $\alpha_4 = 30$

3 - For pipe exit flow; projecting type,

$$K_r = 1, \text{ or } \alpha = f^{-1}$$

4 - For pipe entrance flow; Inward projecting type,

$$K_r = 0.78 \text{ or } \alpha = 0.78 f^{-1}$$

Utilization of equation (4.14) yields the following expressions :

1 - For flow through pipes,

$$h_L = 128 \sqrt{L} m / (\pi \rho g D^4) \quad (4.17)$$

2 - For flow through Tees and Elbows,

$$h_L = 128 \sqrt{\alpha} m / (\pi \rho g D^3) \quad (4.18)$$

3 - For pipe exit flow; projecting type,

$$h_L = 8 m^2 / (\pi^2 \rho^2 g D^4) \quad (4.19)$$

4 - For pipe entrance flow; Inward projecting type,

$$h_L = 6,24 m^2 / (\pi^2 \rho^2 g D^4) \quad (4.20)$$

4.3 THEORETICAL ESTIMATION OF UNEQUAL FLOW RATES IN DIFFERENT COLLECTOR RISERS

The previous investigations of flow inside the thermosyphon solar water heating system are generally based on the assumption of equal fluid mass flow rates through the risers of the collector . In practice, however, the fluid mass flow rates through different risers will not be equal. Therefore an investigation of the effect of these

unequal flow rates on the system performance is considered in the present study. A theoretical method of mass flow rate estimation is developed for a tubular liquid flat plate collector with fluid inlet and exit ports located at the same side of the collector. The present method takes into account the unequal mass flow rates in different collector risers and permits prediction of riser mass flow rates.

Fluid flow in the network shown schematically in Figure 4.3 may consist of,

- 1 - Laminar flow only
- 2 - Laminar and transitional flows
- 3 - Laminar, transitional and turbulent flows
- 4 - Transitional and turbulent flows
- 5 - Turbulent flow only

Laminar flow is the dominant flow pattern in thermosyphon solar water heating systems because the gravity induced flow head is quite small compared to flow heads in pumped flow systems. Therefore the theoretical analysis will be restricted to a study of laminar flow only. It is of convenience to express the head loss for laminar flow in the following form,

$$H = \pi \rho g h_L / (128 \nu) \quad (4.21)$$

$$H = K m \quad (4.22)$$

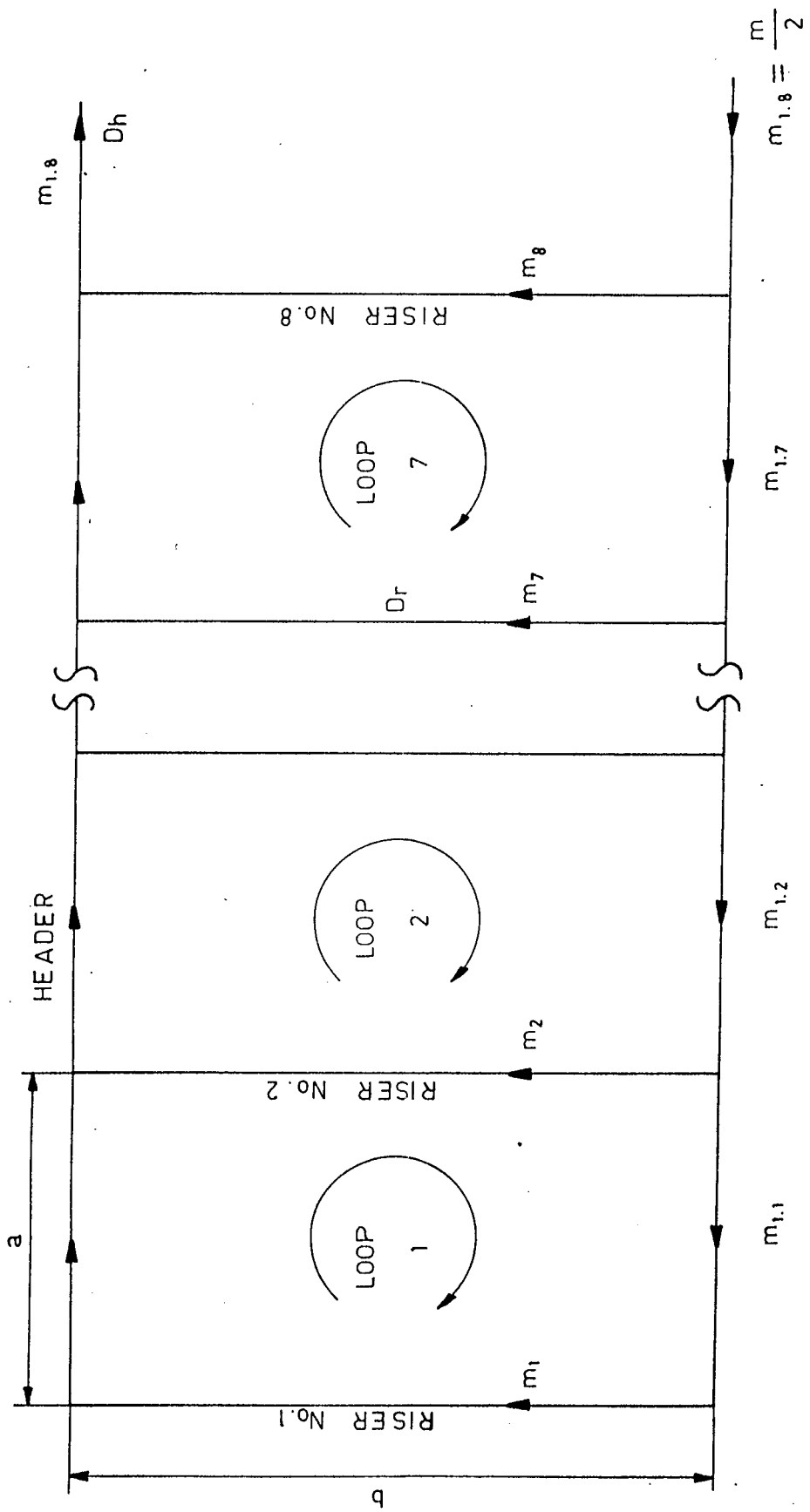


Fig.4.3 Schematic of Flow Net-Work in Collector Risers

where,

$$K = L / D^4 \quad \text{for pipes}$$

$$K = \alpha / D^3 \quad \text{for fittings}$$

The collector network shown schematically in Figure 4.3 is analysed as outlined below,

1 - Analysis for riser no.1 : The flow through riser no.1 is shown schematically below,

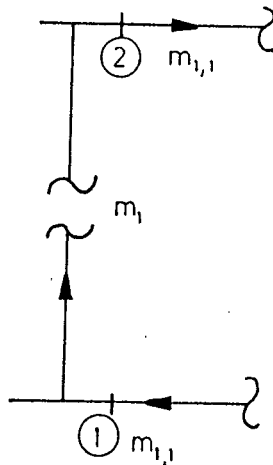


Fig.4.4 Flow Through Riser no.1

This flow includes the following flow resistances,

- One Tee-branch flow (separation)
- One riser flow
- One Tee-branch flow (union)

The head loss between point 1 and 2 is expressed by,

$$H_1 = K_1 m_{1,1} \quad (4.23)$$

where,

$$K_1 = \alpha_2 / D_h^3 + b / D_r^4 + \alpha_3 / D_r^3$$

$$m_{1,1} = m_1 \quad (4.24)$$

$$H_1 = \pi \rho g h_{L_1} / (128 V) \quad (4.25)$$

2 - Analysis for loop no.1 : The flow through loop no.1 is shown schematically below,

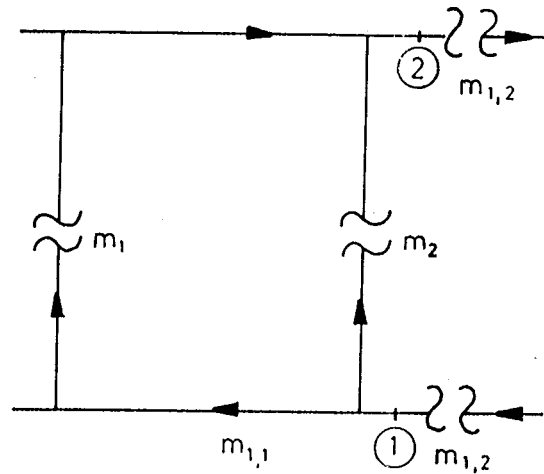


Fig.4.5 Flow Through Loop no.1

This loop includes the following flow resistances,

- i. Flow through riser no.1,
 - One Tee-thru flow (separation)
 - One header flow
 - Flow through riser no.1 (i.e., K_1)

- One header flow
 - One Tee-thru flow (union)
- ii. Flow through riser no.2,
- One Tee-branch flow (separation)
 - One riser flow
 - One Tee-branch flow (union)

The head loss between point 1 and 2 is expressed by,

$$H_2 = K_2 m_{1,2} \quad (4.26)$$

where,

$$K_2 = ((\alpha_1 + \alpha_3) / D_h^3 + 2 a / D_h^4 + K_1)(1 + \gamma_1)^{-1}$$

$$\gamma_1 = ((\alpha_1 + \alpha_3) / D_h^3 + 2 a / D_h^4 + K_1) /$$

$$(\alpha_2 / D_h^3 + b / D_r^4 + \alpha_3 / D_r^3)$$

$$m_1 + m_2 = m_{1,2} \quad (4.27)$$

Application of mechanical energy equation to loop no.1 yields,

$$H_2 = ((\alpha_1 + \alpha_3) / D_h^3 + 2 a / D_h^4 + K_1) m_{1,1} =$$

$$(\alpha_2 / D_h^3 + b / D_r^4 + \alpha_3 / D_r^3) m_2 \quad (4.28)$$

Combining equation (4.27) and equation (4.28) yields,

$$m_{1,1} = (1 + \gamma_1)^{-1} m_{1,2} \quad (4.29)$$

$$H_2 = \pi \left\{ g h_{L_2} / (128V) \right\} \quad (4.30)$$

Analyses for the other loops are carried out similarly to the analysis of loop no.1. The resulting equations for loops no.2, 3, 4, 5 and 6 are given in Appendix 4. The resulting equations for loop no.7 are given below,

$$H_8 = K_8 m_{1,8} \quad (4.31)$$

where,

$$K_8 = ((\alpha_1 + \alpha_3) / D_h^3 + 2 a / D_h^4 + K_7)(1 + \gamma_7)^{-1}$$

$$\gamma_7 = ((\alpha_1 + \alpha_3) / D_h^3 + 2 a / D_h^4 + K_7) /$$

$$(\alpha_2 / D_h^3 + b / D_r^4 + \alpha_3 / D_r^3)$$

$$m_{1,7} + m_8 = m_{1,8} \quad (4.32)$$

Application of mechanical energy equation to loop no.1 yields,

$$H_8 = ((\alpha_1 + \alpha_3) / D_h^3 + 2 a / D_h^4 + K_7) m_{1,7} =$$

$$(\alpha_2 / D_h^3 + b / D_r^4 + \alpha_3 / D_r^3) m_8 \quad (4.33)$$

$$m_{1,7} = (1 + \gamma_7)^{-1} m_{1,8} \quad (4.34)$$

$$H_8 = \pi \rho g h_{L_8} / (128V) \quad (4.35)$$

$$m_{1,8} = m / 2 \quad (4.36)$$

Combining equation (4.31), (4.35) and (4.36); one obtains the collector characteristic. The collector characteristic, h_{L_8} , may be written in terms of mass flow rate through the collector in the following form,

$$h_{L_8} = 64 V K_8 m / (\pi \rho g) \quad (4.37)$$

The expression presented above is utilized in the next section to predict the mass flow rate thru the solar collector system studied experimentally.

Substitution of the following system parameters,

- Inside diameter of riser, D_r
- Inside diameter of header, D_h
- Riser length, b
- Distance between risers, a

into the developed mass flow rate equations yields the mass flow rate of each riser separately. The mass flow rate relationships for the collector risers are given in Chapter 5.

4.4 THE SYSTEM CHARACTERISTIC FOR THE THERMOSYPHONIC LOOP AND THE PREDICTION OF THE THERMOSYPHONIC MASS FLOW RATE FOR LAMINAR FLOW

The closed loop thermosyphonic cycle schematically shown in figure (4.2) includes following fittings losses,

- One pipe sudden inlet (exit from the jacket)
- Cold line pipe length and one elbow
- Tee - branch (separation)
- Pipe length (entrance to header)
- Collector head loss
- Pipe length (exit from header)
- Tee - branch (union)
- Hot line pipe length and one elbow
- Pipe sudden exit (entrance to the jacket)

The head loss in the thermosyphonic loop is written as,

$$\begin{aligned}
 h_L = & 6.24 \text{ m}^2 / (\pi^2 \rho^2 g D_h^4) + 128 \sqrt{L_1} \text{ m} / (\pi \rho g D_p^4) + \\
 & 128 \sqrt{\alpha_4} \text{ m} / (\pi \rho g D_p^3) + 128 \sqrt{L_2} \text{ m} / (\pi \rho g D_p^4) + \\
 & 64 \sqrt{\alpha_2} \text{ m} / (\pi \rho g D_h^3) + 64 \sqrt{a} \text{ m} / (\pi \rho g D_h^4) + \\
 & 64 \sqrt{K_8} \text{ m} / (\pi \rho g) + 64 \sqrt{a} \text{ m} / (\pi \rho g D_h^4) + \\
 & 64 \sqrt{\alpha_3} \text{ m} / (\pi \rho g D_h^3) + 128 \sqrt{L_4} \text{ m} / (\pi \rho g D_p^4) +
 \end{aligned}$$

$$128 \sqrt{\alpha_4} m / (\pi \rho g D_p^3) + 128 \sqrt{L_5} m / (\pi \rho g D_p^4) +$$

$$8 m^2 / (\pi^2 \rho^2 g D_h^4) \quad (4.38)$$

Equation (4.38) is simplified to the following form,

$$h_L = C_2 m^2 + C_3 m \quad (4.39)$$

where ;

$$C_2 = 14,24 / (\pi^2 \rho^2 g D_h^4)$$

$$C_3 = 128 ((L_1+L_2+L_4+L_5) / D_p^4 + 2 \alpha_4 / D_p^3 +$$

$$\frac{1}{2} \cdot (\alpha_2 + \alpha_3) / D_h^3 + a / D_h^4 + K_8 / 2) / (\pi \rho g)$$

Combining equation (4.8) and equation (4.39) , one obtains

$$C_2 m^2 + C_3 m = C_1 (T_2 - T_1) \quad (4.40)$$

The overall energy balance for the collector yields,

$$Q_{uc} = m \cdot C_p \cdot (T_2 - T_1) \quad (4.41)$$

Substitution of equation (4.41) into equation (4.40) gives,

$$m^3 + C_4 m^2 + C_5 = 0 \quad (4.42)$$

where ,

$$C_4 = C_3 / C_2$$

$$C_5 = - C_1 Q_{uc} / (C_p \cdot C_2)$$

Equation (4.42) yields the mass flow rate through the collectors. Equation (4.41) is then used to determine the temperature difference between collector inlet and exit. Equation (4.36), (4.34) and (4.32), (A4.24) and (A4.22), (A4.19) and (A4.17), (A4.14) and (A4.12), (A4.9) and (A4.7), (A4.4) and (A4.2), (4.29) and (4.27), and (4.24) are successfully used to determine the flow rate through each riser of the collector.

CHAPTER 5

RESULTS AND DISCUSSION

5.1 EVALUATION OF RESULTS

Two computer programs were developed in the Applesoft Basic Language using an Apple IIe microcomputer for the evaluation of the experimental measurements and the theoretical results. The computer program listing for the evaluation of the experimental data is given in Appendix 3. The computer program listing for the evaluation of the theoretical results is given in Appendix 5.

Computer program for experimental data evaluation takes fixed and variable parameters as inputs and gives computed system performance variables as outputs. The fixed and variable input parameters and outputs of this program are outlined below.

1 - Fixed inputs :

- Total collector area, AC
- Collector heat loss coefficient, UL
- Collector fluid specific heat, CP
- Surface emissivity of the uninsulated part of the tank, E
- Heat exchanger heat transfer surface area, AJ
- Stefan-Boltzmann constant, SF

2 - Variable inputs :

- Inside room air temperature, TA
- Collectors total heat input rate, QI
- Collector inlet temperature, CI
- Collector exit temperature, CE
- Tank inlet temperature, TI
- Tank exit temperature, TE

3 - Outputs :

- Collectors useful heat input rate, QC
- Collector side thermosyphonic mass flow rate, MC
- Heat exchanger heat loss coefficient, US
- Net heat input rate to the heat exchanger, QS
- Heat exchanger load side mass flow rate, MT
- Cold side (load) capacity rate, CR
- Hot side (collector) capacity rate, CR
- Minimum capacity rate, CM
- Theoretical effectiveness for a counter flow heat exchanger, ET
- Effectiveness of the heat exchanger-storage tank unit, EO
- Heat exchanger overall heat transfer coefficient, UH
- Heat exchanger NTU value, NTU

The interactive computer program for evaluation of the theoretical results takes fixed and variable inputs, and yields computed system performance output quantities. The inputs and outputs for this computer program are listed below.

1 - Fixed inputs :

- Inside room air temperature, TA

- Total collector area, CA
 - Distance between two risers, A
 - Length of riser, B
 - Circulation fluid specific heat, CB
 - Collector total heat loss coefficient, UL
 - Collector inlet temperature, TG
 - Density of circulating fluid, DW
 - Gravitational acceleration, G
 - Fitting loss coefficient for T-thru flow ;
separation, F1
 - Fitting loss coefficient for T-branch flow ;
separation, F2
 - Fitting loss coefficient for T-thru, branch flow ;
union, F3
 - Fitting loss coefficient for 90° Elbow, F4
- 2 - Variable inputs :
- Heat input rate to the collectors, QF
 - Riser inside diameter, DR
 - Header inside diameter, DH
 - Connecting pipe inside diameter, DP
 - Connecting pipe total length, LP
 - Connecting pipe vertical length, LV
- 3 - Outputs :
- Coefficient of volume expansion of circulating
fluid, CE
 - Dynamic viscosity of circulating fluid, DV
 - Thermal conductivity of circulating fluid, K
 - Collector thermosyphonic head loss characteristic, HC

- Thermosyphonic mass flow rate, M
- Thermosyphonic system thermostatic head, HT
- Collector inlet-exit temperature difference, TF
- Useful heat input rate to the collectors, QI

The interactive computer program for the theoretical results was used to study the effects of heat input rate to the collectors, collector riser inside diameter, collector header inside diameter, connecting pipe inside diameter, connecting pipe total length and connecting pipe vertical length on the thermosyphonic system performance parameters which were selected to be the mass flow rate, the temperature difference between collector inlet and exit, and the thermostatic head loss. The outputs from the computer program for the evaluation of experimental measurements are given in Appendix 3. The outputs from the computer program for the evaluation of theoretical results are given in Appendix 5.

5.2 DISCUSSION OF THE EFFECTS OF SYSTEM PARAMETERS ON SYSTEM PERFORMANCE

The effect of collector header inside diameter size on thermosyphonic system mass flow rate, collector inlet-exit temperature difference and the total system head loss are shown in Figures 5.1, 5.2 and 5.3 respectively. The computer program was run four times by taking four different header inside diameters which are equal to 0.0216, 0.0272, 0.0359 and 0.0368 m. It is seen from these figures that an increase in the header inside diameter results in an increase

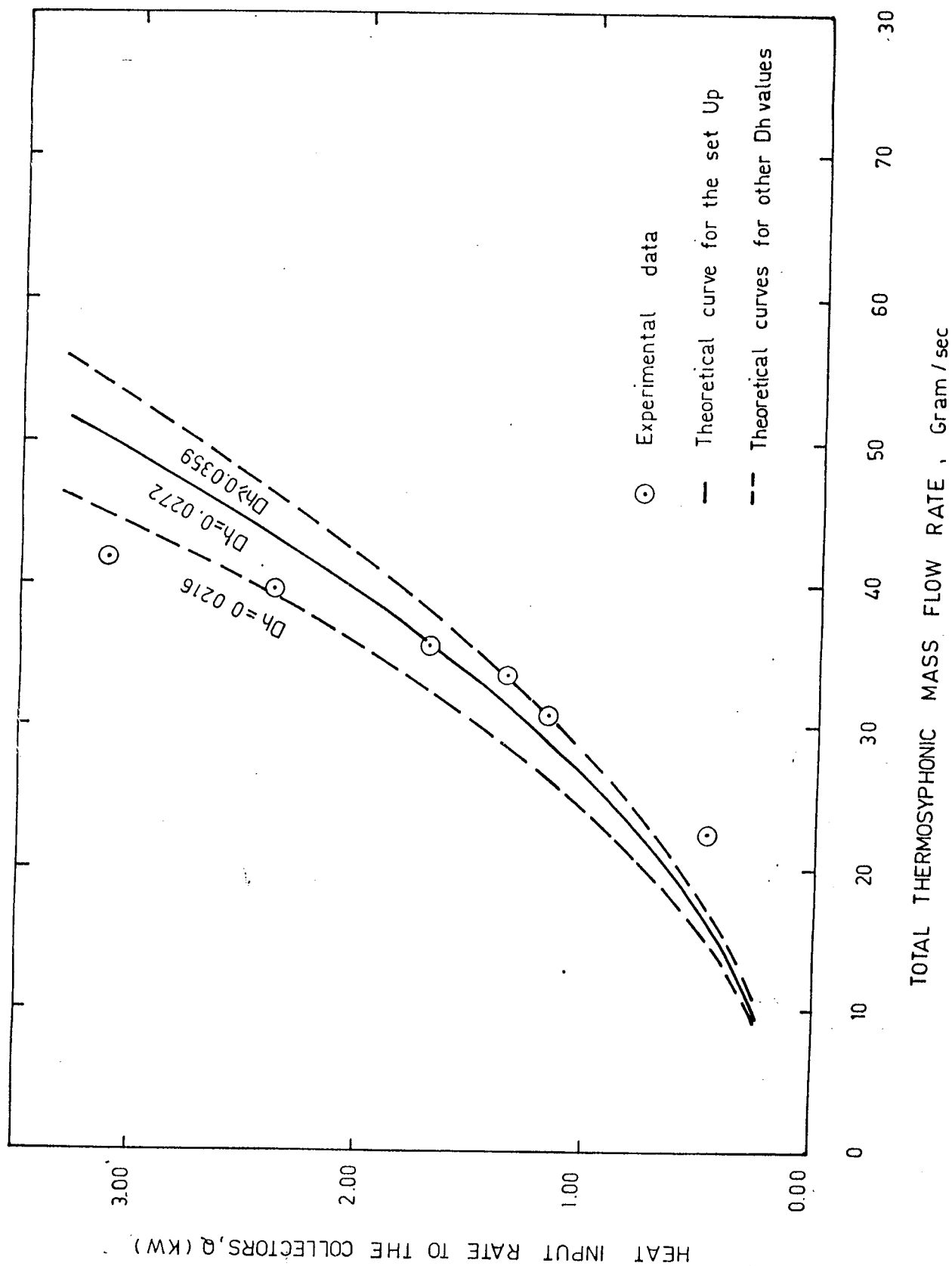


Fig.5.1 The Effect of D_h on the Total Thermosiphonic Mass Flow Rate

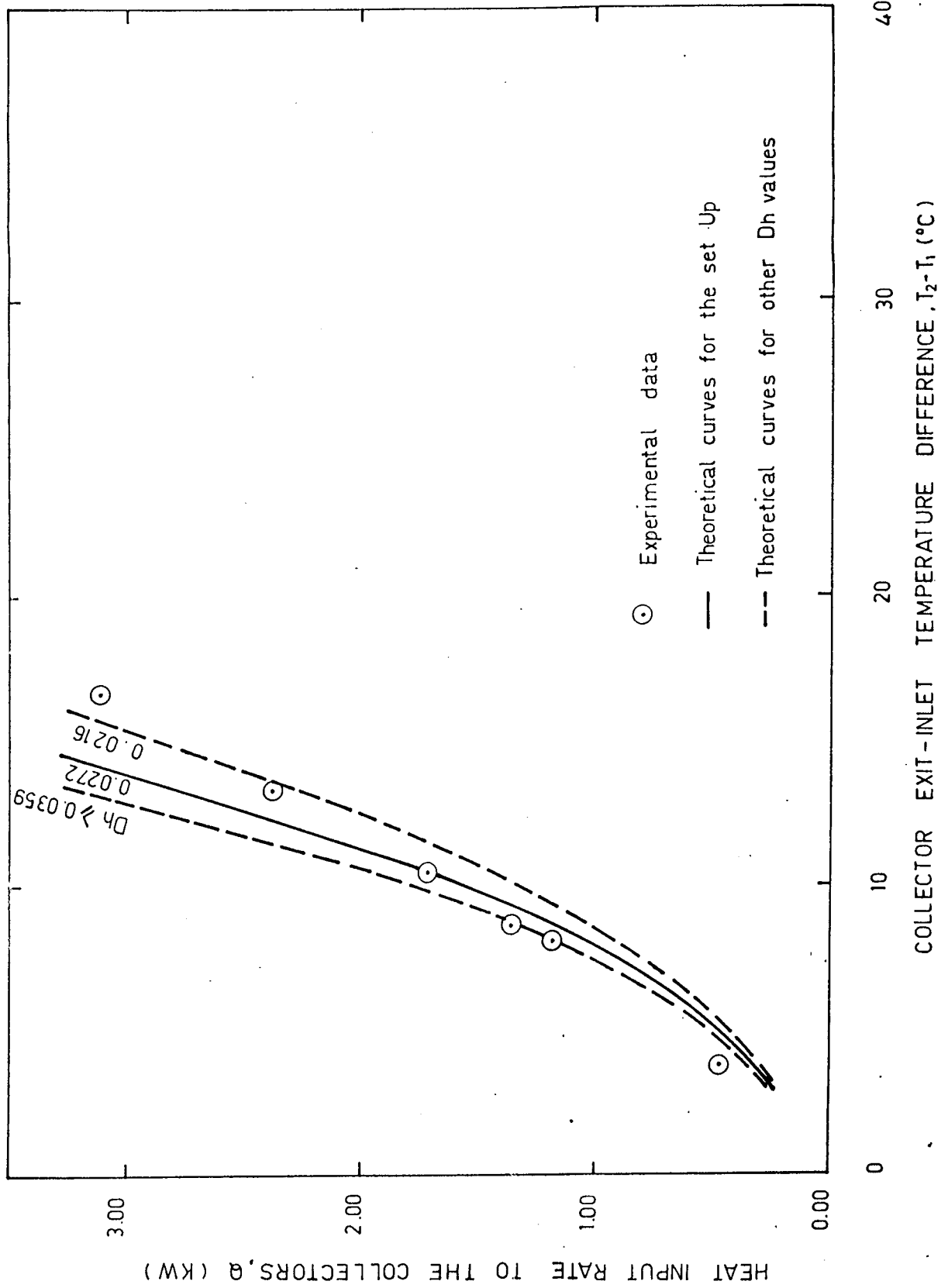


Fig.5.2 The Effect of Dh on the Collector Exit-Inlet Temperature Difference

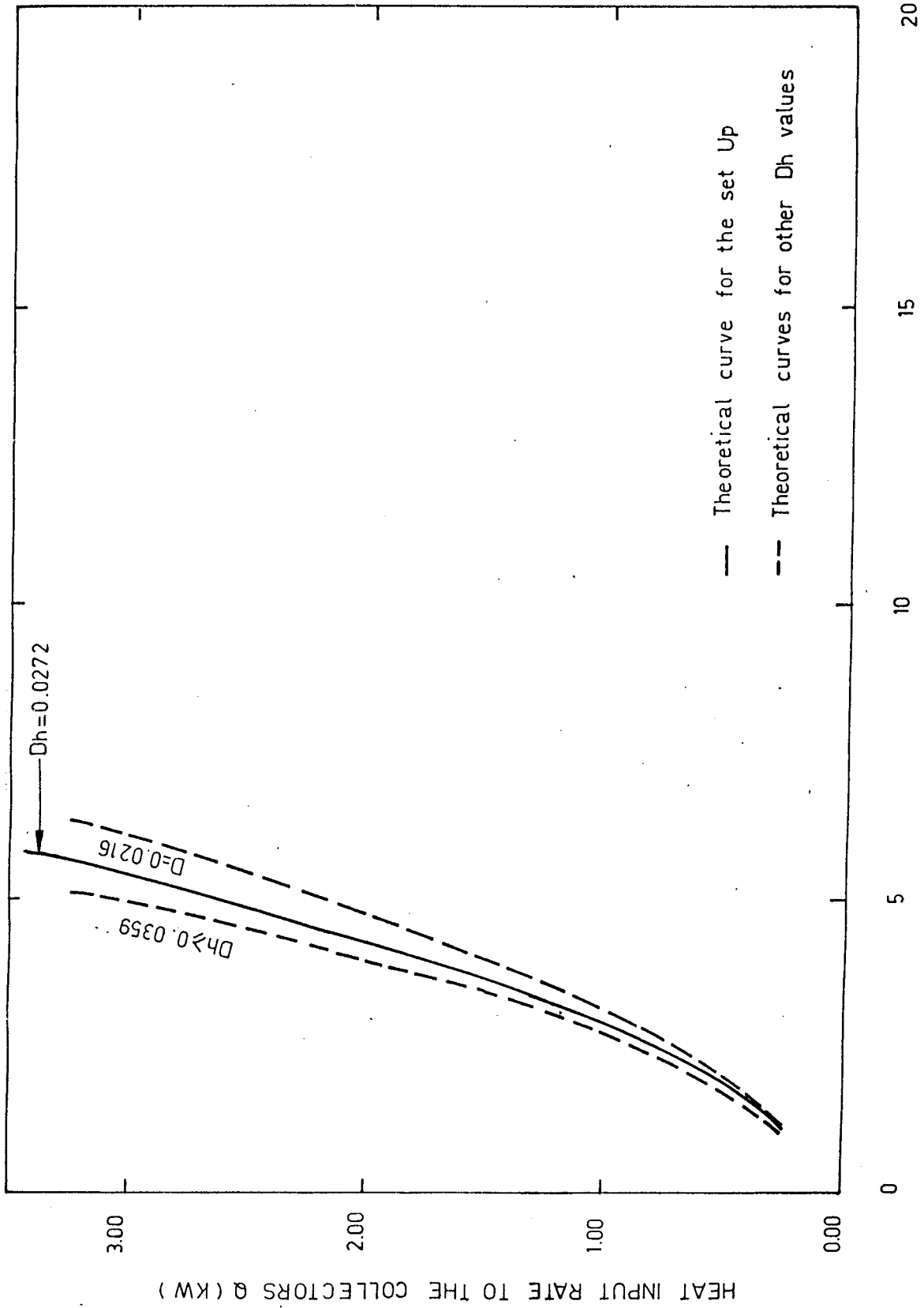


Fig.5.3 The Effect of Dh on the Total Thermosyphonic Head

in the system mass flow rate, and corresponding decreases in collector inlet-exit temperature difference and the total system head loss. It was observed from the outputs of the computer program that the effect of header inside diameter on the mass flow rate, collector inlet-exit temperature difference and the total system head loss disappears with increasing header inside diameter. Considering the present experimental set up, header inside diameters above 0.0359 m does not have any effect on system performance. The solid line curves in Figures 5.1, 5.2 and 5.3 are the theoretical curves obtained from computer outputs corresponding to the experimental set up condition. The experimental data shown by circled points in these figures represent the experimental points obtained from the computer output of the program for the evaluation of experimental measurements. The general trend observed in these figures indicates that the effect of header inside diameter size on the system performance is small. Acceptable agreement between the experimental data and the theoretical analysis is observed particularly at 1-2 kW heat input rates to the collectors. Deviations between the experimental results and the theoretical results are observed at small and large values of heat input rate to the collectors. A reason for deviations between theoretical results and experimental measurements may be the assumption of laminar flow in the system. Reynolds number increases in the system with increasing heat input rates to the collectors. The Reynolds number in the connecting pipes and the eighth riser were

calculated in order to judge for the regime of flow in the pipes. The riser mass flow rate was estimated for each riser by using the developed expressions in Chapter 4 and Appendix 4. The theoretical analysis developed in this study for unequal flow rates in collector risers gives mass flow rates of each riser separately for the collector used in the experimental set up as shown in Figure 5.4.

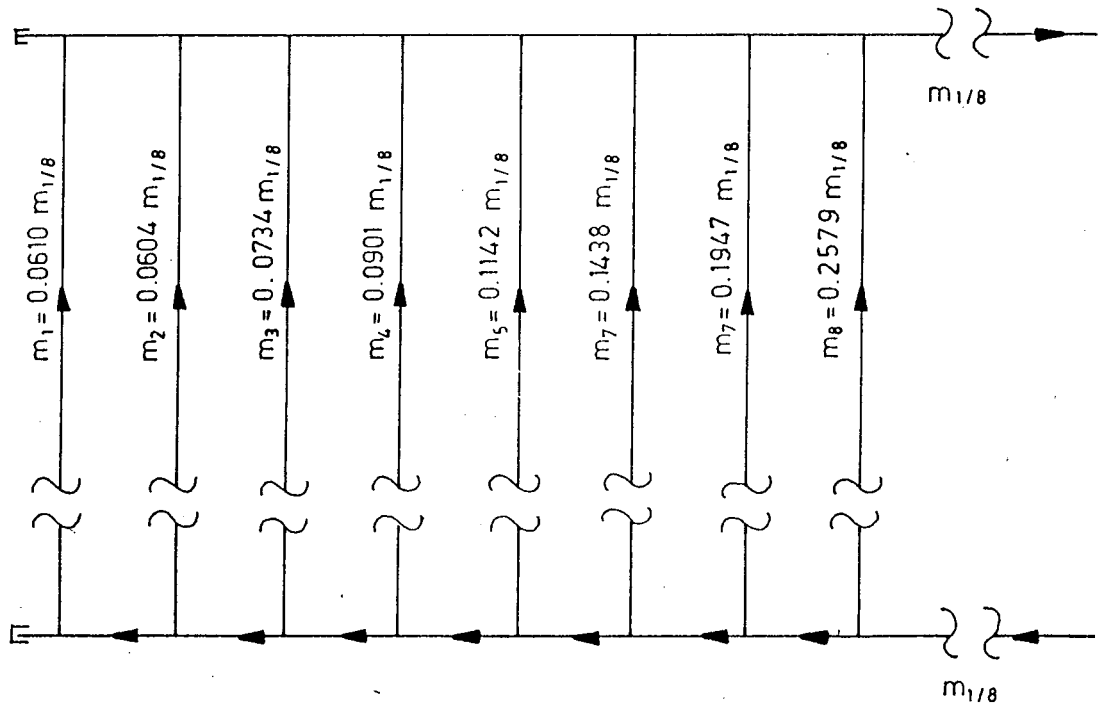


Fig.5.4 Theoretical Mass Flow Rate Relationships for the Solar Collector Manufactured by ÇILTUĞ A.Ş.

The estimated Reynolds number in the connecting pipe and in the 8th riser are given in Table 3.

Table 3. The Estimated Reynolds Number in the
Connecting Pipe and the 8th Riser

Exp. no.	Re in the 8th riser	Re in the connecting pipe
4	599	3421
5	665	3794
6	772	4398

It is observed from Table 3 that the Reynolds number in the connecting pipe is larger than 2000 indicating transitional flow. If the flow is transitional then the friction factor will be larger than the friction factor in laminar flow. Increase of friction factor will result in an increase in the total system hydraulic resistance and this may be the reason for the deviation between experimental measurements and theoretical predictions.

The effects of riser inside diameter change on the thermosyphonic mass flow rate, collector inlet-exit temperature difference and total system head loss are shown in Figures 5.5, 5.6 and 5.7. The theoretical computation was repeated for five different riser inside diameters corresponding to 0.0088, 0.0125, 0.016, 0.0216 and 0.0272 m respectively. From Figures 5.5, 5.6 and 5.7 it is seen that an increase in riser inside diameter results in an increase in mass flow rate and a corresponding decreases in collector inlet-exit temperature difference and total system head loss. Considering the present experimental set up riser inside diameters larger

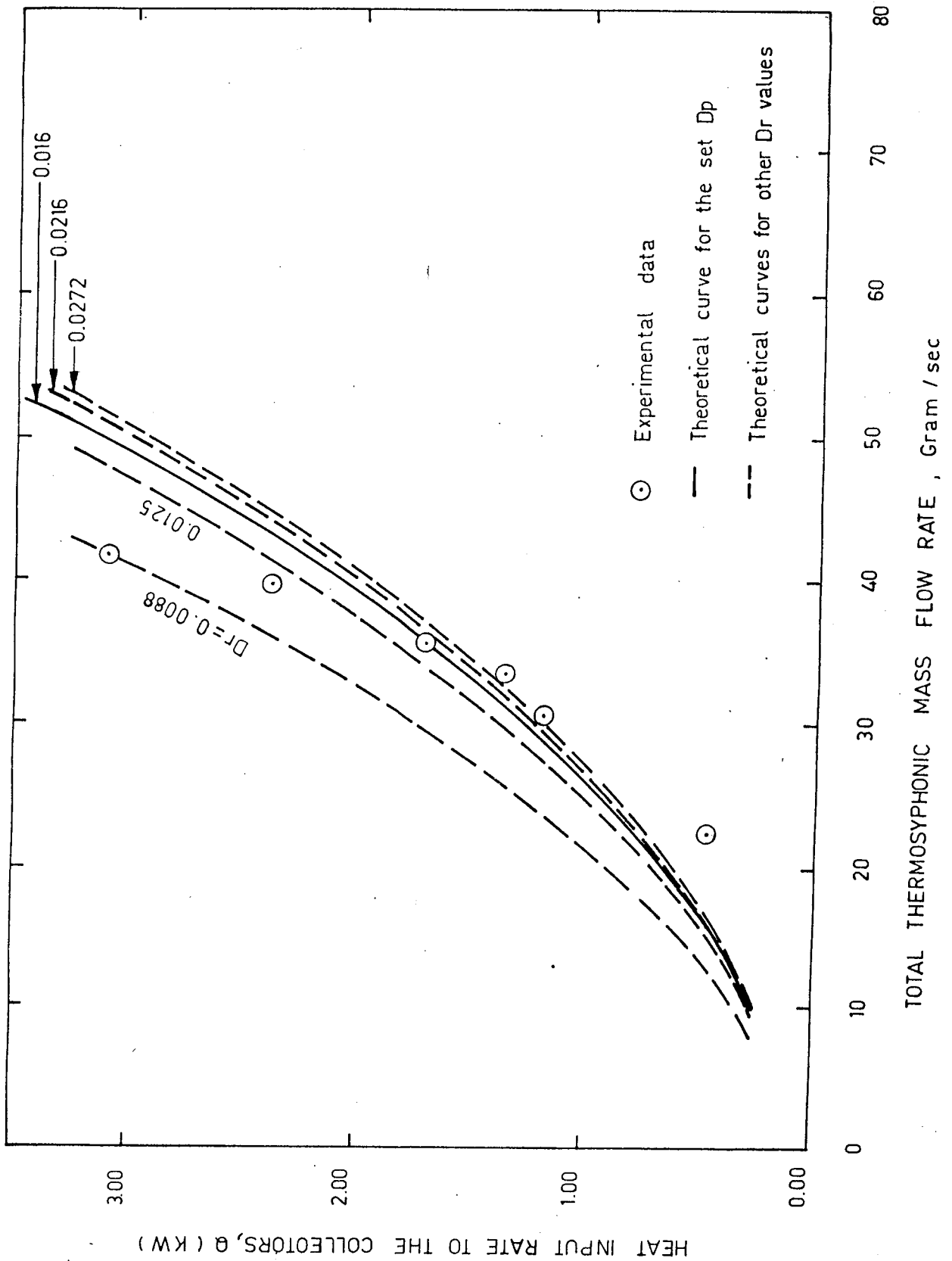


Fig.5.5 The Effect of D_r on the Total Thermosyphonic Mass Flow Rate

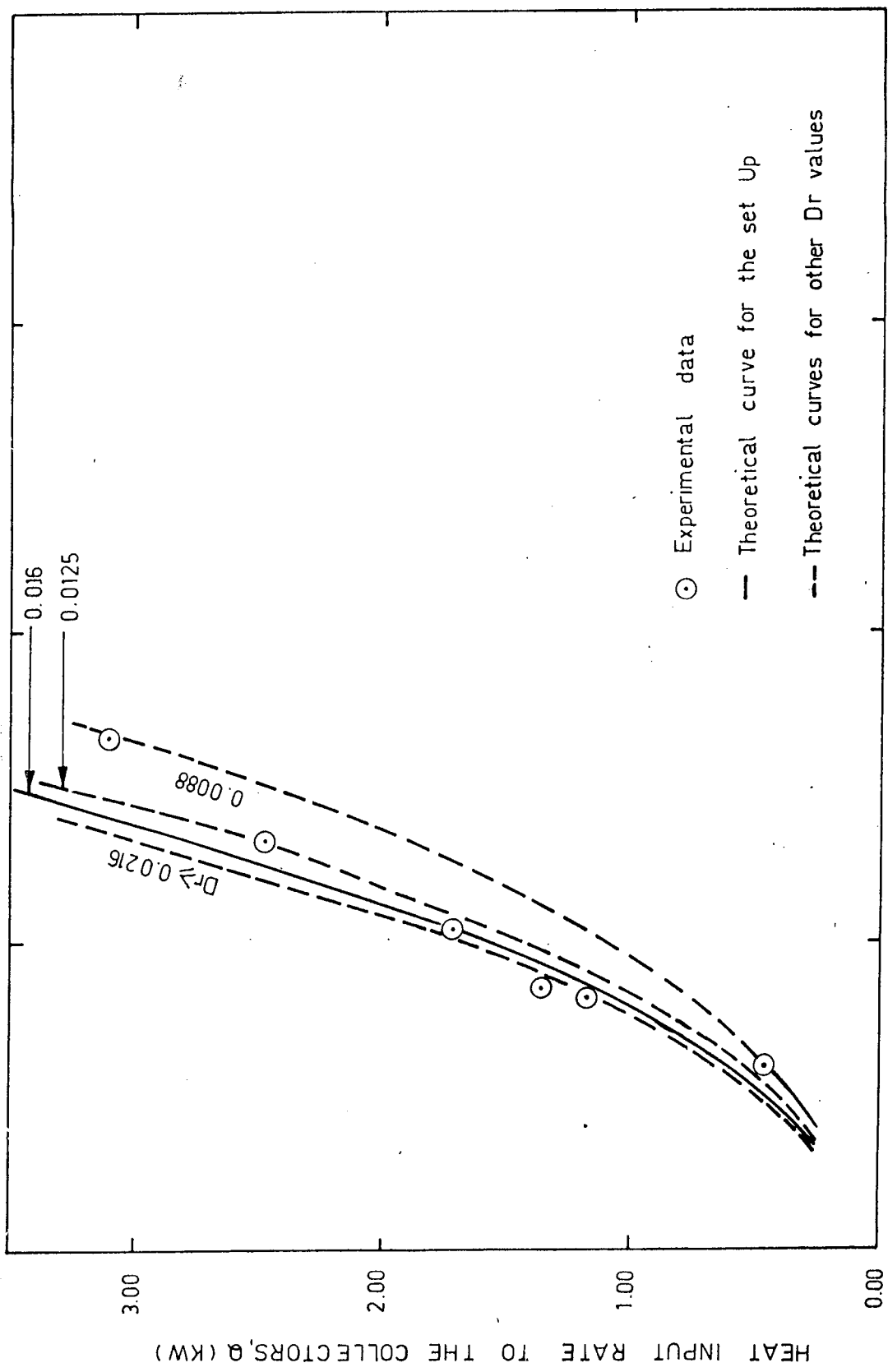


Fig. 5.6 The Effect of Dr on the Collector Exit-Inlet Temperature Difference

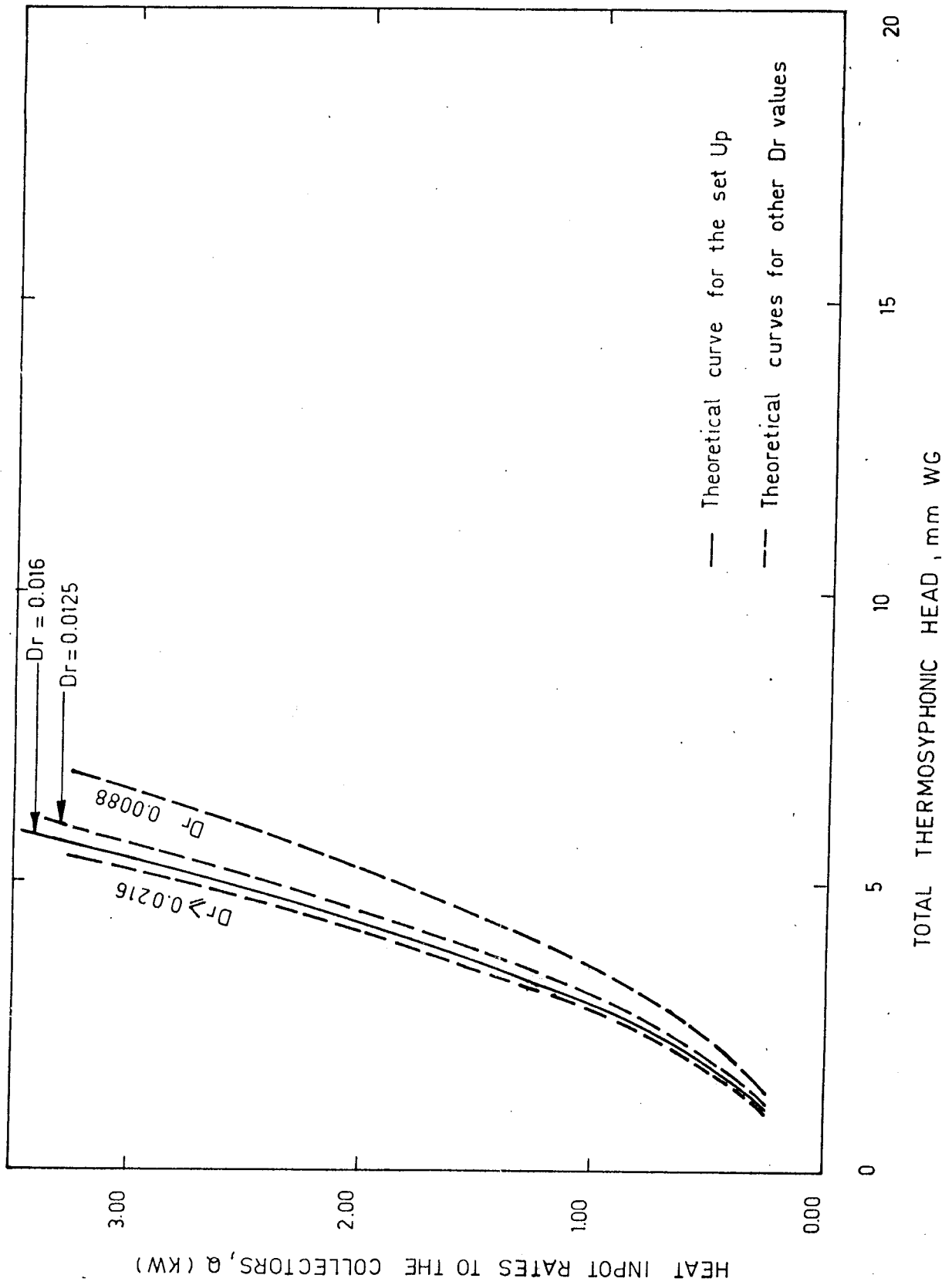


Fig.5.7 The Effect of Dr on the Total Thermosyphonic Head

than 0.0216 m does not have any effect on the collector inlet-exit temperature difference and the total system head loss. The effect of the riser inside diameter size on system performance is observed to be small. Deviations of the experimental data from the theoretical curve for the experimental set up is observed at small and large values of the heat input rate to the collectors.

The effects of connecting pipe inside diameter size on the thermosyphonic system mass flow rate, collector inlet-exit temperature difference and total system head loss are shown in Figures 5.8, 5.9 and 5.10. The theoretical computation was performed for four different connecting pipe inside diameters equal to 0.0125, 0.016, 0.0216 and 0.272 m respectively. It is seen from these figures that an increase in the connecting pipe inside diameter results in an increase in the system mass flow rate and corresponding decreases in the collector inlet-exit temperature difference and system total head loss. The effect of connecting pipe inside diameter on system performance is observed to be quite significant. The deviation between experimental and theoretical results follows a similar trend as in Figures 5.1, 5.2, 5.5 and 5.6.

In present commercial applications the conventional thermosyphonic solar heating systems are of almost identical design with the storage tank located right above the collectors. The distance between the collector top and the tank bottom in these systems usually varies between 25 to 35 centimeters. It is of practical interest to study the system performance of non-conventional thermosyphonic

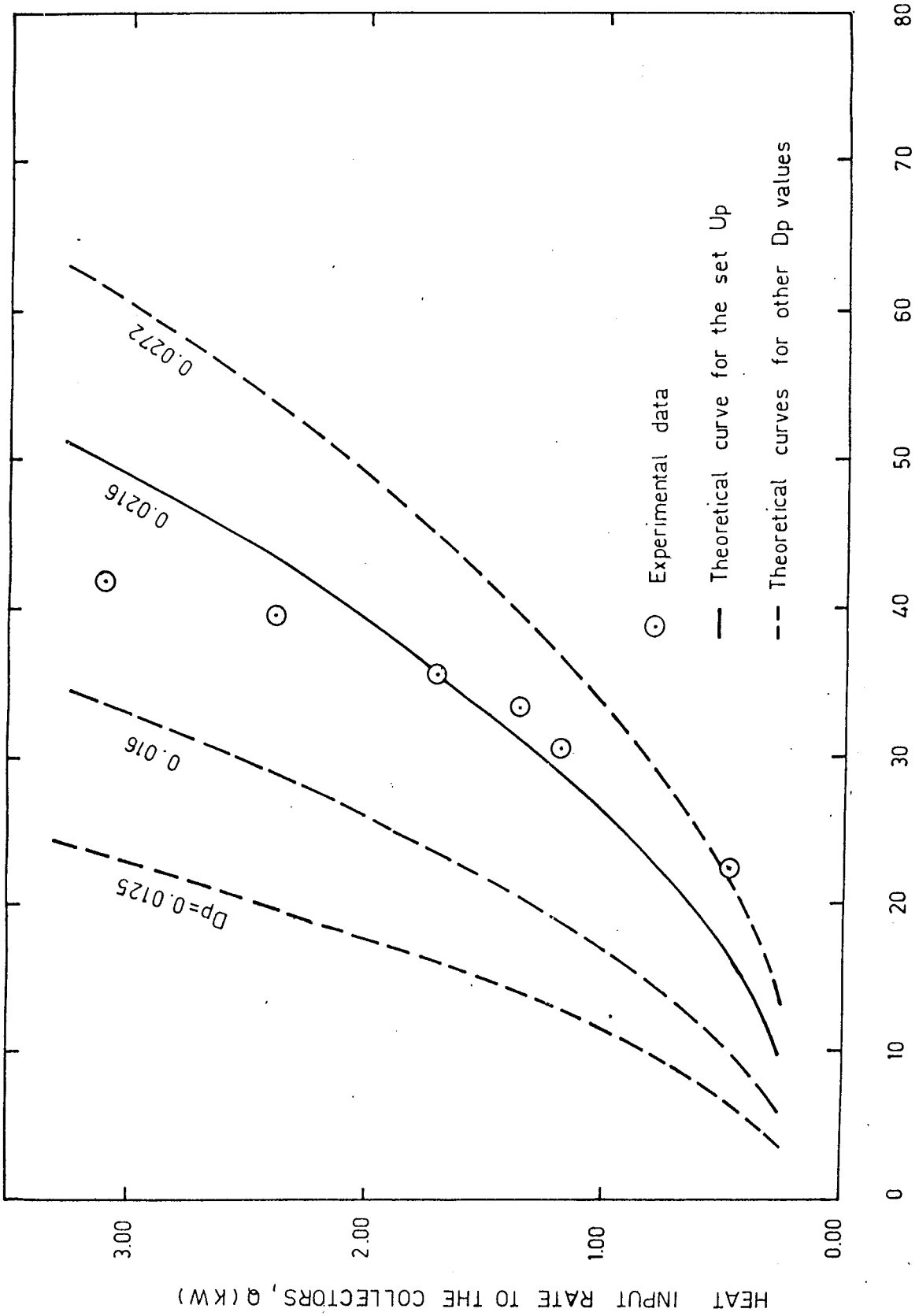


Fig.5.8 The Effect of D_p on the Total Thermosyphonic Mass Flow Rate

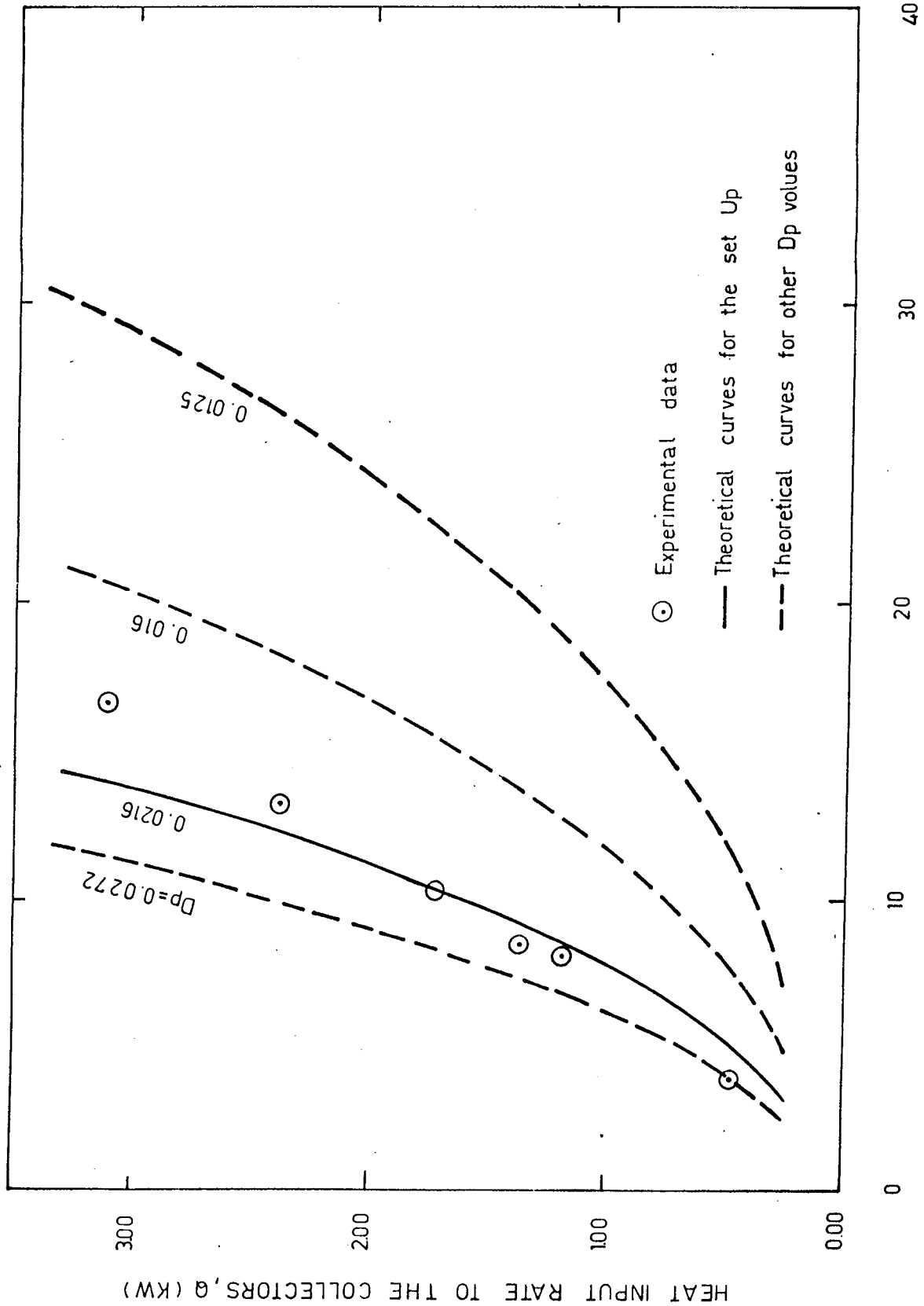


Fig.5.9 The Effect of D_p on the Collector Exit-Inlet Temperature Difference

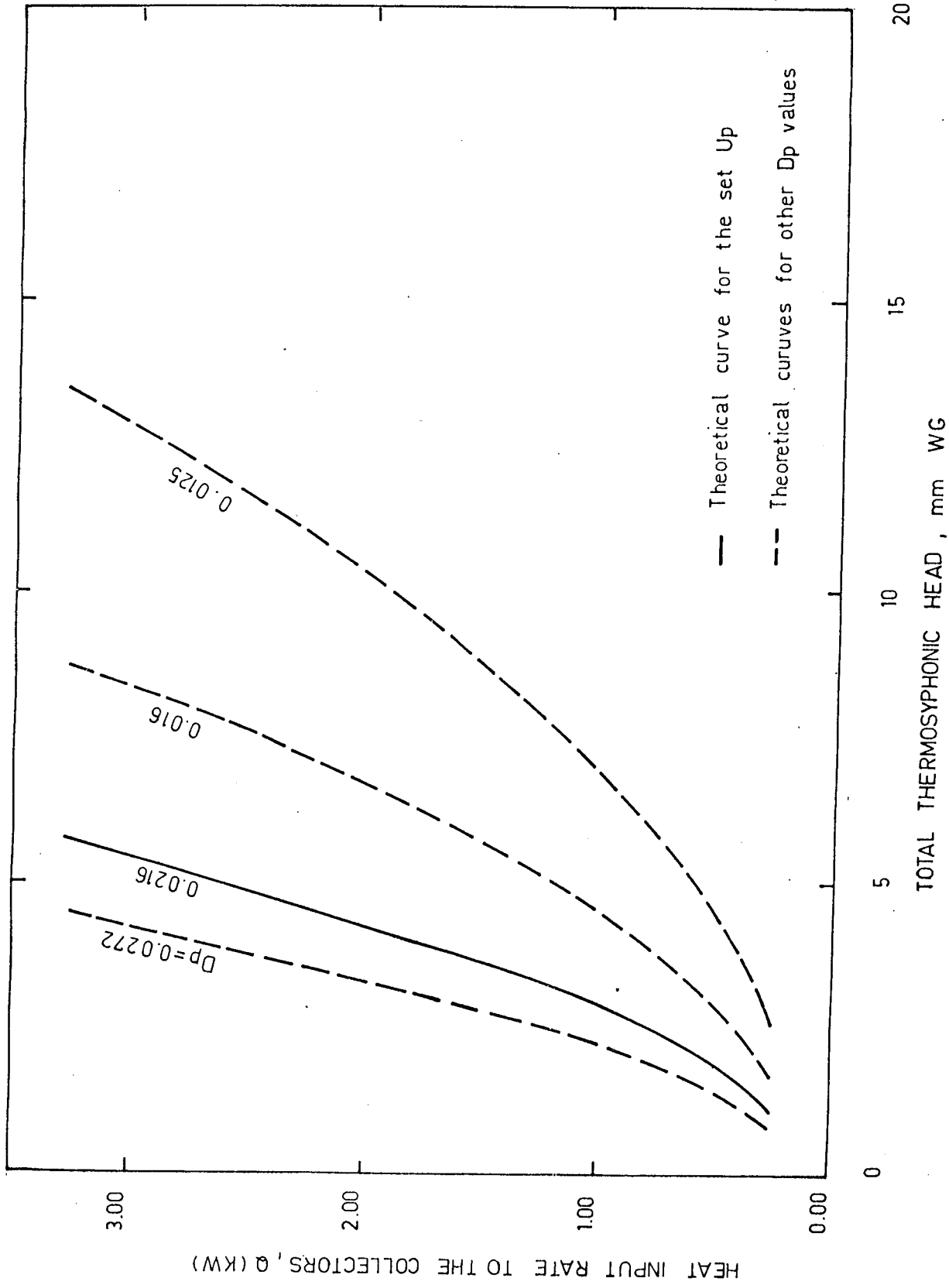


Fig.5.10 The Effect of D_p on the Total Thermosyphonic Head

systems where the collector top-storage tank bottom vertical distance and the collector-storage tank horizontal distance are different from the standard design values. Generally, very little is known about the performance of these unconventional system orientations. To investigate the performance of such systems proper input values were given to the computer program by increasing the total connecting pipe length incrementally. In one set of computations only the horizontal distance between the collectors and the storage tank was changed. In a second set of computations only the vertical distance between the collector top and the storage tank bottom was changed.

The effects of total connecting pipe length on thermosyphonic system mass flow rate, collector inlet-exit temperature difference and total system head loss are shown in Figures 5.11, 5.12 and 5.13. The theoretical computation has been done for six different connecting pipe lengths which are equal to 3.903, 4.303, 4.867, 6.867, 10.867 and 18.867 respectively. From Figures 5.11, 5.12 and 5.13, it is seen that an increase in the connecting pipe length results in a decrease in system mass flow rate and corresponding increases in collector inlet-exit temperature difference and system total head loss. The deviation between experimental and theoretical results are similar to those in the previous figures. It is observed from Figure 5.12 that an increase in the connecting pipe length from 4.867 m to 18.867 m increases

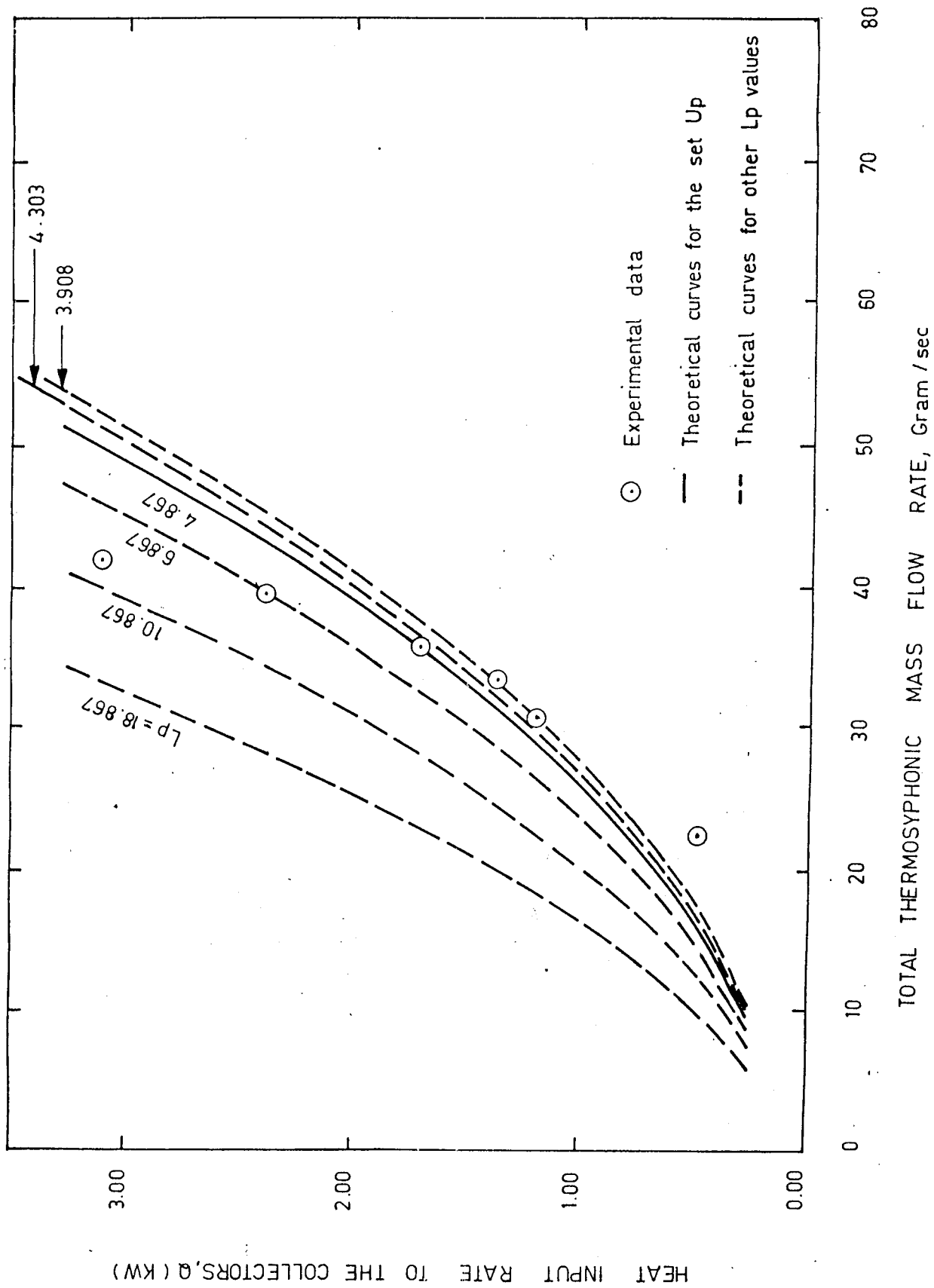


Fig.5.11 The Effect of L_p on the Total Thermosyphonic Mass Flow Rate

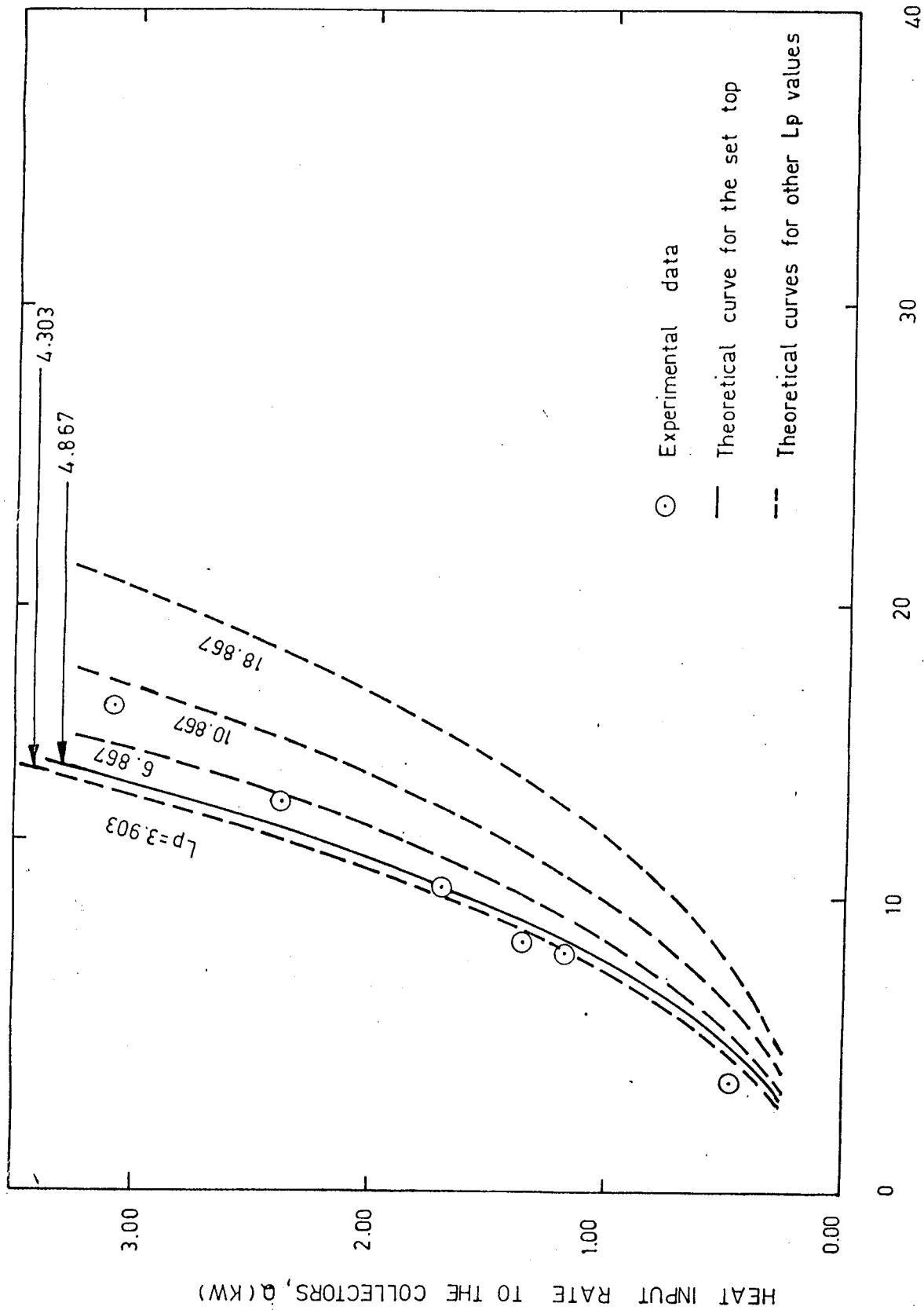
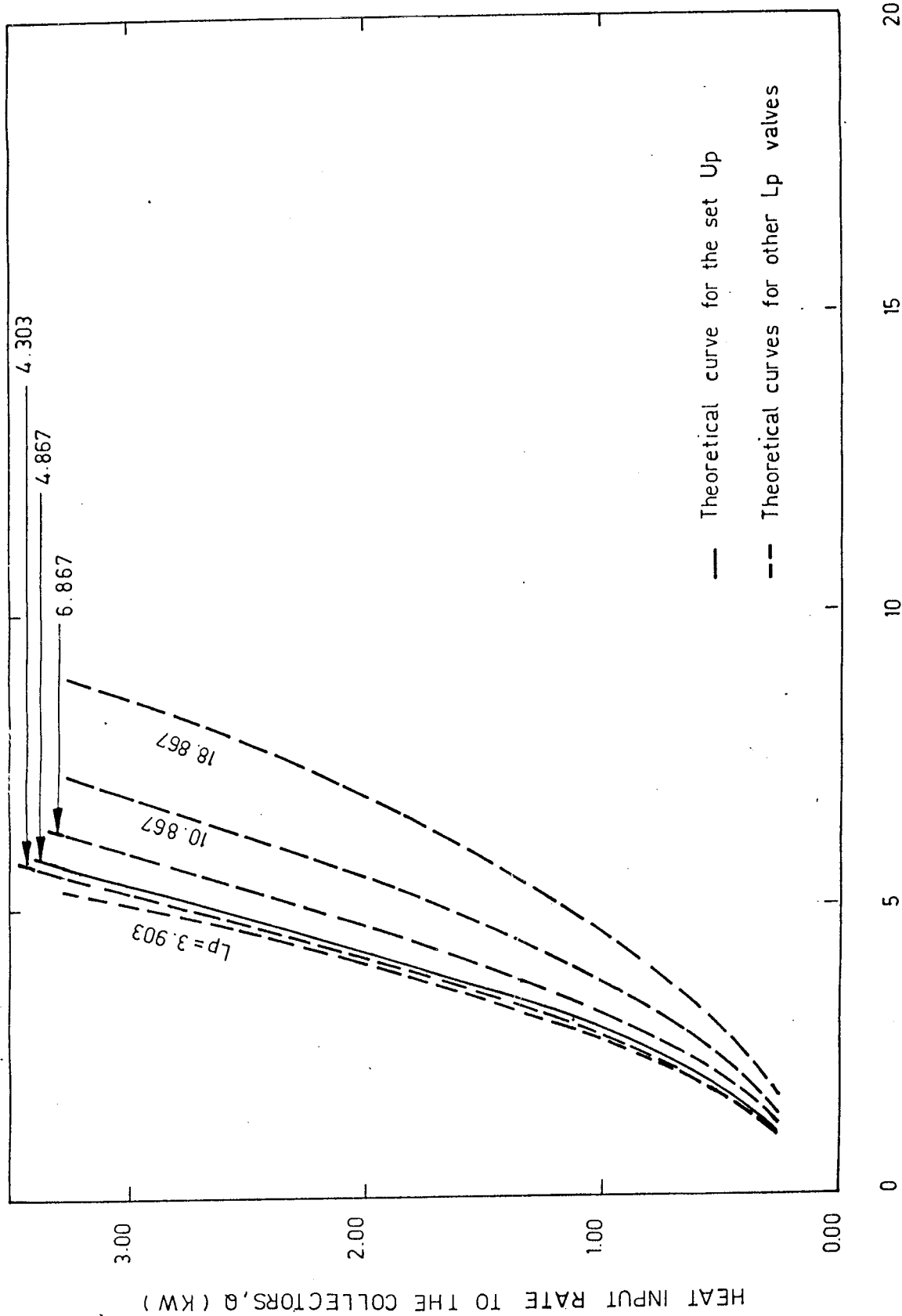


Fig. 5.12 The Effect of L_p on the Collector Exit-Inlet Temperature Difference



TOTAL THERMOSYPHONIC HEAD, mm WG

Fig.5.13 The Effect of Lp on the Total Thermosyphonic Head

the collector inlet-exit temperature difference by about 30 percent. For non-conventional systems with large collector to storage tank horizontal distance, these figures present a quantitative estimate on the amount of decrease in the mass flow rate and the increase in the system head loss, as well as the increase in the operating temperature difference in the system. In practice such system performance information may prove useful, should a system design engineer be in a position to judge for the installation of a non-standard system.

The effects of vertical length of the connecting pipes on thermosyphonic system mass flow rate, the collector inlet-exit temperature difference and the system total head loss are shown in Figures 5.14, 5.15 and 5.16. The theoretical computation was repeated for five different vertical lengths of the connecting pipe which are equal to 0.785, 1.385, 1.985, 2.585 and 3.185 m respectively. From Figures 5.14, 5.15 and 5.16, it is seen that an increase in the vertical length of the connecting pipes results in an increase in the mass flow rate and the total head loss, and a corresponding decrease in collector inlet-exit temperature difference. It is noted that an increase in the vertical length of the connecting pipes increases the thermostatic head. This results in larger mass flow rates and decreases the system temperature difference. This in turn means that system thermal performance will be better and the thermosyphon system will operate at a higher overall thermal efficiency when

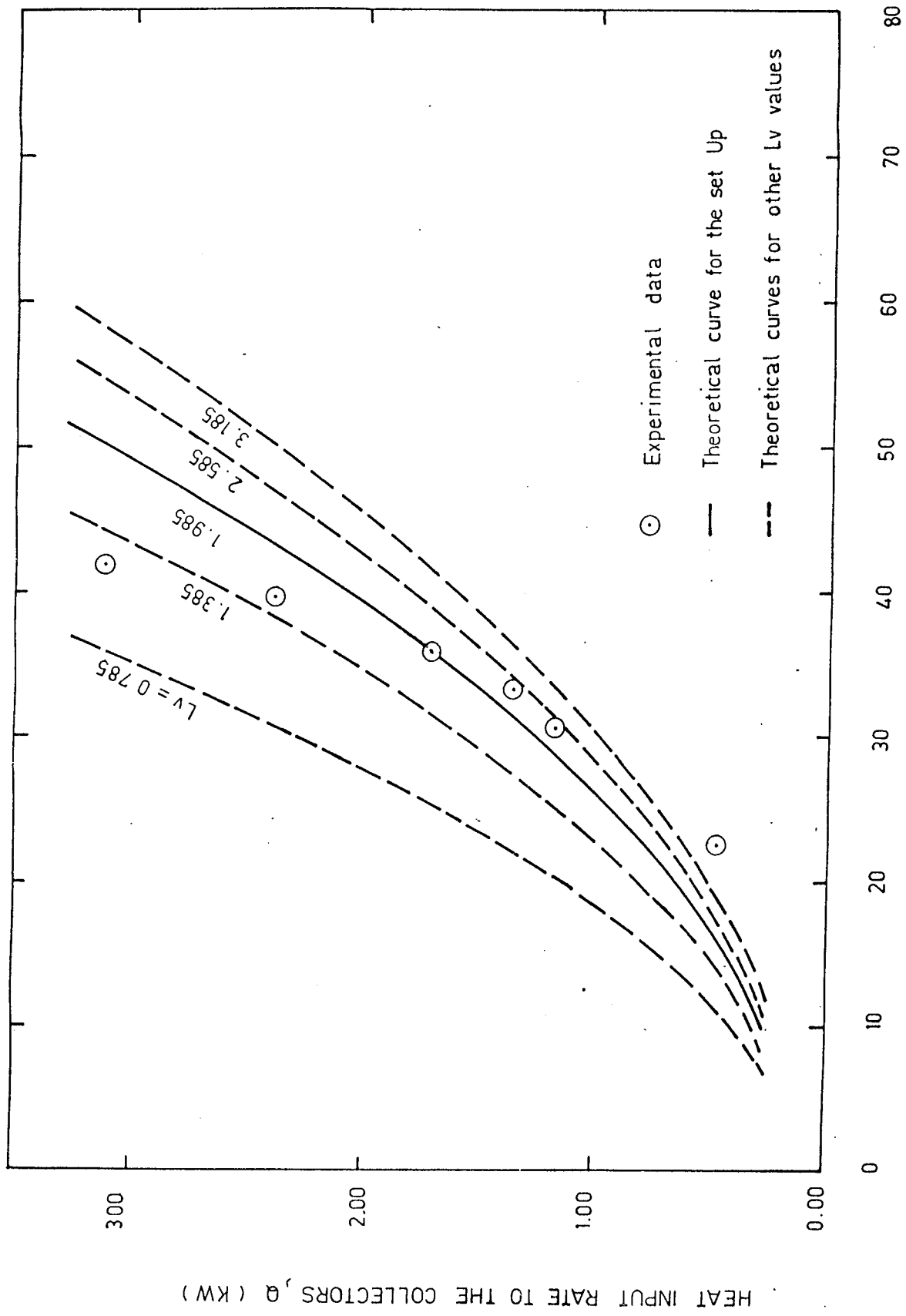


Fig.5.14 The Effect of Lv on the Total Thermosyphonic Mass Flow Rate

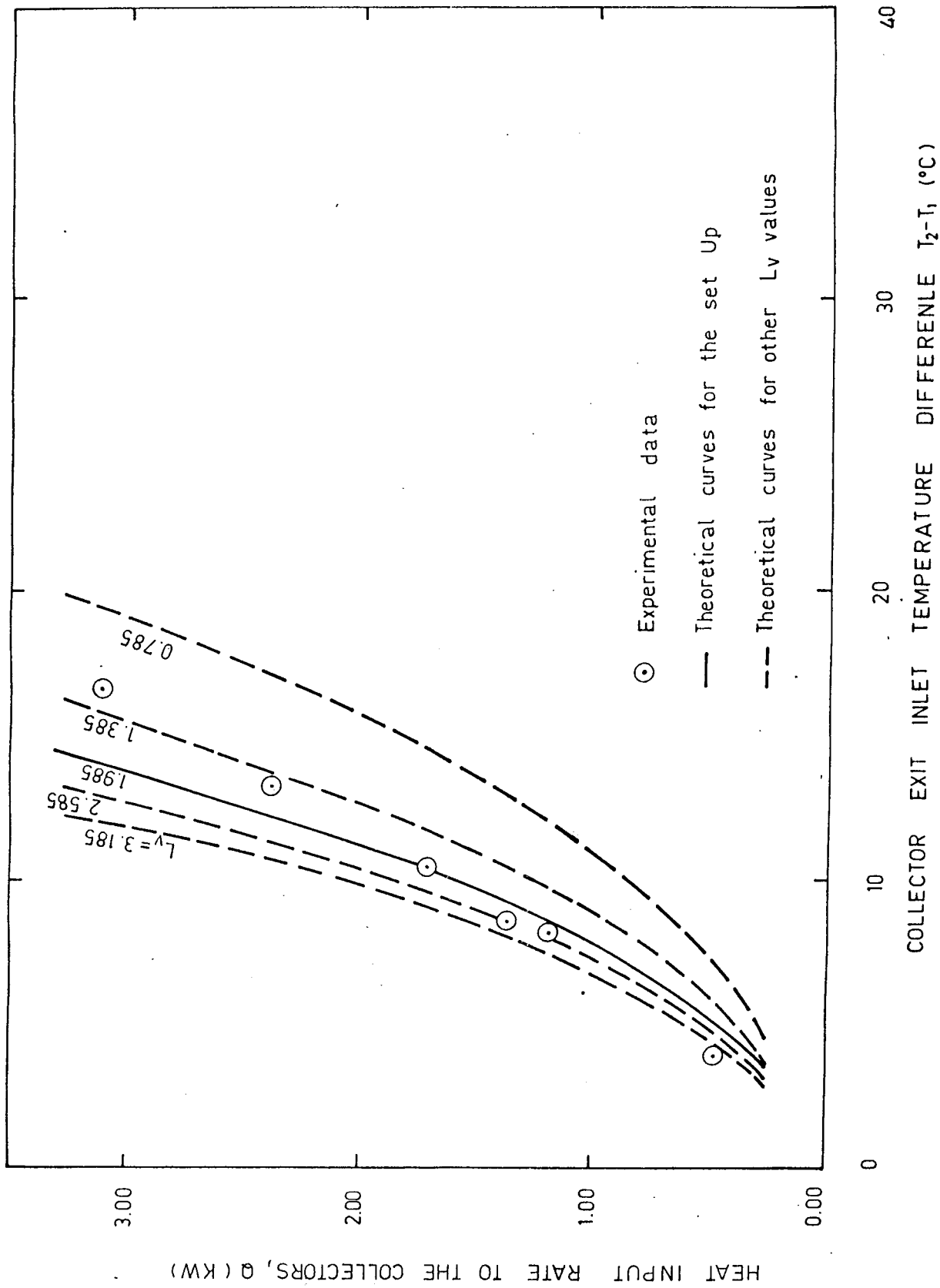


Fig.5.15 The Effect of L_v on the Collector Exit-Inlet Temperature Difference

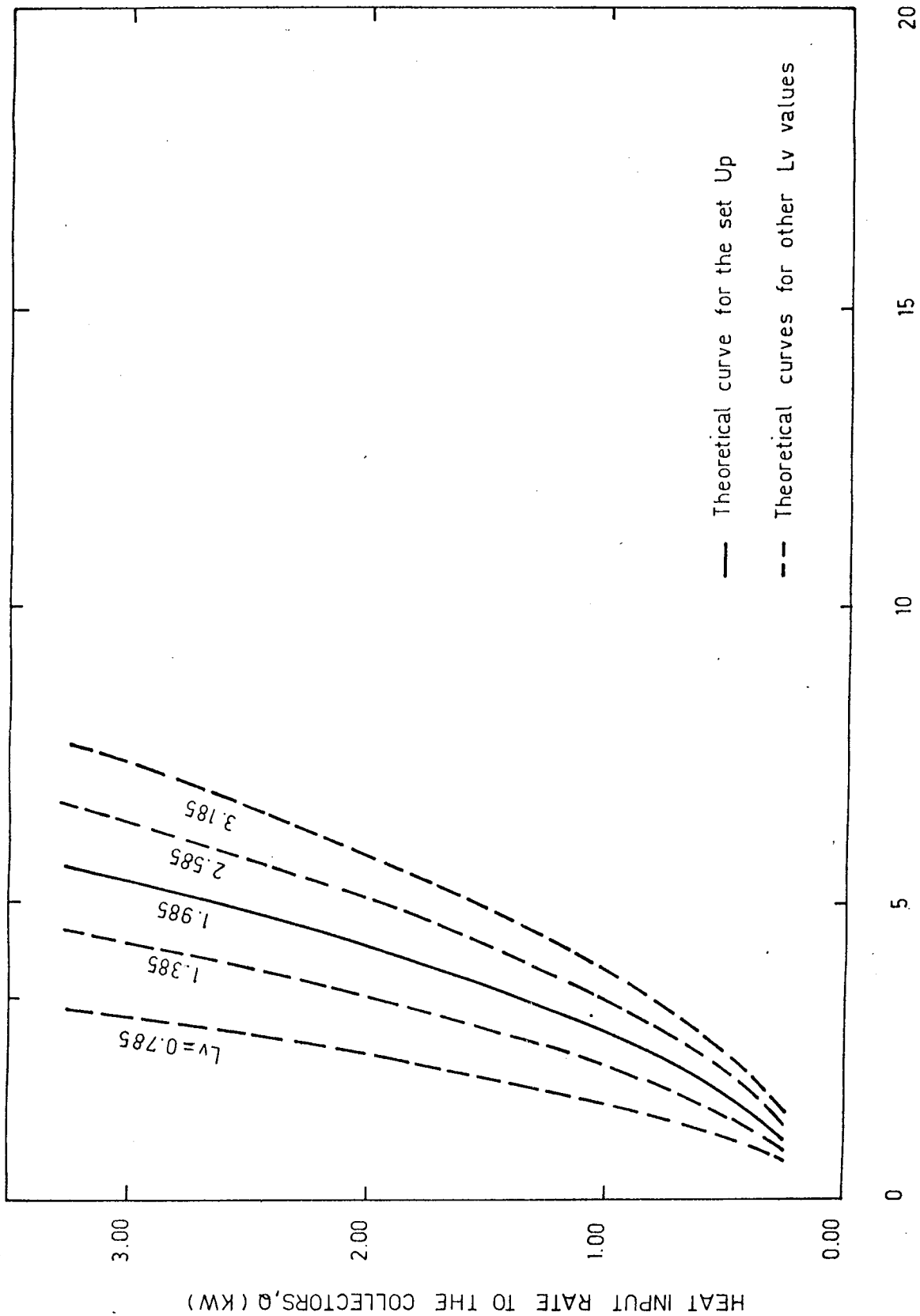


Fig.5.16 The Effect of L_v on the Total Thermosyphonic Head

operating under solar heating conditions.

The experimental value for the effectiveness of the heat exchanger-storage tank unit is compared with the theoretical effectiveness of a counter flow heat exchanger in Table 4.

Table 4. Comparison of the Experimental Effectiveness Value of the Storage Tank-Heat Exchanger with the Theoretical Effectiveness Value for a Counter Flow Heat Exchanger

$C_{\min.} / C_{\max.}$ (experimental)	ϵ (Theoretical)	ϵ (Experimental)
0.22	0.2701	0.2702
0.46	0.8636	0.8618
0.40	0.8909	0.8894
0.52	0.8529	0.8512
0.58	0.8409	0.8393
0.78	0.7725	0.7708

It is seen from the Table 4 that the effectiveness-NTU relationship of the storage tank-heat exchanger unit compares well with the corresponding theoretical relationship for a counter flow heat exchanger. As a consequence of this observation it is noted that the storage tank-heat exchanger unit may be considered as a counter flow heat exchanger when analysing the effect

of the storage tank-heat exchanger unit on the solar heating system thermal performance.

The experimental U-values, overall heat transfer coefficient, of the storage tank-heat exchanger unit are shown in Figures 5.17 and 5.18 as a function of heat input rates to the collectors and storage tank cold side inlet-exit temperature difference respectively. From Figure 5.17 it is seen that the U-value increases with increasing heat input rate to the collectors. From Figure 5.18 it is seen that the U-value increases with increasing tank inlet-exit temperature difference. It is noted that the magnitude of the U-values depicted in these figures are smaller by an order of magnitude from the U-values for forced circulation water to water heat exchangers. The U-values for the latter type heat exchangers generally lie in the 850-1700 W/m² °C range (14). Because of the heat exchanger unit in a double loop thermosyphon system, the collectors are forced to operate at a higher temperature with a corresponding reduction in system thermal efficiency. The percent decrease in system efficiency may be determined from the following formula (16).

$$\frac{F_R'}{F_R} = \frac{1}{1 + \left(\frac{A_c F_R U_L}{(m C_p)_c} \right) \left(\frac{(m C_p)_c}{\epsilon (m C_p)_{\min}} \right)} \quad (5.1)$$

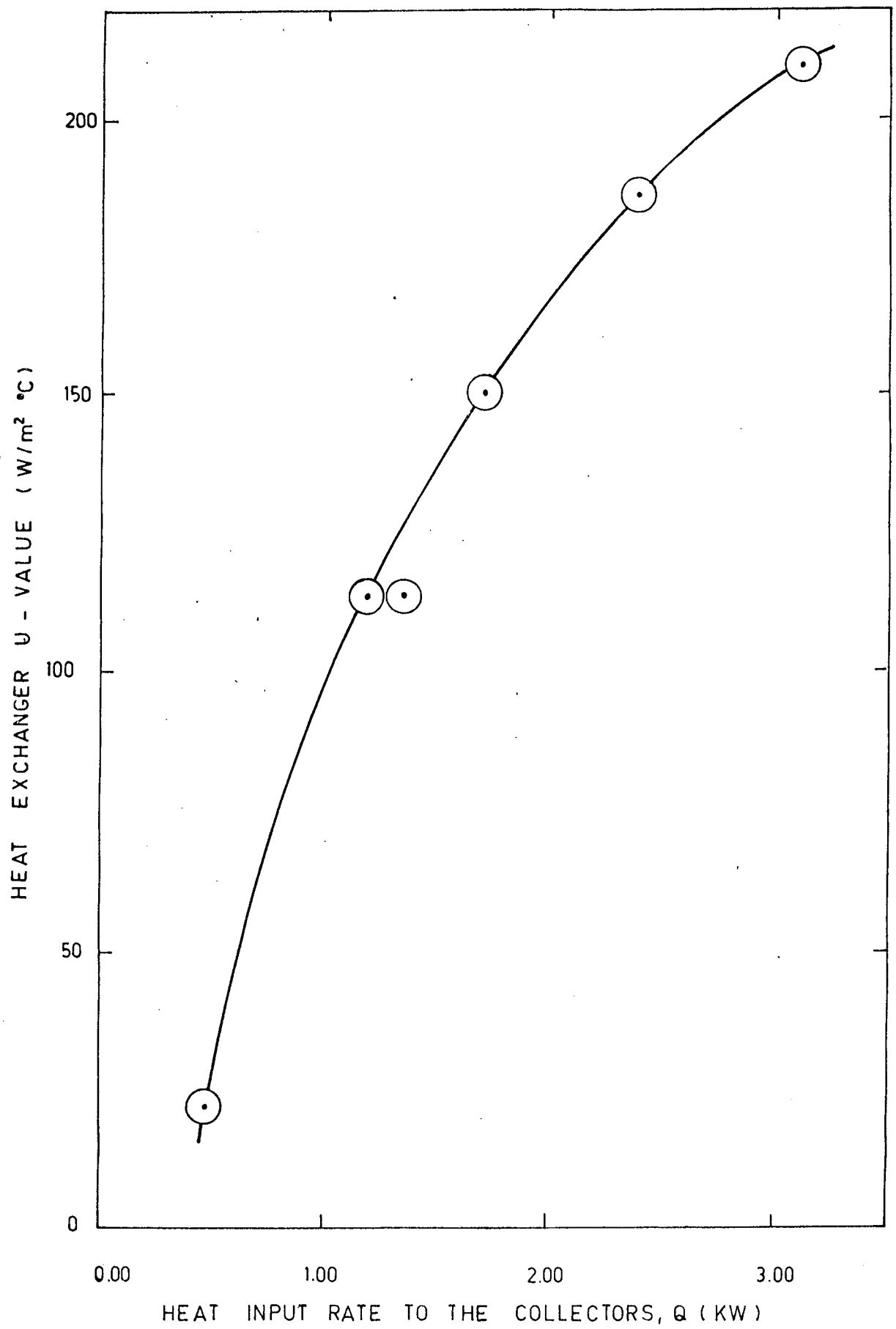


Fig.5.17 Experimental U-Value Versus Heat Input Rate to the Collectors

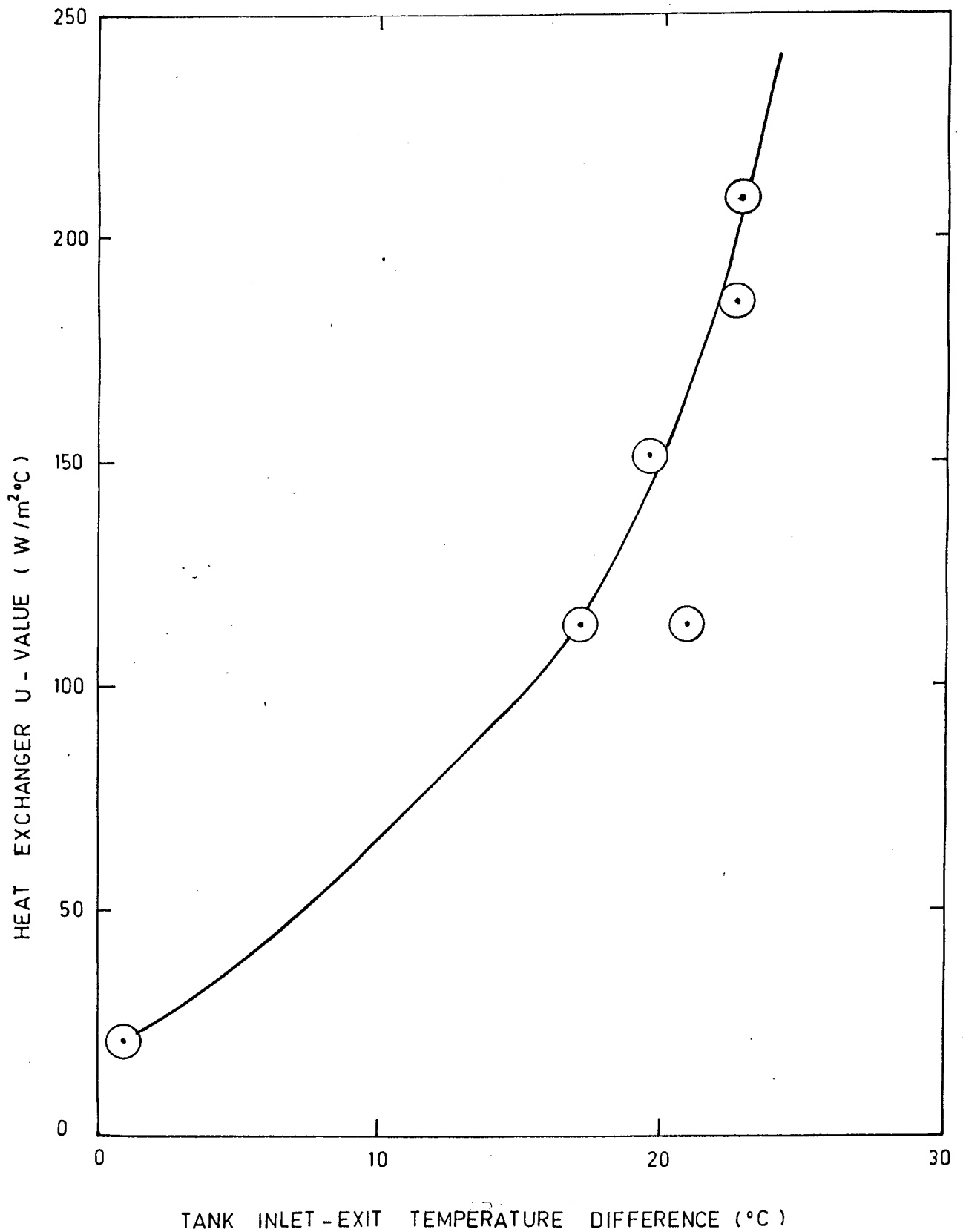


Fig.5.18 Experimental U-Value Versus Tank Inlet-Exit Temperature Difference

The ratio F_R' / F_R represents the decrease in system efficiency resulting from the use of a heat exchanger in the double loop thermosyphon system. The value of F_R' / F_R was estimated for the present system as follows :

The U_L value corresponding to operation under solar insolation for the collectors used in the experimental set up was taken as $7.5 \text{ W/m}^2 \text{ }^\circ\text{C}$ from graph 6.4.4.c (16).

The F_R values for the collector used in the experimental set up was calculated from equations given in (16) as a function of experimental mass flow rate through the collectors. The estimated reductions in system thermal efficiency for the present thermosyphon system are given in Table 5.

Table 5. Percent Reduction in Double Loop Thermosyphon System Efficiency Because of the Storage Tank-Heat Exchanger Unit

Exp. no.	\dot{m} /Collector	F_R	$(\epsilon)_{he}$	F_R' / F_R
1	0.011245	0.747	0.27027	0.633
2	0.01534	0.771	0.86180	0.804
3	0.01677	0.776	0.88936	0.788
4	0.01786	0.780	0.85120	0.85
5	0.019825	0.786	0.83925	0.88
6	0.020965	0.789	0.77079	0.88

It is seen from Table 5 that depending on the solar insolation intensity, the present system will absorb 12-36 % less energy than a single loop thermosyphon system of similar construction.

CHAPTER 6

CONCLUSION

The experimental U-value of the hot water heat storage tank-heat exchanger unit increases with increasing heat input rates to the system. The experimental U-values are on the order of $50-200 \text{ W / m}^2 \text{ }^\circ\text{C}$. These values are an order of magnitude smaller than the U-values for forced flow water to water heat exchangers. It is found that the effectiveness - NTU relationship of the water storage tank-heat exchanger unit is in agreement with that of a counter flow heat exchanger. The reduction in system thermal efficiency under solar heating conditions due to the use of a double loop cycle is found to vary from 12 % to 36 % depending on the heat input rate to the system.

The theoretical results indicate unequal mass flow rates in the collector risers contrary to the assumptions in the previous theoretical models. For the set up studied experimentally, the theoretical mass flow rate in the last riser of the collector is approximately 4 times the mass flow rate in the first riser of the collector.

The connecting pipes inside diameter size is found to have a significant effect on system performance. An increase in the inside diameter of the connecting pipes will increase the thermal performance of the system.

The computer program yields a quantitative measure on the effects of system geometric parameters on the thermosyphonic mass flow rate, the collector inlet-exit temperature difference and the system head loss. The theoretical analysis is based on the laminar flow assumption and deviations between the experimental and theoretical results are observed when the Reynolds number is larger than the critical Reynolds number in the connecting pipes. The predictions from the computer program are in reasonable agreement with the experimental data when the flow in the system is in the laminar regime. The interactive computer program presented is a general computer code for thermosyphon solar water heaters and can be used to predict the performance of systems with other geometric dimensions.

CHAPTER 7

RECOMMENDATIONS FOR FURTHER STUDY

One of the aims of the experimental part of this study was to measure the flow non-uniformity in the collector risers and its effect on the thermosyphonic mass flow rate, collector inlet-exit temperature difference and on the total thermosyphonic head of the double loop solar water heating system.

Experimental measurements of the riser mass flow rates were not successful because of the following reasons :

1 - The collector tube fin construction was not identical for all fins resulting in unequal heat input rates into different risers of the collectors.

2 - Thermocouples were located on the outer surface of riser tubes for the measurement of mean inside tube water temperature. It was later estimated that there is a significant temperature difference between the mean water temperature in the riser tubes and the outside tube surface temperature. The measurements (on the outside tube surface) therefore did not represent mean tube water temperature.

Because of the reasons stated above, it was not possible to determine, experimentally, the mass flow rate

in risers and it was not possible to verify the non-uniform riser mass flow rate predictions obtained from the theoretical analysis. It is therefore recommended that future experimental work to be performed for precision measurement of riser water mass flow rates.

There is no technical information in the available literature regarding the theoretical U-values for the storage tank-heat exchanger unit used in the experimental set up. The present experimental measurements of this parameter is in dimensional form and it was not possible to generalize the measurements to other water storage tank-exchanger units with different geometric dimensions. It is therefore also suggested that future theoretical study is necessary for the prediction of the overall U-value of the storage tank-heat exchanger unit.

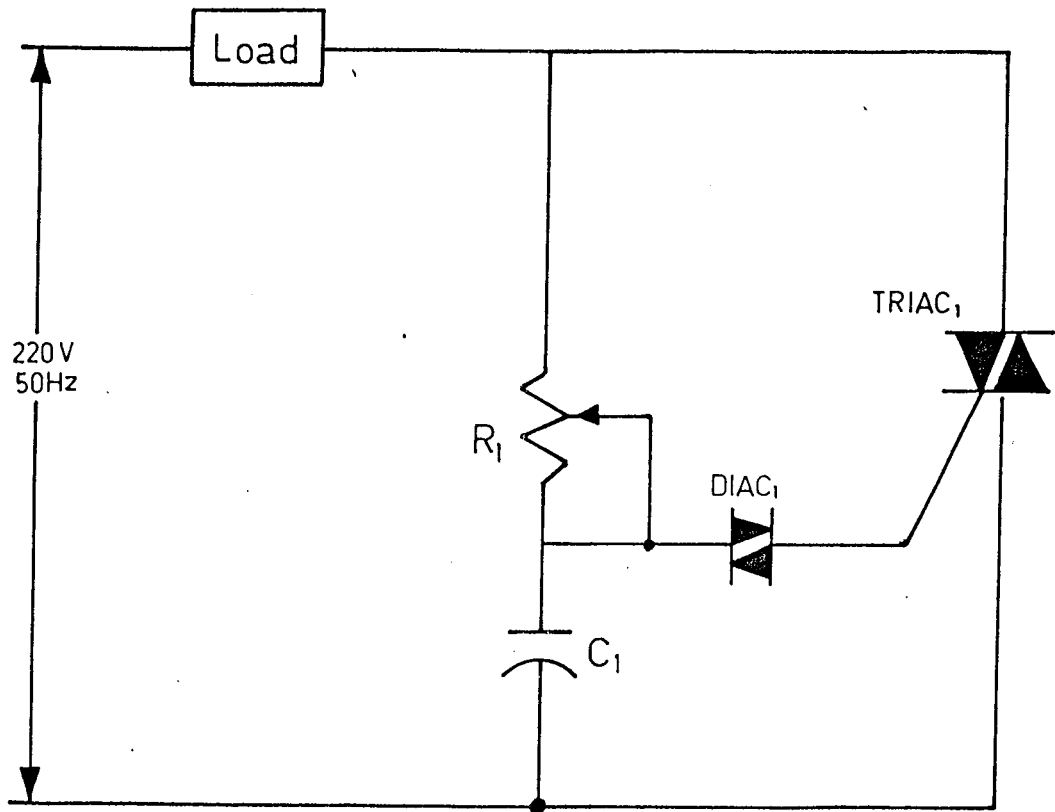
REFERENCES

- 1 - D.J. Close, The Performance of Solar Water Heaters with Natural Circulation, Solar Energy 12, pp 163-182 (1968).
- 2 - Y. Zvirin, A. Shitzer and G. Grossman, The Natural Circulation Solar Heater-Models with Linear and Non-linear Temperature Distributions, Int. J. Heat Mass Trans. 20, pp 997-999 (1977).
- 3 - A. Shitzer, D. Kalmanoviz, Y. Zvirin and G. Grossman, Experiments with a Flat Plate Solar Water Heating System in Thermosyphonic Flow, Solar Energy 22, pp 27-35 (1979).
- 4 - C.L. Gupta and H.P. Garg, System in Solar Water Heaters with Natural Circulation, Solar Energy 12, pp 163-182 (1968).
- 5 - B.J. Huang, Similarity Theory of Solar Water Heater with Natural Circulation, Solar Energy 25, pp 105-116 (1980).
- 6 - K.S. Ong, A Finite-Difference Method to Evaluate the Thermal Performance of a Solar Water Heater, Solar Energy 16, pp 137-147 (1974).
- 7 - K.S. Ong, An Improved Computer Program for the Thermal Performance of a Solar Water Heater, Solar Energy 18, pp 183-191 (1976).

- 8 - A. Mertol, W. Place, T. Webster and R. Greif (1980),
Thermosyphon Water Heaters with Heat Exchangers. Proc.
Am. Section of ISES, Phoenix, Arizona.
- 9 - FRANCIS DE Winter, Heat Exchanger Penalties in Double-
Loop Solar Water Heating Systems, Solar Energy 17,
pp 335-337 (1975).
- 10 - A.F. Orlando, L. Goldstein Jr., and D. Magnoli, Influence
of Heat Exchanger Effectiveness on the Performance of
Thermosyphon Double Loop Water Heating System, Solar
Energy International Congress, Vol. 2, pp 731-742 ;
16-22 June 1978, Cairo, Egypt.
- 11 - W.L. Dutre, L. Cybers, J. Berghmans and A. Debosscher,
Hot Water Production by means of a Solar Thermosyphon
Loop, Solar Energy International Congress, Vol. 2,
pp 745-766 ; 16-22 June 1978 Cairo, Egypt.
- 12 - Y.F. Wang, Z.L. Li and X.L. Sun, A "once-through" Solar
Water Heating System, Solar Energy 29, pp 541-547 (1982).
- 13 - Vincent Del Toro, Electrical Engineering Fundamentals,
Prentice-Hall, Inc. Englewood Cliffs, New Jersey,(1972).
- 14 - J.P. Holman, Heat Transfer, Fourth Edition, Mc Graw-Hill
Kogakusha , Ltd. , Tokyo,(1976).
- 15 - S. Kakaç and Y. Yener, Convective Heat Transfer,
Pub. No : 65, METU, Ankara,(1980).
- 16 - J.A. Duffie and W.A. Beckman, Solar Engineering of
Thermal Processes, John Wiley and Sons, Inc. (1980).
- 17 - A. Kılıç and A. Öztürk, Güneş Enerjisi, Kipaş Dağıtımçılık,
Cağaloğlu-İstanbul, (1983).

- 18 - N. Deriş, Güneş Enerjisi, Sıcak Su ile Isıtma Tekniği, Sermet Matbaası, İstanbul, (1979).
- 19 - J.P. Holman, Experimental Methods for Engineers, 3rd Edition, Mc Graw-Hill International Book Company, Tokyo, (1978).
- 20 - F.C. Mc Quiston and J.D. Parker, "Heating, Ventilating and Air Conditioning-Analysis and Design", John Willey and Sons, Inc., New York, (1982).
- 21 - J.R. Williams, Solar Energy-Technology and Applications, Ann Arbor Science Publishers, Inc., Michigan, (1974).
- 22 - J.C. Mc Veigh, Sun Power-An Introduction to the Applications of Solar Energy, Pergamon Press, (1977).
- 23 - Low Temperature Engineering Application of Solar Energy, Published by ASHRE, Inc., New York, (1967).
- 24 - Solar Energy Application in Buildings, Edited by A.A.M. Sayigh, Academic Press, Inc, New York, (1978).
- 25 - Solar Energy Engineering, Edited by A.A.M. Sayigh, Academic Press, Inc., New York, (1977).
- 26 - Murrey R. Spiegel, Mathematical Handbook of Formulas and Tables, Schaum's Outline Series in Mathematics, Mc Graw-Hill Book Company, (1968).
- 27 - S. Kakaç and Y. Yener, Heat Conduction, METU Publication no:60, ANKARA, (1979).
- 28 - Türk Standartları, TSE, Water Heater (Heat Exchanger), TS 736/Nisan 1969.
- 29 - SCR Applications Handbook, Edited by Richard G. Hoft, California, (1977).

APPENDIX 1



TRIAC TRIGGERING CIRCUIT

APPENDIX 2

ESTIMATION OF THE OVERALL HEAT LOSS COEFFICIENTS

a . Estimation of the Collector Overall Heat Loss

Coefficient, U_c :

The heat losses occur through top, bottom and edges of the collector to the environment. The resistances for collector heat losses consist of the resistance to heat flow through the insulation and, the combined convection and radiation resistance to the environment. The insulation resistance is large compared to the combined convective-radiative resistance outside the collector and the latter resistance is neglected.

The edge loss is estimated by assuming one-dimensional side ways heat flow around the perimeter of the collector system. This loss coefficient is then converted to a per unit collector area based coefficient when estimating the overall loss coefficient of the collector.

The collector top and back loss coefficients are written as follows :

$$U_b = U_t = k_{ins.} / t_{ins.} \quad (A2.1)$$

The edge loss coefficient referenced to the collector area is written as,

$$U_e = (UA)_{\text{edge}} / A_c \quad (\text{A2.2})$$

The collector overall heat loss coefficient, U_c , is the sum of the top, bottom, and edge loss coefficients.

$$U_c = U_b + U_t + U_e \quad (\text{A2.3})$$

From equations (A2.1), (A2.2) and (A2.3), the overall heat loss coefficient for the collector used in our experiment is found as,

$$U_c = 2.62 \text{ W} / \text{m}^2 \cdot \text{°C}$$

(The collector surface area is equal to 1.8 square meters.)

b . The Jacketed Hot Water Heat Storage Tank Overall

Heat Loss Coefficient Estimation, U_{he} :

The heat losses from the tank to the environment occur from the following three sections,

- 1 - Insulation over the jacket
- 2 - Insulated side surface of the tank
- 3 - Uninsulated side surface of the tank.

The loss coefficient for the first two heat losses may be determined with the same procedure as described in part(a).

Letting U_g to be the heat loss coefficient for the water jacket and U_{si} to be the heat loss coefficient for the

insulated part of the tank, the following heat loss coefficients are written :

$$U_s = \frac{k_{ins.}}{r_i \cdot \ln(r_o / r_i)} \cdot \frac{A_s}{A_j} \quad (A2.4)$$

$$U_{si} = \frac{k_{ins.}}{r_i \cdot \ln(r_o / r_i)} \cdot \frac{A_p}{A_j} +$$

$$\frac{k_{ins.}}{t_{ins.}} \cdot \frac{A_f}{A_j} \quad (A2.5)$$

The thermal resistance on the uninsulated side surface of the tank consists of outside air resistance, steel side wall thermal resistance and inside water thermal resistance. The latter two resistances are small and can be neglected. The outside air heat transfer coefficient is estimated by using the following equation,

$$h = 1.42 \left(\frac{T_w - T_a}{d} \right)^{1/4} + \epsilon \sigma (T_w^2 + T_a^2)(T_w + T_a) \quad (A2.6)$$

where T_a is the outside air temperature and T_w is the inside water temperature.

The overall loss coefficient for the hot water storage tank referenced to the jacket to tank heat transfer

surface area is written as,

$$U_{he} = U_s + U_{si} + h \cdot \frac{A_f}{A_j} \quad (A2.7)$$

The numerical values of the first two loss coefficients for the storage tank used in the experimental study are,

$$U_s = 1.12 \text{ W / m}^2 \cdot \text{ }^\circ\text{C}$$

$$U_{si} = 0.37 \text{ W / m}^2 \cdot \text{ }^\circ\text{C}$$

The resulting overall heat loss coefficient for the jacketed hot water heat storage tank takes the following form,

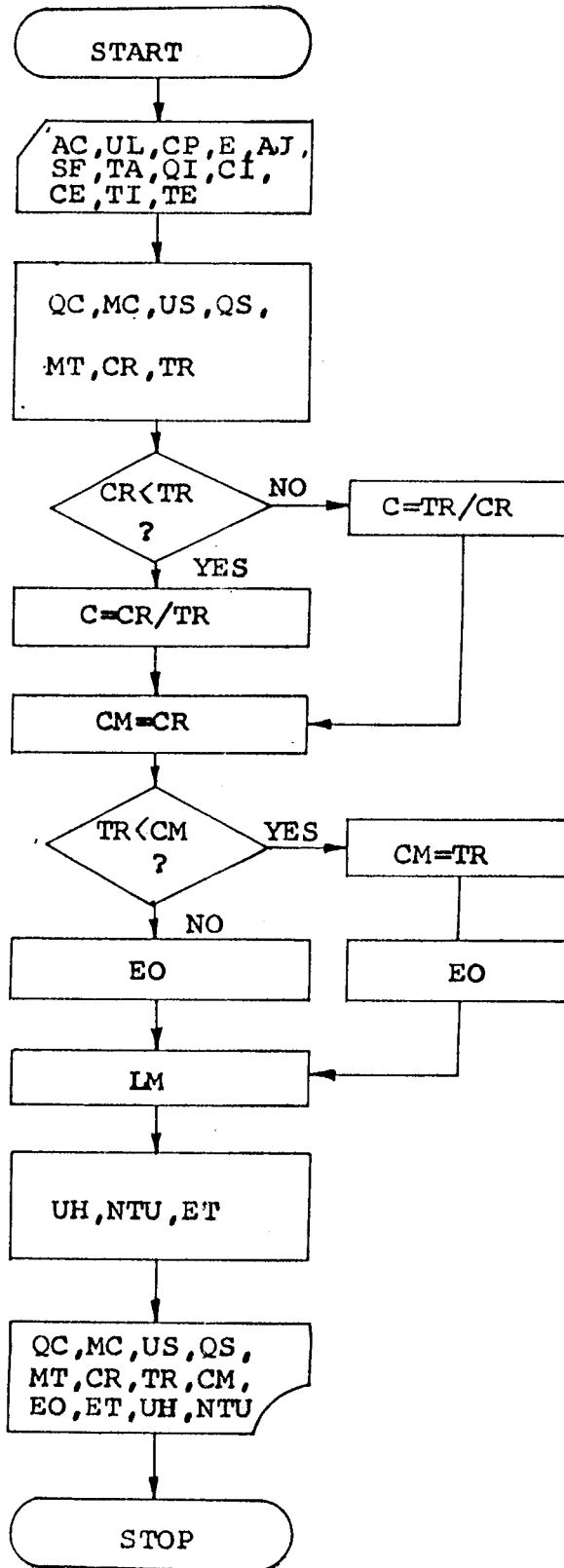
$$U_{he} = 1.49 + 0.155(T_w - T_a)^{1/4} + 0.087 \epsilon \sigma (T_w^2 + T_a^2)(T_w + T_a) \quad (A2.8)$$

The jacket to tank heat transfer surface area, A_j , is 1.45 m^2 .

APPENDIX 3

THE FLOWCHART FOR EXPERIMENTAL DATA EVALUATION

COMPUTER PROGRAM



LIST 10,470

```
10 REM          COMPUTER PROGRAM FOR EXPERIMENTAL DATA EVALUATION

20 REM ** FIXED VARIABLES **
30 D$ = CHR$(4):
40 AC = 3.6: REM  COLLECTOR AREA
50 UL = 2.62: REM  COLLECTOR HEAT LOSS COEFFICIENT
60 CP = 4.174: REM  COLLECTOR FLUID SPECIFIC HEAT
70 E = 0.95: REM  SURFACE EMMISIVITY
80 AJ = 1.45: REM  HEAT EXCHANGER SURFACE AREA
90 SF = 5.6697E - 8: REM  STEPHAN-BOLTZMAN CONSTANT
100 REM ** END OF FIXED CONSTANTS SECTION **

110 REM ** INPUT VARIABLES **
120 REM  INPUT AIR TEMPERATURE
130 TA = 25.5
140 REM  COLLECTOR TOTAL HEAT INPUT
150 QI = 3.104
160 REM  COLLECTOR INLET TEMPERATURE
170 CI = 38.25
180 REM  COLLECTOR EXIT TEMPERATURE
190 CE = 54.85
200 REM  TANK INLET TEMPERATURE
210 TI = 25.4
220 REM  TANK EXIT TEMPERATURE
230 TE = 48.1
240 REM ** END OF INPUT SECTION **

250 REM  EVALUATION OF EXPERIMENTAL RESULTS
260 QC = QI - UL * AC * ((CI + CE) / 2 - TA) / 1000
270 MC = QC / (CP * (CE - CI))
280 US = 1.49 + .155 * ((TE + TI) / 2 - TA) ^ 0.25 + .087 * E * SF * (((TE + TI) / 2) ^ 2 + TA ^
2) * ((TE + TI) / 2 + TA))
290 QS = QC - US * AJ * ((TE + TI) / 2 - TA) / 1000
300 MT = QS / (CP * (TE - TI))
310 CR = MC * CP
320 TR = MT * CP: IF CR < TR THEN C = CR / TR
330 IF CR > TR THEN C = TR / CR
340 CM = CR: IF TR < CM THEN CM = TR: EO = (TE - TI) / (CE - TI): GOTO 360
350 EO = (CE - CI) / (CE - TI)
360 LM = ((CI - TI) - (CE - TE)) / LOG ((CI - TI) / (CE - TE))
370 UH = QS / (LM * AJ)
380 NTU = (UH * AJ) / CM
390 ET = (1 - EXP (- NTU * (1 - C))) / (1 - C * EXP (- NTU * (1 - C)))
400 REM ** END OF EXPERIMENTAL EVALUATION SECTION **

410 REM  PRINTER OUTPUT SECTION
420 PRINT D$;"PR#1": PRINT : PRINT :
430 PP$ = CHR$(13): REM  RETURN CODE
440 WRITE = 49568
450 PI$ = CHR$(27): REM  PRINTER INITILIZE
460 PRINT PI$;"5":
470 PRINT CHR$(27);"B": REM  CANCEL BUZZER
```

LIST 480,810

```
480 PRINT SPC( 19);"-----"
490 PRINT SPC( 19);"COMPUTER OUTPUT FOR EXPERIMENTAL COMPUTATIONS"
500 PRINT SPC( 19);"-----": PRINT : PRINT : PRINT : PRI
NT : PRINT :
510 PRINT SPC( 19);"LIST OF FIXED INPUTS FOR COMPUTATION"
520 PRINT SPC( 19);"-----": PRINT :
530 CALL WRITE:"          COLLECTOR AREA (M2) ..... = ",AC;FB.5,PP$:
540 CALL WRITE:"          SURFACE EMISSIVITY ..... = ",E;FB.5,PP$:
550 CALL WRITE:"          HEAT EXCHANGER SURFACE AREA (M2) ..... = ",AJ;FB.5,PP$:
560 PRINT : PRINT : PRINT :
570 PRINT SPC( 19);"LIST OF VARIABLE INPUTS FOR COMPUTATION"
580 PRINT SPC( 19);"-----": PRINT :
590 CALL WRITE:"          COLLECTOR INLET TEMP (C) ..... = ",CI;FB.5,PP$:
600 CALL WRITE:"          AIR TEMPERATURE (C) ..... = ",TA;FB.5,PP$:
610 CALL WRITE:"          COLLECTOR TOTAL HEAT INPUT (KW) ..... = ",QI;FB.5,PP$:
620 CALL WRITE:"          COLLECTOR EXIT TEMPERATURE (C)..... = ",CE;FB.5,PP$:
630 CALL WRITE:"          TANK INLET TEMPERATURE (C) ..... = ",TI;FB.5,PP$:
640 CALL WRITE:"          TANK EXIT TEMPERATURE (C) ..... = ",TE;FB.5,PP$:
650 PRINT : PRINT : PRINT :
660 PRINT SPC( 19);"LIST OF OUTPUTS FROM COMPUTATION"
670 PRINT SPC( 19);"-----": PRINT
680 CALL WRITE:"          COLLECTOR USEFUL HEAT (KW) ..... = ",QC;FB.5,PP$:
690 CALL WRITE:"          COLL. MASS FLOW RATE (KG/S) ..... = ",MC;FB.5,PP$:
700 CALL WRITE:"          HEAT EXCHANGER LOSS COEFF (W/M2-C).... = ",US;FB.5,PP$:
710 CALL WRITE:"          HEAT EXCHANGER NET HEAT INPUT (KW) ... = ",QS;FB.5,PP$:
720 CALL WRITE:"          HEAT EXCHANGER MASS FLOW RATE (KG/S) . = ",MT;FB.5,PP$:
730 CALL WRITE:"          HOT SIDE CAPACITY RATE (KJ/S-C) ..... = ",CR;FB.5,PP$:
740 CALL WRITE:"          COLD SIDE CAPACITY RATE (KJ/S-C) ..... = ",TR;FB.5,PP$:
750 CALL WRITE:"          MINIMUM CAPACITY RATE (KJ/S-C) ..... = ",CM;FB.5,PP$:
760 CALL WRITE:"          EFFECTIVENESS-T ..... = ",EO;FB.5,PP$:
770 CALL WRITE:"          EFFECTIVENESS-F ..... = ",ET;FB.5,PP$:
780 CALL WRITE:"          HEAT EXCHANGER U-VALUE (KW/M2-C) ..... = ",UH;FB.5,PP$:
790 CALL WRITE:"          HEAT EXCHANGER NTU ..... = ",NTU;FB.5,PP$:
800 PRINT CHR$( 12):
810 END
```

EXPERIMENT NO.1

COMPUTER OUTPUT FOR EXPERIMENTAL COMPUTATIONS

LIST OF FIXED INPUTS FOR COMPUTATION

COLLECTOR AREA (M2)	=	3.60000
SURFACE EMISSIVITY	=	0.95000
HEAT EXCHANGER SURFACE AREA (M2)	=	1.45000

LIST OF VARIABLE INPUTS FOR COMPUTATION

COLLECTOR INLET TEMP (C)	=	35.05000
AIR TEMPERATURE (C)	=	25.00000
COLLECTOR TOTAL HEAT INPUT (KW)	=	0.47450
COLLECTOR EXIT TEMPERATURE (C).....	=	38.90000
TANK INLET TEMPERATURE (C)	=	24.65000
TANK EXIT TEMPERATURE (C)	=	25.50000

LIST OF OUTPUTS FROM COMPUTATION

COLLECTOR USEFUL HEAT (KW)	=	0.36155
COLL. MASS FLOW RATE (KG/S)	=	0.02249
HEAT EXCHANGER LOSS COEFF (W/M2-C).....	=	1.57140
HEAT EXCHANGER NET HEAT INPUT (KW) ...	=	0.36138
HEAT EXCHANGER MASS FLOW RATE (KG/S) .	=	0.10185
HOT SIDE CAPACITY RATE (KJ/S-C)	=	0.09390
COLD SIDE CAPACITY RATE (KJ/S-C)	=	0.42515
MINIMUM CAPACITY RATE (KJ/S-C)	=	0.09390
EFFECTIVENESS-T	=	0.27017
EFFECTIVENESS-F	=	0.27006
HEAT EXCHANGER U-VALUE (KW/M2-C)	=	0.02105
HEAT EXCHANGER NTU	=	0.32510

EXPERIMENT NO.2

COMPUTER OUTPUT FOR EXPERIMENTAL COMPUTATIONS

LIST OF FIXED INPUTS FOR COMPUTATION

COLLECTOR AREA (M2)	=	3.60000
SURFACE EMISSIVITY	=	0.95000
HEAT EXCHANGER SURFACE AREA (M2)	=	1.45000

LIST OF VARIABLE INPUTS FOR COMPUTATION

COLLECTOR INLET TEMP (C)	=	35.65000
AIR TEMPERATURE (C)	=	24.60000
COLLECTOR TOTAL HEAT INPUT (KW)	=	1.18000
COLLECTOR EXIT TEMPERATURE (C)	=	43.75000
TANK INLET TEMPERATURE (C)	=	23.85000
TANK EXIT TEMPERATURE (C)	=	41.00000

LIST OF OUTPUTS FROM COMPUTATION

COLLECTOR USEFUL HEAT (KW)	=	1.03757
COLL. MASS FLOW RATE (KG/S)	=	0.03068
HEAT EXCHANGER LOSS COEFF (W/M2-C)	=	1.74968
HEAT EXCHANGER NET HEAT INPUT (KW)	=	1.01772
HEAT EXCHANGER MASS FLOW RATE (KG/S)	=	0.01421
HOT SIDE CAPACITY RATE (KJ/S-C)	=	0.12809
COLD SIDE CAPACITY RATE (KJ/S-C)	=	0.05934
MINIMUM CAPACITY RATE (KJ/S-C)	=	0.05934
EFFECTIVENESS-T	=	0.86180
EFFECTIVENESS-F	=	0.86363
HEAT EXCHANGER U-VALUE (KW/M2-C)	=	0.11295
HEAT EXCHANGER NTU	=	2.76010

EXPERIMENT NO.3

COMPUTER OUTPUT FOR EXPERIMENTAL COMPUTATIONS

LIST OF FIXED INPUTS FOR COMPUTATION

COLLECTOR AREA (M2)	=	3.60000
SURFACE EMISSIVITY	=	0.95000
HEAT EXCHANGER SURFACE AREA (M2)	=	1.45000

LIST OF VARIABLE INPUTS FOR COMPUTATION

COLLECTOR INLET TEMP (C)	=	35.75000
AIR TEMPERATURE (C)	=	23.90000
COLLECTOR TOTAL HEAT INPUT (KW)	=	1.70400
COLLECTOR EXIT TEMPERATURE (C).....	=	46.10000
TANK INLET TEMPERATURE (C)	=	23.25000
TANK EXIT TEMPERATURE (C)	=	42.70000

LIST OF OUTPUTS FROM COMPUTATION

COLLECTOR USEFUL HEAT (KW)	=	1.54342
COLL. MASS FLOW RATE (KG/S)	=	0.03572
HEAT EXCHANGER LOSS COEFF (W/M2-C).....	=	1.75946
HEAT EXCHANGER NET HEAT INPUT (KW) ...	=	1.52026
HEAT EXCHANGER MASS FLOW RATE (KG/S) .	=	0.01872
HOT SIDE CAPACITY RATE (KJ/S-C)	=	0.14912
COLD SIDE CAPACITY RATE (KJ/S-C)	=	0.07816
MINIMUM CAPACITY RATE (KJ/S-C)	=	0.07816
EFFECTIVENESS-T	=	0.85120
EFFECTIVENESS-F	=	0.85290
HEAT EXCHANGER U-VALUE (KW/M2-C)	=	0.15000
HEAT EXCHANGER NTU	=	2.78274

EXPERIMENT NO.4

COMPUTER OUTPUT FOR EXPERIMENTAL COMPUTATIONS

LIST OF FIXED INPUTS FOR COMPUTATION

COLLECTOR AREA (M2)	=	3.60000
SURFACE EMISSIVITY	=	0.95000
HEAT EXCHANGER SURFACE AREA (M2)	=	1.45000

LIST OF VARIABLE INPUTS FOR COMPUTATION

COLLECTOR INLET TEMP (C)	=	36.50000
AIR TEMPERATURE (C)	=	23.30000
COLLECTOR TOTAL HEAT INPUT (KW)	=	2.38000
COLLECTOR EXIT TEMPERATURE (C).....	=	49.75000
TANK INLET TEMPERATURE (C)	=	23.00000
TANK EXIT TEMPERATURE (C)	=	45.45000

LIST OF OUTPUTS FROM COMPUTATION

COLLECTOR USEFUL HEAT (KW)	=	2.19301
COLL. MASS FLOW RATE (KG/S)	=	0.03965
HEAT EXCHANGER LOSS COEFF (W/M2-C).....	=	1.77225
HEAT EXCHANGER NET HEAT INPUT (KW) ...	=	2.16493
HEAT EXCHANGER MASS FLOW RATE (KG/S) .	=	0.02310
HOT SIDE CAPACITY RATE (KJ/S-C)	=	0.16551
COLD SIDE CAPACITY RATE (KJ/S-C)	=	0.09643
MINIMUM CAPACITY RATE (KJ/S-C)	=	0.09643
EFFECTIVENESS-T	=	0.83925
EFFECTIVENESS-F	=	0.84093
HEAT EXCHANGER U-VALUE (KW/M2-C)	=	0.18567
HEAT EXCHANGER NTU	=	2.79179

EXPERIMENT NO.5

----- COMPUTER OUTPUT FOR EXPERIMENTAL COMPUTATIONS -----

LIST OF FIXED INPUTS FOR COMPUTATION

COLLECTOR AREA (M2)	=	3.60000
SURFACE EMISSIVITY	=	0.95000
HEAT EXCHANGER SURFACE AREA (M2)	=	1.45000

LIST OF VARIABLE INPUTS FOR COMPUTATION

COLLECTOR INLET TEMP (C)	=	38.25000
AIR TEMPERATURE (C)	=	25.50000
COLLECTOR TOTAL HEAT INPUT (KW)	=	3.10400
COLLECTOR EXIT TEMPERATURE (C).....	=	54.85000
TANK INLET TEMPERATURE (C)	=	25.40000
TANK EXIT TEMPERATURE (C)	=	48.10000

LIST OF OUTPUTS FROM COMPUTATION

COLLECTOR USEFUL HEAT (KW)	=	2.90545
COLL. MASS FLOW RATE (KG/S)	=	0.04193
HEAT EXCHANGER LOSS COEFF (W/M2-C).....	=	1.77445
HEAT EXCHANGER NET HEAT INPUT (KW) ...	=	2.87651
HEAT EXCHANGER MASS FLOW RATE (KG/S) .	=	0.03035
HOT SIDE CAPACITY RATE (KJ/S-C)	=	0.17502
COLD SIDE CAPACITY RATE (KJ/S-C)	=	0.12671
MINIMUM CAPACITY RATE (KJ/S-C)	=	0.12671
EFFECTIVENESS-T	=	0.77079
EFFECTIVENESS-F	=	0.77250
HEAT EXCHANGER U-VALUE (KW/M2-C)	=	0.20937
HEAT EXCHANGER NTU	=	2.39578

EXPERIMENT NO.6

----- COMPUTER OUTPUT FOR EXPERIMENTAL COMPUTATIONS -----

LIST OF FIXED INPUTS FOR COMPUTATION

COLLECTOR AREA (M2)	=	3.60000
SURFACE EMISSIVITY	=	0.95000
HEAT EXCHANGER SURFACE AREA (M2)	=	1.45000

LIST OF VARIABLE INPUTS FOR COMPUTATION

COLLECTOR INLET TEMP (C)	=	37.60000
AIR TEMPERATURE (C)	=	23.40000
COLLECTOR TOTAL HEAT INPUT (KW)	=	1.36400
COLLECTOR EXIT TEMPERATURE (C).....	=	46.10000
TANK INLET TEMPERATURE (C)	=	22.60000
TANK EXIT TEMPERATURE (C)	=	43.50000

LIST OF OUTPUTS FROM COMPUTATION

COLLECTOR USEFUL HEAT (KW)	=	1.18997
COLL. MASS FLOW RATE (KG/S)	=	0.03354
HEAT EXCHANGER LOSS COEFF (W/M2-C).....	=	1.76362
HEAT EXCHANGER NET HEAT INPUT (KW) ...	=	1.16530
HEAT EXCHANGER MASS FLOW RATE (KG/S) .	=	0.01335
HOT SIDE CAPACITY RATE (KJ/S-C)	=	0.13999
COLD SIDE CAPACITY RATE (KJ/S-C)	=	0.05575
MINIMUM CAPACITY RATE (KJ/S-C)	=	0.05575
EFFECTIVENESS-T	=	0.88936
EFFECTIVENESS-F	=	0.89092
HEAT EXCHANGER U-VALUE (KW/M2-C)	=	0.11358
HEAT EXCHANGER NTU	=	2.95387

APPENDIX 4

EXPRESSIONS FOR MASS FLOW RATE

ESTIMATION OF THE COLLECTOR RISERS

1 - For riser no.3,

$$H_3 = K_3 \cdot m_{1,3} \quad (A4.1)$$

where,

$$K_3 = ((\alpha_1 + \alpha_3) / D_h^3 + 2 a / D_h^4 + K_2) (1 + \gamma_2)^{-1}$$

$$\gamma_2 = ((\alpha_1 + \alpha_3) / D_h^3 + 2 a / D_h^4 + K_2) /$$

$$(\alpha_2 / D_h^3 + b / D_r^4 + \alpha_3 + D_r^3)$$

$$m_{1,2} + m_2 = m_{1,3} \quad (A4.2)$$

$$\gamma_2 \cdot m_{1,2} = m_3 \quad (A4.3)$$

$$m_{1,2} = (1 + \gamma_2)^{-1} \cdot m_{1,3} \quad (A4.4)$$

$$H_3 = \pi \rho g \cdot h_{L3} / (128 V) \quad (A4.5)$$

2 - For riser no.4,

$$H_4 = K_4 \cdot m_{1,4} \quad (\text{A4.6})$$

where,

$$K_4 = ((\alpha_1 + \alpha_3) / D_h^3 + 2 a / D_h^4 + K_3)(1 + \gamma_3)^{-1}$$

$$\gamma_3 = ((\alpha_1 + \alpha_3) / D_h^3 + 2 a / D_h^4 + K_3) /$$
$$(\alpha_2 / D_h^3 + b / D_r^4 + \alpha_3 / D_r^3)$$

$$m_{1,3} + m_4 = m_{1,4} \quad (\text{A4.7})$$

$$\gamma_3 \cdot m_{1,3} = m_4 \quad (\text{A4.8})$$

$$m_{1,3} = (1 + \gamma_3)^{-1} \cdot m_{1,4} \quad (\text{A4.9})$$

$$H_4 = \pi \rho g \cdot h_{L4} / (128 \gamma) \quad (\text{A4.10})$$

3 - For riser no.5,

$$H_5 = K_5 \cdot m_{1,5} \quad (\text{A4.11})$$

where,

$$K_5 = ((\alpha_1 + \alpha_3) / D_h^3 + 2 a / D_h^4 + K_4)(1 + \gamma_4)^{-1}$$

$$\gamma_4 = ((\alpha_1 + \alpha_3) / D_h^3 + 2 a / D_h^4 + K_4) /$$

$$(\alpha_2 / D_h^3 + b / D_r^4 + \alpha_3 / D_r^3)$$

$$m_{1,4} + m_5 = m_{1,5} \quad (A4.12)$$

$$\gamma_4 \cdot m_{1,4} = m_5 \quad (A4.13)$$

$$m_{1,4} = (1 + \gamma_4)^{-1} \cdot m_{1,5} \quad (A4.14)$$

$$H_5 = \pi \rho g \cdot h_{L5} / (128 V) \quad (A4.15)$$

4 - For riser no.6,

$$H_6 = K_6 \cdot m_{1,6} \quad (A4.16)$$

where,

$$K_6 = ((\alpha_1 + \alpha_3) / D_h^3 + 2 a / D_h^4 + K_5)(1 + \gamma_5)^{-1}$$

$$\gamma_5 = ((\alpha_1 + \alpha_3) / D_h^3 + 2 a / D_h^4 + K_5) /$$

$$(\alpha_2 / D_h^3 + b / D_r^4 + \alpha_3 / D_r^3)$$

$$m_{1,5} + m_6 = m_{1,6} \quad (\text{A4.17})$$

$$\gamma_5 \cdot m_{1,5} = m_6 \quad (\text{A4.18})$$

$$m_{1,5} = (1 + \gamma_5)^{-1} \cdot m_{1,6} \quad (\text{A4.19})$$

$$H_6 = \pi \rho g \cdot h_{L_6} / (128V) \quad (\text{A4.20})$$

5 - For riser no.7,

$$H_7 = K_7 \cdot m_{1,7} \quad (\text{A4.21})$$

Where,

$$K_7 = ((\alpha_1 + \alpha_3) / D_h^3 + 2a / D_h^4 + K_6)(1 + \gamma_6)^{-1}$$

$$\gamma_6 = ((\alpha_1 + \alpha_3) / D_h^3 + 2a / D_h^4 + K_6) /$$

$$(\alpha_2 / D_h^3 + b / D_r^4 + \alpha_3 / D_r^3)$$

$$m_{1,6} + m_7 = m_{1,7} \quad (\text{A4.22})$$

$$\gamma_6 \cdot m_{1,6} = m_7 \quad (\text{A4.23})$$

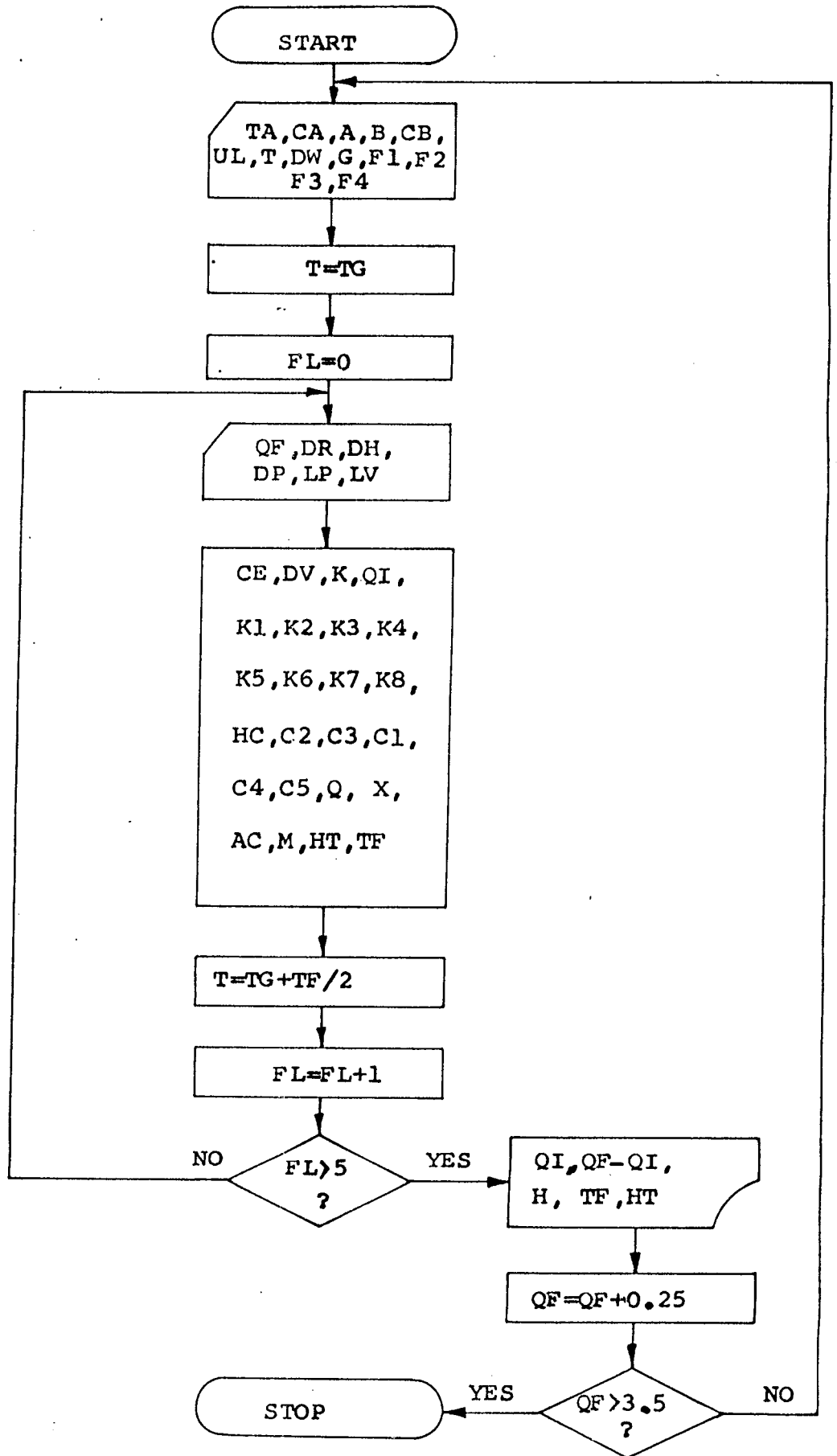
$$m_{1,6} = (1 + \gamma_6)^{-1} \cdot m_{1,7} \quad (\text{A4.24})$$

$$H_6 = \pi \rho g \cdot h_{L_7} / (128V) \quad (\text{A4.25})$$

APPENDIX 5

THE FLOWCHART FOR THEORETICAL RESULTS EVALUATION

COMPUTER PROGRAM



LIST 10,480

```
10 REM INTERACTIVE COMPUTER EVALUATION OF THE THEORETICAL RESULTS
20 REM      ** START INTERACTIVE INPUT ROUTINE **
30 D$ = CHR$(4):
40 T = 35.65:QI = .25:DR = .016:A = .114:B = 1.821:DH = .0272:DP = .0216:LP = 4.867:LV = 1.985:CB
= 4.174:UL = 2.62:CA = 3.6:TA = 24.6
50 HOME : PRINT : PRINT : PRINT :BY = 0: PRINT D$;"PR#3":
60 PRINT " 1) COLLECTOR INLET TEMPERATURE (C) ..... T = ";T
70 PRINT " 2) HEAT INPUT RATE FOR TWO COLLECTORS (KW) ..... QI = ";QI
80 PRINT " 3) RISER INSIDE DIAMETER (M) ..... DR = ";DR
90 PRINT " 4) DISTANCE BETWEEN TWO RISERS (M) ..... A = ";A
100 PRINT " 5) LENGTH OF RISER (M) ..... B = ";B
110 PRINT " 6) HEADER INSIDE DIAMETER (M) ..... DH = ";DH
120 PRINT " 7) CONNECTION PIPE INSIDE DIAMETER (M) ..... DP = ";DP
130 PRINT " 8) CONNECTION PIPE TOTAL LENGTH (M) ..... LP = ";LP
140 PRINT " 9) CONNECTION PIPE VERTICAL LENGTH (M) ..... LV = ";LV
150 PRINT "10) COLLECTOR FLUID SPECIFIC HEAT (KJ/KG-C) ..... CB = ";CB
160 PRINT "11) COLLECTOR OVERALL HEAT LOSS COEFF (W/M2-C) ..... UL = ";UL
170 PRINT "12) COLLECTOR AREA (M2) ..... CA = ";CA
180 PRINT "13) AMBIANT AIR TEMPERATURE (C) ..... TA = ";TA
190 PRINT :TG = T: REM TG IS COLLECTOR INLET TEMP
200 PRINT : PRINT :QF = QI: REM QF IS THE HEAT INPUT TO THE COLLECTORS
210 PRINT "INPUT 14 TO START PROGRAM "
220 INPUT "WHICH INPUT VALUE DO YOU WANT TO CHANGE ? = ";SS
230 HOME : ON SS GOTO 240,250,260,270,280,290,300,310,320,330,340,350,360,380
240 INPUT "COLLECTOR INLET TEMPERATURE (C) ..... T = ";T: GOTO 380
250 INPUT "HEAT INPUT RATE FOR TWO COLLECTORS (KW) ..... QI = ";QI: GOTO 380
260 INPUT "RISER INSIDE DIAMETER (M) ..... DR = ";DR: GOTO 380
270 INPUT "DISTANCE BETWEEN TWO RISERS (M) ..... A = ";A: GOTO 380
280 INPUT "LENGTH OF RISER (M) ..... B = ";B: GOTO 380
290 INPUT "HEADER INSIDE DIAMETER (M) ..... DH = ";DH: GOTO 380
300 INPUT "CONNECTION PIPE INSIDE DIAMETER (M) ..... DP = ";DP: GOTO 380
310 INPUT "CONNECTION PIPE TOTAL LENGTH (M) ..... LP = ";LP: GOTO 380
320 INPUT "CONNECTION PIPE VERTICAL LENGHT (M) .....LV = ";LV: GOTO 380
330 INPUT "COLLECTOR FLUID SPECIFIC HEAT (KJ/KG-C) ..... CB = ";CB: GOTO 380
340 INPUT "COLLECTOR OVERALL HEAT LOSS COEFF (W/M2-C) ..... UL = ";UL: GOTO 380
350 INPUT "COLLECTOR AREA (M2) ..... CA = ";CA: GOTO 380
360 INPUT "AMBIANT AIR TEMPERATURE (C) ..... TA= ";TA: GOTO 380
370 REM      ** END OF INPUT ROUTINE **

380 REM ** FIXED PROPERTY AND PARAMETRIC VALUES ARE GIVEN BELOW **
390 IF SS < > 14 GOTO 50
400 DW = 986: REM DW IS DENSITY OF WATER
410 G = 9.81: REM G IS GRAVITATIONAL ACCELERATION
420 F1 = 20: REM F1 IS FITTING LOSS COEFF T-THRU FLOW SEPARATION
430 F2 = 60: REM F2 IS FITTING LOSS COEFF T-BRANCH FLOW SEPARATION
440 F3 = 40: REM F3 IS FITTING LOSS COEFF THRU,BRANCH FLOW UNION
450 F4 = 30: REM F4 IS FITTING LOSS COEFF 90 DEGREE ELBOW
460 PI = 3.1416: REM PI CONSTANT
470 GOTO 1340
480 REM ** END OF ROUTINE **
```

LIST 490,910

```
490 REM **** PRINTER NUMERIC OUTPUT SUBROUTINE ****
500 REM ----- DD(I) INPUT VALUES 0 <= I <= 9
510 REM ----- DS (I)NUMBER OF DECIMAL SPACES
520 REM ----- UU(I) LENGHT OF REAL NUMBER ON OUTPUT
530 REM ----- DD$(I) CONTAINS THE RESULT ON RETURN
540 FOR I = 0 TO 9:ES(I) = 1 / 10 ^ DS(I): NEXT
550 FOR I = 0 TO 9:DD(I) = INT (DD(I) / ES(I) + 0.5) * ES(I): NEXT
560 FOR I = 0 TO 9:EE$(I) = STR$(DD(I)): NEXT
570 FOR I = 0 TO 9:MM(I) = LEN (EE$(I)): NEXT
580 FOR I = 0 TO 9:DD(I) = INT (DD(I)): NEXT
590 FOR I = 0 TO 9:DD$(I) = STR$(DD(I)):IL = LEN (DD$(I)):
600 LI = IL + 1 + DS(I):EE$(I) = LEFT$(EE$(I),LI)
610 IF EE$(I) = DD$(I) THEN EE$(I) = EE$(I) + "."
620 LL(I) = LEN (DD$(I)):PP = UU(I) - LL(I) - DS(I) - 1: IF VAL (EE$(I)) = 0 THEN GOTO 640
630 IF VAL (EE$(I)) < 1 THEN PP = PP + 1
640 FOR J = 1 TO PP:EE$(I) = " " + EE$(I): NEXT
650 PP = UU(I) - LEN (EE$(I)): IF PP = 0 GOTO 670
660 FOR J = 1 TO PP:EE$(I) = EE$(I) + " ": NEXT
670 NEXT
680 FOR I = 0 TO 9:DD$(I) = EE$(I): NEXT
690 RETURN
700 REM ** END OF PRINTER NUMERIC OUTPUT SUBROUTINE **

710 REM ** SUBROUTINE FOR COMPUTING COEFF OF VOL EXPANSION (CE) **
720 REM ** SUBROUTINE NEEDS TEMP(C) AS INPUT INTO VARIABLE T **
730 REM ** SUBROUTINE RETURNS AS OUTPUT THE VALUE FOR CE (1/C) **
740 A1 = 6.48E + 10:A2 = - 1.438E + 9:
750 CE = (A1 + A2 * (60 - T)) * K * DV / (6 * DW ^ 2 * CB) / 1000
760 RETURN
770 REM ** END OF SUBROUTINE **

780 REM ** SUBROUTINE FOR COMPUTING DYNAMIC VISCOSITY (DV) **
790 REM ** SUBROUTINE NEEDS TEMP(C) AS INPUT INTO VARIABLE T **
800 REM ** SUBROUTINE RETURNS THE VALUE FOR DV (KG/M-S) **
810 A1 = 2.1482:A2 = - 8.435:A3 = 8078.4:A4 = 8.435:A5 = 120
820 DV = 0.1 / ((A1 * ((T + A2) + (A3 + (T - A4) ^ 2) ^ 0.5)) - A5)
830 RETURN
840 REM ** END OF SUBROUTINE **

850 REM ** SUBROUTINE FOR COMPUTING THERMAL CONDUCTIVITY (K) **
860 REM ** SUBROUTINE NEEDS TEMP(C) AS INPUT INTO VARIABLE T **
870 REM ** SUBROUTINE RETURNS AS OUTPUT THE VALUE FOR K (W/M-C) **
880 T1 = T * 9 / 5 + 32
890 K = (0.34 + 0.000416 * (T1 - 50)) / 5.778E - 1
900 RETURN
910 REM ** END OF SUBROUTINE **
```

LIST 920,1330

```
920 REM SUBROUTINE FOR DETERMINING THE COLLECTOR CHARACTERISTIC
930 K1 = F2 / DH ^ 3 + B / DR ^ 4 + F3 / DR ^ 3:KE = (F1 + F3) / DH ^ 3 + 2 * A / DH ^ 4
940 K2 = (K1 + KE) * K1 / (2 * K1 + KE)
950 K3 = (K2 + KE) * K1 / (K2 + KE + K1)
960 K4 = (K3 + KE) * K1 / (K3 + KE + K1)
970 K5 = (K4 + KE) * K1 / (K4 + KE + K1)
980 K6 = (K5 + KE) * K1 / (K5 + KE + K1)
990 K7 = (K6 + KE) * K1 / (K6 + KE + K1)
1000 KB = (K7 + KE) * K1 / (K7 + KE + K1)
1010 HC = 64 * DV * KB / (PI * DW ^ 2 * G): REM HC IS COLLECTOR CHARACTERISTIC COEFF
1020 RETURN
1030 REM ** END OF SUBROUTINE **

1040 REM SUBROUTINE FOR DETERMINING THERMOSYPHONIC SYSTEM CHARACTERISTIC
1050 C2 = 14.24 / (PI ^ 2 * DW ^ 2 * G * DH ^ 4)
1060 C3 = (128 * DV / (PI * DW ^ 2 * G)) * (LP / DP ^ 4 + 2 * F4 / DP ^ 3 + 0.5 * (F2 + F3) / DH
^ 3 + A / DH ^ 4 + 0.5 * KB)
1070 RETURN
1080 REM ** END OF SUBROUTINE **

1090 REM SUBROUTINE FOR THERMOSTATIC HEAD LOSS COEFFICIENT
1100 C1 = 0.5 * CE * LV
1110 RETURN
1120 REM ** END OF SUBROUTINE **

1130 REM SUBROUTINE FOR MASS FLOW RATE DETERMINATION
1140 C4 = C3 / C2
1150 C5 = - C1 * Q1 / (CB * C2)
1160 Q = - (C4 ^ 2) / 9:R = (- 27 * C5 - 2 * C4 ^ 3) / 54
1170 X = (R / (- Q ^ 3) ^ 0.5)
1180 AC = - ATN (X / SQRT (- X * X + 1)) + 1.5708
1190 M = 2 * (- Q) ^ 0.5 * COS (AC / 3) - C4 / 3
1200 RETURN
1210 REM ** END OF SUBROUTINE **

1220 REM SUBROUTINE FOR THERMATIC HEAD COMPUTATION
1230 HT = C2 * (M ^ 2) + C3 * M
1240 RETURN
1250 REM ** END OF SUBROUTINE **

1260 REM SUBROUTINE FOR TEMP DIFFERENCE COMPUTATION
1270 TF = Q1 / (M * CB)
1280 RETURN
1290 REM ** END OF SUBROUTINE **

1300 REM SUBROUTINE FOR USEFUL HEAT RATE COMPUTATION
1310 QI = QF - UL * CA * (T - TA) * 0.001
1320 RETURN
1330 REM ** END OF SUBROUTINE **
```


LIST 1340,1790

```
1340 REM ***** MAIN PROGRAM *****
1350 GOSUB 1300: REM CONVERT HEAT INPUT TO USEFUL HEAT INPUT
1360 GOSUB 780: REM COMPUTE DYNAMIC VISCOSITY
1370 GOSUB 850: REM COMPUTE THERMAL CONDUCTIVITY
1380 GOSUB 710: REM COMPUTE COEFF OF VOL EXPANSION
1390 GOSUB 920: REM COMPUTE COLLECTOR CHARACTERISTIC
1400 GOSUB 1040: REM COMPUTE SYSTEM CHARACTERISTIC
1410 GOSUB 1090: REM COMPUTE THERMOSTATIC HEAD LOSS COEFF
1420 GOSUB 1130: REM COMPUTE MASS FLOW RATE
1430 GOSUB 1220: REM COMPUTE TOTAL HEAD LOSS
1440 GOSUB 1260: REM COMPUTE TEMPERATURE DIFFERENCE
1450 FL = FL + 1
1460 IF FL = 5 THEN FL = 0: GOTO 1480:
1470 T = TG + TF / 2: GOTO 400: REM ITERATE IF FL IS NOT ZERO
1480 IF BY = 1 GOTO 1500: REM DO NOT WRITE PARAMETRIC VALUES
1490 GOSUB 1600: REM PRINT PARAMETRIC VALUES
1500 D1 = QI:D2 = QF - QI:D3 = M:D4 = TF:D5 = HT:
1510 WRITE = 49568
1520 CALL WRITE:" ",D1;F9.4," ":
1530 CALL WRITE:D2;F9.4," ":
1540 CALL WRITE:D3;F9.4," ":
1550 CALL WRITE:D4;F9.4," ":
1560 CALL WRITE:D5;E4, CHR$(13):
1570 IF QF > 3.3 THEN QF = .25: PRINT : PRINT : PRINT : PRINT : PRINT D$;"PR#0":BY = 0: GOTO 50
1580 QF = QF + .25: GOTO 1340
1590 REM ** END OF MAIN PROGRAM **
```

```
1600 REM ***** PRINTER OUTPUT ROUTINE *****
1610 PRINT D$;"PR#1"
1620 PRINT : PRINT : PRINT :BY = 1
1630 PRINT SPC(19);"-----"
1640 PRINT SPC(19);"COMPUTER OUTPUT FOR THEORETICAL ANALYSIS"
1650 PRINT SPC(19);"-----"
1660 PRINT : PRINT : PRINT :
1670 DD(1) = CA:DS(1) = 4:UU(1) = 10: GOSUB 490
1680 PRINT SPC(13);"COLLECTOR AREA (M2) ..... = ";DD$(1)
1690 DD(1) = T: GOSUB 490
1700 PRINT SPC(13);"COLLECTOR INLET TEMP (C) ..... = ";DD$(1)
1710 DD(1) = DR: GOSUB 490
1720 PRINT SPC(13);"RISER INSIDE DIAMETER (M) ..... = ";DD$(1)
1730 DD(1) = A: GOSUB 490
1740 PRINT SPC(13);"DISTANCE BETWEEN TWO RISERS (M) ..... = ";DD$(1)
1750 DD(1) = B: GOSUB 490
1760 PRINT SPC(13);"LENGTH OF RISER (M) ..... = ";DD$(1)
1770 DD(1) = DH: GOSUB 490
1780 PRINT SPC(13);"HEADER INSIDE DIAMETER (M) ..... = ";DD$(1)
1790 DD(1) = DP: GOSUB 490
```

LIST 1800,1930

```
1800 PRINT SPC( 13);"CONNECTION PIPE I.D. (M) ..... = ";DD$(1)
1810 DD(1) = LP: 60SUB 490
1820 PRINT SPC( 13);"CONNECTION PIPE TOTAL LENGTH (M) ..... = ";DD$(1)
1830 DD(1) = LV: 60SUB 490
1840 PRINT SPC( 13);"CONNECTION PIPE VER. LENGTH (M) ..... = ";DD$(1)
1850 DD(1) = CB: 60SUB 490
1860 PRINT SPC( 13);"COLLECTOR FLUID SP. HEAT (KJ/KG-C) ... = ";DD$(1)
1870 DD(1) = UL: 60SUB 490
1880 PRINT SPC( 13);"COLL. OVERALL HEAT LOSS CDEFF (W/M2-C) = ";DD$(1)
1890 PRINT : PRINT : PRINT : PRINT : PRINT
1900 PRINT SPC( 17);"QI"; SPC( 8);"QF-QI"; SPC( 12);"M"; SPC( 11);"TF"; SPC( 10);"HT"
1910 PRINT SPC( 17);"---"; SPC( 8);"-----"; SPC( 12);"--"; SPC( 11);"---"; SPC( 10);"--"
1920 RETURN
1930 REM ** END OF SUBROUTINE **
```

 COMPUTER OUTPUT FOR THEORETICAL ANALYSIS

COLLECTOR AREA (M2)	=	3.6
COLLECTOR INLET TEMP (C)	=	35.65
RISER INSIDE DIAMETER (M)	=	.016
DISTANCE BETWEEN TWO RISERS (M)	=	.114
LENGTH OF RISER (M)	=	1.821
HEADER INSIDE DIAMETER (M)	=	.0272
CONNECTION PIPE I.D. (M)	=	.0216
CONNECTION PIPE TOTAL LENGTH (M)	=	4.867
CONNECTION PIPE VER. LENGTH (M)	=	1.985
COLLECTOR FLUID SP. HEAT (KJ/KG-C) ...	=	4.174
COLL. OVERALL HEAT LOSS COEFF (W/M2-C) =		2.62

QI ---	QF-QI -----	M --	TF ---	HT ---
0.1308	0.1191	0.0099	3.1589	1.088E-03
0.3710	0.1289	0.0169	5.2412	1.857E-03
0.6142	0.1357	0.0220	6.6816	2.411E-03
0.8587	0.1412	0.0262	7.8458	2.871E-03
1.1040	0.1459	0.0299	8.8463	3.276E-03
1.3498	0.1501	0.0332	9.7356	3.642E-03
1.5960	0.1539	0.0362	10.5432	3.980E-03
1.8425	0.1574	0.0391	11.2875	4.295E-03
2.0892	0.1607	0.0417	11.9810	4.593E-03
2.3362	0.1637	0.0443	12.6325	4.876E-03
2.5832	0.1667	0.0467	13.2488	5.146E-03
2.8305	0.1694	0.0490	13.8347	5.406E-03
3.0778	0.1721	0.0512	14.3943	5.656E-03
3.3253	0.1746	0.0533	14.9308	5.898E-03